


1-1-2011

# Reinforced chitosan-based heart valve scaffold and utility of bone marrow-derived mesenchymal stem cells for cardiovascular tissue engineering

Mohammad Z. Albanna  
*Wayne State University*

Follow this and additional works at: [http://digitalcommons.wayne.edu/oa\\_dissertations](http://digitalcommons.wayne.edu/oa_dissertations)

 Part of the [Biomedical Engineering and Bioengineering Commons](#), [Chemical Engineering Commons](#), and the [Materials Science and Engineering Commons](#)

---

## Recommended Citation

Albanna, Mohammad Z., "Reinforced chitosan-based heart valve scaffold and utility of bone marrow-derived mesenchymal stem cells for cardiovascular tissue engineering" (2011). *Wayne State University Dissertations*. Paper 230.

This Open Access Dissertation is brought to you for free and open access by DigitalCommons@WayneState. It has been accepted for inclusion in Wayne State University Dissertations by an authorized administrator of DigitalCommons@WayneState.

**REINFORCED CHITOSAN-BASED HEART VALVE SCAFFOLD AND UTILITY  
OF BONE MARROW-DERIVED MESENCHYMAL STEM CELLS FOR  
CARDIOVASCULAR TISSUE ENGINEERING**

by

**MOHAMMAD ZAKI ALBANNA**

**DISSERTATION**

Submitted to the Graduate School

of Wayne State University,

Detroit, Michigan

in partial fulfillment of the requirements

for the degree of

**DOCTOR OF PHILOSOPHY**

2011

MAJOR: BIOMEDICAL ENGINEERING

Approved by:

---

Advisor

Date

---

---

---

---

## DEDICATION

Dedicated to Mom, Ahmad, Ruba and Layann.....

## ACKNOWLEDGMENTS

The time has come when I must acknowledge those who have affected my life so greatly that this dissertation could not have been possible without them. Although there are far too many to mention, I must pay special tribute to a few.

First, and foremost, I thank God Almighty for all the blessings he has bestowed upon me.

I must thank my queen Ruba and my little princess Layann. You both have touched the very depths of my soul. My love for you is eternal and unconditional. To my parents, Dr. Zaki and Mrs. Mussarah Sweidan: without you none of this could have been possible. To My brother Dr. Ahmad Albanna, you always stood beside me and helped me through every step of my education. My little sisters-Esra and Tasneem: I want to thank you for all your calls and prayers. God could not have blessed me with a better family. To my parents in law, Azmi and Fathia, and their family, thanks all for you support.

I must also thank my advisors and mentors, Professors Howard W. T. Matthew and Henry L. Walter III: Without your patience, help, and faith in my abilities, I would not have finished this dissertation. You have guided me and given me inspiration to continue with my education. I also extend my sincere gratitude to Professors Michele Grimm and Pamela VandeVord, my committee members, for their patience and research support during my Ph.D. research. Moreover, infinite thanks to Dr. Therese Bou-Akl, my mentor and friend.

In addition, I would like to thank the tissue engineering and biomaterials research group members for their help in the lab and Wayne State University for providing me

with the sufficient fund to complete my graduate studies, allowing me the opportunity to expand my knowledge and ability.

Finally, I would like to thank all of my friends who have become brothers over the years specially my best three friends Suhib Rawshdeh, Mahmoud Najeh and Dr. Dawood Yusef. I could not list all of my wonderful friends but you all know who you are and you know you are all in my heart.

## TABLE OF CONTENTS

Dedication_____	ii
Acknowledgements_____	iii
List of Figures_____	xi
List of Tables_____	xv
CHAPTER ONE: INTRODUCTION_____	1
CHAPTER TWO: CHITOSAN AND GLYCOSAMINOGLYCANS IN TISSUE ENGINEERING APPLICATIONS_____	4
2.1 Chitosan_____	4
2.2 Glycosaminoglycans (GAGs)_____	5
CHAPTER THREE: HEART VALVE DISEASES AND TISSUE ENGINEERED HEART VALVES_____	7
3.1 Significance of Heart Valve Diseases in Pediatrics_____	7
3.2 Current Treatments of Defective Aortic Heart Valve_____	9
3.2.1 Mechanical Valves_____	9
3.2.2 Biological Valves_____	9
3.3 Tissue Engineered Heart Valve Approach_____	10
3.4 Parameters Affecting the Tissue Engineered Heart Valve Function_____	11
3.4.1 Scaffold Materials_____	11
3.4.2 Static and Dynamic Culturing of Scaffolds_____	15
CHAPTER FOUR: ADVANCES IN BONE MARROW-DERIVED MESENCHYMAL STEM CELLS FOR CARDIOVASCULAR TISSUE ENGINEERING_____	20
4.1 Isolation of Mesenchymal Stem Cells (MSCs) From Bone Marrow_____	20

4.2 Bone Marrow MSCs in Tissue-Engineered Heart Valves Applications__	20
4.3 Effect of Mechanical stimulations on Bone Marrow-Derived MSCs	
Differentiation and Proliferations_____	21
4.4 Effect of Scaffold Matrix Components on Bone Marrow-Derived MSCs	
differentiation and proliferations_____	22
 CHAPTER FIVE: REINFORCING CHITOSAN-BASED HEART VALVE	
SCAFFOLD USING CHITOSAN FIBERS_____	24
5.1 Introduction_____	24
5.2 Experimental Work_____	26
5.2.1 Materials and Methods_____	26
5.2.2 Formation of Chitosan Fibers Using Gel Extrusion Technique_	27
5.2.3 Formation of Chitosan-Based Heart Valve Scaffold_____	28
5.2.4 Formation of Fiber-Reinforced chitosan-Based Disc Scaffold__	29
5.2.5 Formation of Fiber-Reinforced Chitosan-Based Heart Valve	
Scaffold_____	30
5.2.6 Covalent Immobilization of Heparin onto Chitosan Fibers and	
Formation of Reinforced Scaffolds with chitosan-Heparin	
Fibers_____	30
5.2.7 Mechanical Testing of Fibers and Fiber-Reinforced Scaffolds_	31
5.2.8 Statistical Analysis_____	31
5.3 Results_____	31
5.3.1 Porosity and Mechanical Properties of Heart Valve Scaffolds	
and Chitosan Fibers_____	31

5.3.2 Effect of Fiber Length and Fiber/Scaffold Mass Ratio on Scaffold Mechanical Properties_____	33
5.3.3 Effect of Fiber Reinforcement on Chitosan-Based Heart Valve Scaffolds_____	37
5.3.4 Partial Dissolution of Chitosan Fibers within Chitosan Scaffold_	39
5.3.5 Effect of Heparin Immobilization on Chitosan Fibers Mechanical Properties_____	40
5.3.6 Effects of Fiber Crosslinking and fiber mechanical properties on Scaffold Mechanical Properties_____	43
5.4 Discussion _____	45
5.5 Conclusions and Future Work _____	50
<b>CHAPTER SIX: IMPROVING CHITOSAN FIBER MECHANICAL PROPERTIES THROUGH PHYSICAL AND CHEMICAL TREATMENTS_____</b>	
6.1 Introduction_____	51
6.2 Experimental Work_____	53
6.2.1 Materials and Methods_____	53
6.2.2 Fabrication of Chitosan Fibers Using Polymer Fiber Extrusion Technique_____	53
6.2.3 Measurement of Fiber Diameters_____	54
6.2.4 X-Ray Diffraction (XRD) Analysis of Fiber Microstructure_____	54
6.2.5 Evaluating the Mechanical Properties of Chitosan Fibers_____	55
6.2.6 Statistical Analysis_____	55
6.3 Results_____	55



6.3.1 Effect of Acetic Acid Concentration on Chitosan Fibers	
Mechanical Properties_____	55
6.3.2 Effect of Coagulation Bath pH of Ammonia Solution on	
Chitosan Fibers Mechanical Properties_____	58
6.3.3 Effect of Drying Temperature on Chitosan Fibers Mechanical	
Properties_____	62
6.3.4 Effect of Combined Parameters on the Mechanical Properties	
of Chitosan_____	66
6.4 Discussion_____	69
6.5 Conclusions and Future Work_____	71
CHAPTER SEVEN: ISOLATION, CHARACTERIZATION AND PROLIFERATION	
OF OVINE BONE MARROW- DERIVED MESENCHYMAL STEM CELLS:	
POTENTIAL SOURCE FOR CARDIOVASCULAR TISSUE ENGINEERING	73
7.1 Introduction_____	73
7.1.1 Bone Marrow-Derived Mesenchymal Stem Cells (MSC)_	73
7.1.2 Characterization of Bone Marrow-Derived Mesenchymal Stem	
Cells_____	74
7.1.3 Bone Marrow MSCs in Tissue-Engineered Heart Valves	
Applications_____	74
7.2 Experimental Work_____	75
7.2.1 Isolation of Ovine Bone Marrow Mesenchymal Stem Cells_____	75
7.2.2 Cryopreservation of Sheep Bone Marrow Mesenchymal Stem	
Cells_____	76

7.2.3 Characterization of Bone Marrow-Derived Mesenchymal Stem Cells (MSCs)	76
7.2.4 MSCs Differentiation into Smooth Muscle Cells (SMC)	78
7.2.5 Effect of Serum Concentration on MSCs Proliferation and Attachment	79
7.2.6 Effect of Immobilized GAGS on MSCs Proliferation and Attachment	80
7.3 Results	81
7.3.1 Isolation of Ovine Bone Marrow-Derived MSCs	81
7.3.2 Characterization of MSCs	82
7.3.4 Differentiation of MSCs into Smooth Muscle Cells (SMC)	87
7.3.5 Effect of Serum Concentration on MSCs Proliferation and Attachment	91
7.3.6 MSCs Proliferation GAG-Chitosan Membranes	93
7.4 Discussion	96
7.5 Conclusions and Future Work	100
 CHAPTER EIGHT: EFFECT OF STIFFNESS OF MECHANICALLY IMPROVED CHITOSAN FIBERS ON BONE MARROW- DERIVED MESENCHYMAL STEM CELLS ATTACHMENT, VIABILITY AND PROLIFERATION	
8.1 Introduction	101
8.2 Experimental Work	102
8.2.1 Fabrication of Mechanically Improved Chitosan Fibers	102
8.2.2 MSC Culturing and Seeding	103

8.2.3 MSC Attachment and Viability on Chitosan Fibers with Different Stiffness_____	103
8.2.4 MSCs Cytoskeleton Organization on Mechanically Improved Chitosan Fibers_____	104
8.3 Results_____	105
8.3.1 MSCs Viability and Proliferation on Mechanically Improved Chitosan Fibers_____	105
8.3.2 Cytoskeleton Organization in MSCs Cultured on Mechanically Improved Chitosan Fibers_____	108
8.4 Discussion_____	110
8.5 Conclusions and Future Work_____	111
References_____	112
Abstract_____	129
Autobiographical Statement_____	131

## LIST OF FIGURES

- Figure 1: Chemical structure of chitosan repeating unit. \_\_\_\_\_ 4
- Figure 2: Repeating unit structure of GAGs. \_\_\_\_\_ 6
- Figure 3: Formation of chitosan fibers using gel extrusion technique (left) and Phase contrast image of hydrogel chitosan fibers with average diameter of ~325 $\mu$ m. Scale bar is 250  $\mu$ m. Average diameter was calculated from 40 measurements. \_\_\_\_\_ 28
- Figure 4: (A) Unigraphics® image of trileaflet heart valve mold, (B) Ventricular view of porous chitosan trileaflet heart valve scaffold showing the leaflet (L) and the cylinder (C) and (C) Aortic view of trileaflet heart valve scaffold showing the sinus (S) \_\_\_\_\_ 29
- Figure 5: Stress-strain curve of reinforced scaffold at 0.4 fiber/scaffold mass ratio and unmodified chitosan based scaffold. Reinforced scaffold had a higher strength and strain values compared to unmodified scaffolds. \_\_\_\_\_ 34
- Figure 6: Effect of fiber/scaffold mass ratio on scaffold (A) Strength and (B) Stiffness. (n=7), all values were statistically different from unmodified scaffold. \_\_\_\_\_ 35
- Figure 7: Effect of fibers length on chitosan (A) strength and (B) stiffness. \* indicate a statistical difference (p<0.05). (n=7) \_\_\_\_\_ 36
- Figure 8: Reinforced heart valve scaffold with 2mm fibers length at 1.0 fiber/scaffold mass ratio showing (A) Strength, (B) Maximum Strain and (C) Modulus of elasticity. Values were statistically different at each location between the two conditions (p<0.05). \_\_\_\_\_ 39
- Figure 9: Reinforced scaffolds with chitosan fibers. (Left) phase contrast image of transverse section of scaffold showing the embedded chitosan scaffold were present within the matrix, scale bar 250 $\mu$ m and (Right) transverse section SEM image shows porous chitosan scaffold with fibers embedded, scale bar is 100 microns \_\_\_\_\_ 40
- Figure 10: Effect of crosslinking of chitosan fibers with heparin on fibers (A) diameters, (B) strength, (C) elasticity and (D) stiffness. (n=10) \_\_\_\_\_ 43
- Figure 11: Effects of chitosan fiber and modified heparin fiber mechanical properties on scaffold (A) tensile strength and (B) modulus of elasticity. Error bars indicate standard deviation from 7 samples. Values at each mass ratio for the two

conditions were statistically different except for tensile strength at a ratio of 0.2. \_\_\_\_\_ 44

Figure 12: Effect of acetic acid (AA) concentration on chitosan fibers (A) diameters, (B) strength, (C) elasticity and (D) stiffness. \_\_\_\_\_ 58

Figure 13: Effect of coagulation bath of ammonia solution, (A) chitosan fibers diameters and (B) XRD spectra of chitosan fibers extruded in 10 or 25 wt% ammonia solutions. (\*  $p < 0.05$ ) \_\_\_\_\_ 60

Figure 14: Effect of coagulation bath ammonia solution on chitosan fibers mechanical properties, (A) fiber strength, (B) fiber elasticity and (C) fiber stiffness. \_\_\_\_\_ 62

Figure 15: Effect of drying temperature on chitosan fiber diameters \_\_\_\_\_ 63

Figure 16: XRD spectra of chitosan fibers annealed at different temperature (A) and height ratio of crystalline to amorphous peaks (B) \_\_\_\_\_ 64

Figure 17: Effect of annealing temperature on (A) chitosan fibers strength, (B) fibers elasticity and (C) fibers stiffness. \_\_\_\_\_ 66

Figure 18: Representative Stress-Strain curve of different chitosan fibers formed with combined parameters \_\_\_\_\_ 67

Figure 19: Effect of combing parameters on (A) fiber strength, (B) fiber elasticity and (C) fiber stiffness \_\_\_\_\_ 69

Figure 20: Cell attachment and morphology of MSCs at passage 0 during isolation, Objective is 10X \_\_\_\_\_ 81

Figure 21: Subculturing of MSCs up to passage 4, objective is 10X \_\_\_\_\_ 82

Figure 22: MSCs differentiation into adipocytes. Formation of oil vacuoles indicating MSCs differentiation into adipocytes at Day 20, Objective 20X \_\_\_\_\_ 83

Figure 23: Morphological changes in MSCs during their differentiation into osteocytes, Objective 20X \_\_\_\_\_ 84

Figure 24: Von Kossa and safranin-O staining at higher magnification, upper panel, and the whole culture plate, lower panel \_\_\_\_\_ 85

Figure 25: Morphological changes of MSCs during their differentiation into Chondrocytes, Objective 4X _____	86
Figure 26: H&E, Safranin-O and Masson's Trichrome staining confirm the differentiation of MSCs into chondrocytes _____	87
Figure 27: Morphological changes of MSCs during differentiation into SMCs, Objective 10X _____	88
Figure 28: $\alpha$ -SMAActin staining confirms that both MSCs cultured in growth medium or differentiation medium differentiated into SMC, Objective 20X _____	89
Figure 29: Amount of Actin production in MSC cultured in growth medium or differentiation medium _____	90
Figure 30: $\alpha$ -SMAActin staining of MSC of Passage 0 cultured in DMEM culture medium without FBS for 1 day, Objective 20X _____	90
Figure 31: Growth rate of MSC cultured for 5 days in growth medium or differentiation medium _____	91
Figure 32: Effect of serum concentration in culture medium on MSCs attachment and spreading, Objective 10X _____	92
Figure 33: Effect of Serum concentration on MSCs proliferation for 5 days culture. ____	93
Figure 34: Cell morphology of MSC cultured on different immobilized GAGs, HS (Heparan Sulfate), Hep (Heparin Sodium), C4S (Chondroitin-4-Sulfate), HA (hyaluronic Acid), Chit (Chitosan) and TCP (Tissue Culture Plate). Objective is 10X. _____	95
Figure 35: Effect of different immobilized GAGs on MSC proliferation for 8 days in static culture. _____	95
Figure 36: Stiffness for mechanically improved chitosan fiber _____	106
Figure 37: Alamar Blue results of MSC proliferation for 6 days on different fibers with different stiffness values. _____	106
Figure 38: Live/ Dead assay showing MSC attachment and viability on day 3 and 5 of culture for chitosan fibers with different stiffness values, red-dead cells and green-live cells _____	107

Figure 39: Cytoskeleton organization in MSCs on day 9 of culture when cultured on (A) Fibers dried at RT, (B) fibers dried at RT and Immobilized with Heparin, (C) Fibers annealed at 195 °C, arrow points to fluorescent chitosan fiber and (D) MSCs cultured on Tissue culture plate, red: f-actin, blue: nucleus, Objective 20X. \_\_\_\_\_ 109

## LIST OF TABLES

Table 1: Pore size of heart valve scaffold at different locations _____	32
Table 2: Mechanical properties of chitosan fibers and chitosan based scaffolds _____	32
Table 3: Mechanical properties of chitosan based heart valve scaffold compared to human pulmonary and aortic valves _____	33



## CHAPTER ONE

### INTRODUCTION

Current mechanical and biological replacements lack the ability to grow and remodel with the patient, a limitation that hinders their use in pediatric patients to replace the defective aortic or pulmonary valves. Tissue engineered heart valve is a promising approach to address current problems associated with mechanical and biological valves and provide a suitable valve replacement to pediatric patients. However, tissue engineered heart valve scaffolds made of chitosan, collagen or fibrin still lack the mechanical integrity and the structural maturity to withstand the hemodynamic environment in the heart. Additionally, cell type and source are still among the major issues that greatly affect the cell proliferation and the interaction with the biomaterial.

Chitosan has been used extensively for many tissue engineering applications. However, like many other hydrogel polymers, chitosan has many attractive biological and biocompatibility properties but modest mechanical properties which limit its use in load-bearing tissue engineering applications.

MSCs isolated from bone marrow are an attractive promising source in the field of tissue engineering and regenerative medicine. Their use in new cell-based therapeutic strategies such as mesenchyme-derived tissue repair showed a great hope to expand their use so far.

The main focus of this research study is to improve the mechanical properties of chitosan-based heart valve scaffold and to utilize bone marrow-derived mesenchymal

stem cells (MSCs) for cardiovascular tissue engineering applications. The driving hypothesis for this research study is that ***improving the mechanical properties of a chitosan-based heart valve scaffold to comparable heart valve properties will improve the bone marrow–derived mesenchymal stem proliferation and direct their differentiation into heart valve cells.***

The specific aims of this study are:

- (1) To evaluate the mechanical properties of chitosan scaffolds and chitosan fibers and then to evaluate the effectiveness of chitosan fibers reinforcement as a method for enhancing the mechanical properties of chitosan-based heart valve scaffolds. The working hypothesis for this aim is that ***embedding chitosan fibers within chitosan-based scaffold will improve its mechanical properties.***
- (2) To evaluate the effect of various physical and chemical modifications on chitosan fibers to further improve their mechanical properties and test modified fiber biocompatibility for tissue engineering applications. The working hypothesis for this aim is ***that improving the mechanical properties through physical and chemical modifications will further improve the mechanical properties of chitosan-based scaffolds.***
- (3) To isolate, characterize and utilize ovine bone marrow-derived mesenchymal stem cells for cardiovascular tissue engineering applications.
- (4) To evaluate the effect of different immobilized GAGs on MSCs morphology, attachment, spreading and proliferation. The working hypothesis for this aim is that ***immobilized GAGs on chitosan substrates will modulate growth factors and bind matrix proteins to improve MSCs attachment and proliferation.***

- (5) To evaluate the effect of chitosan fibers stiffness on MSCs attachment, spreading and proliferation. The working hypothesis for this aim is that ***improving the matrix stiffness will improve MSCs proliferation and direct their differentiation into heart valve-like cells.***

## CHAPTER TWO

## CHITOSAN AND GLYCOSAMINOGLYCANS IN TISSUE ENGINEERING

## APPLICATIONS

## 2.1 Chitosan

Chitosan is a semicrystalline polysaccharide that is formed by repeating units of N-acetyl-D-glucosamine and D-glucosamine (Madihally and Matthew, 1999). The degree of crystallinity is highly depended on the degree of deacetylation, while the rate of degradation is dependent on the degree of deacetylation. Chitosan is insoluble in most organic solvents in addition to water, however, it is soluble in dilute acid solutions ( $\text{pH} < 5$ ). Its Molecular weight ranges between 100 kDa and 1000 kDa.

Chitosan has been shown to be useful biomaterial in many tissue engineering applications such as a wound dressing material (Kratz *et al.*, 1997) and drug delivery vehicle (Aiedeh *et al.*, 1997). It has many attractive biodegradable, biocompatible, non-antigenic, non-toxic and bio-functional properties which expanded its use in different tissue engineering applications (Madihally and Matthew, 1999; VandeVord *et al.*, 2002). Figure 1 shows the chemical structure of a repeating unit in a chitosan molecule.

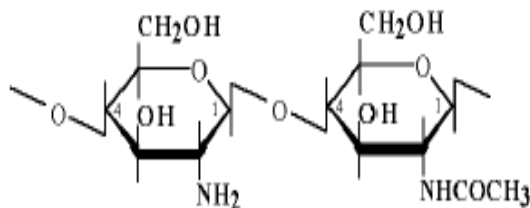
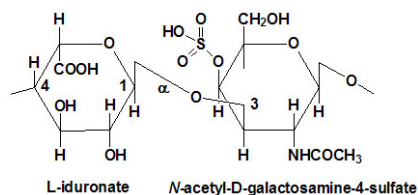
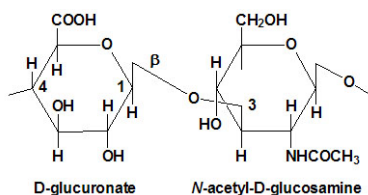


Figure 1: Chemical structure of chitosan repeating unit.

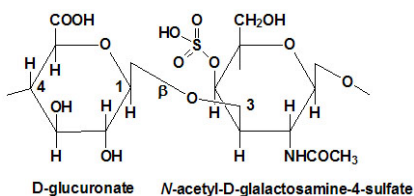
## 2.2 Glycosaminoglycans (GAGs)

Glycosaminoglycans (GAGs) are highly sulfated heteropolysaccharide, which have acidic sulfate and/or carboxyl groups. GAGs are covalently bound to core proteins forming macromolecules called proteoglycans (Lindahl and Hook, 1978). They are found on the cell surface or in the extracellular matrices. GAGs are negatively charged macromolecules that can be immobilized on different surfaces including chitosan substrates (Chupa *et al.*, 2000). Proteoglycans plays a key role as tissue organizers, influence cell growth and the maturation of specialized tissues and modulate growth-factor activities (Madihally *et al.*, 1999; Matthews *et al.*, 2000; Cho *et al.*, 2008).

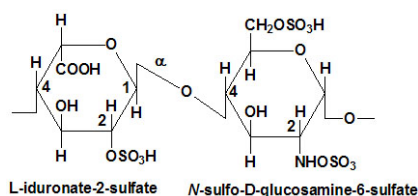
The six major types of GAGs according to their structure of repeating disaccharide units are: hyaluronic acid (HA), dermatan sulfate (DS), chondroitin sulfate (CS), heparin sodium (Hep), heparan sulfate (HS) and Keratan sulfate (KS). All GAGs have a sulfate group and covalently attached to proteins as protoglycans except HA. Heparin is the most highly sulfated GAG and possesses the highest molecular charge density.



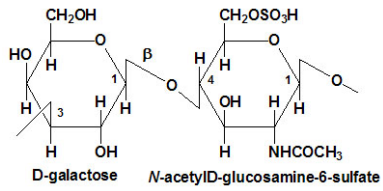
### Hyaluronic Acid (HA)



### Dermatan Sulfate (DS)



**Chondroitin 4- and 6-sulfates (C-4-S Heparin and Heparan sulfates(HS) and C-6-S)**



**Keratan Sulfates(KS)**

Figure 2: Repeating unit structure of GAGs.

## CHAPTER THREE

### HEART VALVE DISEASES AND TISSUE ENGINEERED HEART VALVES

#### 3.1 Significance of Heart Valve Diseases in Pediatrics

Congenital heart defects are the leading cause of mortality in pediatrics around the globe as they are the most common type of birth defects. 8 of every 1,000 newborns are affected by heart defects. In the United States alone, more than 35,000 babies are born with one or more congenital heart defects ranging from mild to severe defects. 7,000 babies are born with severe heart defects in the aortic or pulmonary valve (Flanagan and Pandit, 2003; Zimmermann and Eschenhagen, 2003; Neuenschwander and Hoerstrup, 2004; Sarkar *et al.*, 2007; Akhtar and Ahmed, 2008; Filova *et al.*, 2009).

Congenital heart defects include: (1) atrial septal defects where a hole is present in septum between the two atria allowing the mixing of the oxygenated and the deoxygenated blood between the two sides of the heart, (2) aortic stenosis which refers to an obstruction to blood flow between the left ventricle and the aorta. The causes of this obstruction can result from a muscular obstruction below the aortic valve, obstruction at the aortic valve itself or an immediate narrowing above the aortic valve. However, the most common aortic stenosis is the obstruction at the valve itself termed as aortic valvar stenosis.

Bicuspid aortic valve (BAV) is the most common abnormality that occurs to the aortic valve when two leaflets are existed instead of three leaflets. The leaflets in BAV are often less pliable and more thickened and the lines of separation between the leaflets (i.e. commissures) are fused together to compensate the loss of the third leaflet.

The aortic valve in this case would not open and close freely. To compensate the malfunction of the aortic valve, the left ventricle should provide extra force to eject the blood into the aorta, which often results in ventricular hypertrophy as a result of ventricular muscle thickening. In severe aortic valve obstruction where ventricular muscle is unable to compensate adequately, patients may develop cardiac failure, which is a common case in newborn infants.

Newborn babies with severe aortic stenosis usually develop cardiac failure in the first few days of life which necessitates an instant treatment by either balloon dilation of the valve or surgery. Balloon dilation valvuloplasty is usually completed at the time of catheterization through the umbilical artery for newborns (Filova *et al.*, 2009). Surgical valvotomy or open heart procedure is used when simple balloon dilation is not sufficient. This procedure involves the opening of the valve along the lines of commissures. Complete surgical aortic valve replacement will be necessary when aortic valve is obstructed by severe calcium deposits in the leaflets or when the valve ring is small and underdeveloped. Ross procedure for aortic valve replacement is commonly used to replace the defective aortic valve with the patient's own pulmonary valve where the pulmonary valve will be replaced with a homograft valve (i.e. human donor valve). The main advantage of this procedure is that the replaced aortic valve continues to grow with the child. However, the availability of a donor pulmonary valve and immune system rejection are some of the major hindrances for this approach.

The implantation of a mechanical or biological valve in the aortic valve place is traditionally used when no donor valves are available for immediate implantation. In 2003, the number of patients who required heart valve transplantation was 295,000



patients (Filova *et al.*, 2009). This number is expected to reach 850,000 patients by 2050 (Yacoub and Takkenberg, 2005). Current heart valve replacements use mechanical valves in 60% of the replacement cases while biological valves are used in remaining 40% of replacement cases (Mol and Hoerstrup, 2004).

## **3.2 Current Treatments of Defective Aortic Heart Valve**

### **3.2.1 Mechanical Valves**

Mechanical valve is a non physiological design that resides in close contact with the blood resulted in causing turbulent blood flow. The use of these valves requires a lifetime of anticoagulation therapy. Due to the modest lifespan of these valves, that is 15 years, they are mainly used in adults patients.

Mechanical valves lack the ability to grow with the patient which limits their use in pediatric patients. Hemolysis and platelet activations are some of the main side effects that result from the turbulent blood flow. Apart from this, problems in fertile females may occur due to embryo-toxicity of warfarin and other substances used in anticoagulation therapies (Neuenschwander and Hoerstrup, 2004).

### **3.2.2 Biological Valves**

Biological valves (xenografts and autografts) have been used in parallel with the mechanical valves over the past decades to treat the defective valves. These valves do not require lifetime anticoagulation; however, they have limited durability due to calcification which shortens their life span to 10 years.

Heterografts valves are decellularized valves which are usually obtained from different species, yet they lack the ability to remodel or grow with patient. These valves have also been shown to have inadequate mechanical properties and immunological concerns (Filova *et al.*, 2009). With all the aforementioned problems, biological valves are not a practical alternative to replace heart valves in newborn patients.

### **3.3 Tissue Engineered Heart Valve Approach**

Replacing the defective heart valve in infants is quite different and far more challenging problem as oppose to adults patients. The replaced valve should be viable, able to grow, remodel and perform its function adequately for a longer period of time. The ultimate goal of all tissue engineered heart valves (TEHV) is to seed cells onto a biodegradable scaffold and transplant it instead of the defective valve. The scaffold is expected to provide adequate amount of mechanical strength to stimulate the growth of new tissue. This scaffold then becomes part of patient's tissue and restores the natural function of the valve after certain amount of time.

Despite the significant research efforts that have been conducted over the past decade to produce optimal TEHV (Shinoka *et al.*, 1995; Niklason and Langer, 1997; Steinhoff *et al.*, 2000; Flanagan and Pandit, 2003; Zimmermann and Eschenhagen, 2003; Neuenschwander and Hoerstrup, 2004; Sarkar *et al.*, 2007), some of these trials using either synthetic or natural scaffolds were limited by the structural immaturity and the inadequate mechanical properties (Hoerstrup *et al.*, 2000). Researchers have investigated different approaches to improve the mechanical properties of synthetic scaffolds mainly. The majority of these approaches focused on materials

characterizations of scaffolds and/or mechanical conditioning of scaffolds via static and dynamic culturing (Flanagan and Pandit, 2003; Engelmayer *et al.*, 2005).

### **3.4 Parameters Affecting the Tissue Engineered Heart Valve Function**

Despite the wide range of investigated scaffolds as extracellular matrix (ECM) templates for TEHV, current scaffolds still lack the mechanical integrity and the structural maturity to withstand the hemodynamic environment in the heart (Hoerstrup *et al.*, 2000; Sodian *et al.*, 2000; Sodian *et al.*, 2000; Sodian *et al.*, 2000; Sodian *et al.*, 2006). The following sections will focus on the studied parameters that greatly affect the mechanical properties of heart valves scaffolds.

#### **3.4.1 Scaffold Materials**

##### **3.4.1.1 Decellularized Heart Valves Scaffolds**

Using detergents and enzymes, Wilson *et al* (Wilson *et al.*, 1995) developed a protocol in 1995 to decellularize canine heart valves. They removed most of cell membranes, lipids, nucleic acids and the soluble matrix molecules. The amount of collagen and elastin remained in the ECM was suitable to recellularize the valve. Nearly one month after implantation, histology analysis showed no inflammatory response, fractional valvular interstitial cells (VIC) penetration at the valve base and partial endothelial cells formation. However, this study did not provide any long term calcification studies or mechanical properties evaluation.

Bader and colleagues in 1998 (Bader *et al.*, 1998) decellularized porcine aortic valve and reseeded it with human endothelial cells and implanted it again. Their results

demonstrated that there was no evidence of cell throughout the thickness of the leaflet. Collagen formation was comparable to native valve with wavelike structure, however, the presence of huge interfibrillar space was significant, which could explain the low mechanical properties obtained.

In 2000, Steinhoff *et al* (Steinhoff *et al.*, 2000) acellularized sheep heart valve and then reseeded it with myofibroblasts for six days and then with endothelial cells for two days. Acellularized and reseeded valves were then implanted in a sheep model. For three months, the reseeded valves and the acellularized valves showed normal function. However, after that, the acellularized valves showed partial degradation and no new tissue formation, while the reseeded valves showed confluent endothelial surface, myofibroblasts, and collagen I. Histological analysis showed inflammatory response led to calcification. Additionally, leaflet thickness increased which caused a valve stenosis limiting the free opening and closing of the valve.

SynerGraft™ valve is a commercial decellularised valve available through CryoLife Incorporation in the US. human studies showed early failure of the valve within the first year of implantation due to structural failure and/or rapid deterioration (Simon *et al.*, 2003).

#### **3.4.1.2 Natural Polymers Heart Valve Scaffolds**

Among the most two investigated natural scaffolds for TEHV are fibrin gel and collagen (Ye *et al.*, 2000; Jockenhoevel *et al.*, 2001; Grassl *et al.*, 2002; Neidert *et al.*, 2002; Tschoeke *et al.*, 2009; Koch *et al.*, 2010). Fibrin gel is a biodegradable polymer that can be produced easily and quickly from blood. Fibrin gel has many attractive properties which make it a good candidate for heart valve scaffolds. Fabrication of fibrin

gel scaffold from patient's blood is an easy process and eliminates any risk of immunological rejection. The degradation rate of this scaffold can be easily controlled. Also homogenous distribution of cells can be achieved when manufacturing scaffold (cell/fibrin tissue structure) (Jockenhoevel *et al.*, 2001; Flanagan and Pandit, 2003; Zhou *et al.*, 2006; Sarkar *et al.*, 2007). However, when fibrin gel structure was used to fabricate trileaflet scaffold, the mechanical properties of the structure were not adequate for implantation (Ye *et al.*, 2000).

Collagen was investigated to fabricate heart valve scaffolds (Chevallay and Herbage, 2000; Rothenburger *et al.*, 2001; Taylor *et al.*, 2002); however collagen scaffolds were shown to be very weak and require Dacron mesh to strengthen them. Additionally, collagen scaffolds have been shown to perform poorly over contraction which reduces the matrix permeability (Lewus and Nauman, 2005; Sarkar *et al.*, 2007).

#### **3.4.1.3 Synthetic Polymers Heart Valve Scaffolds**

Polyglycolic acid (PGA), polylactic acid (PLA), and their copolymers (PGLA) are among the most synthetic polymers that have been investigated extensively in fabricating TEHV (Flanagan and Pandit, 2003; Sarkar *et al.*, 2007). The first use of PGA was in 1995 by Shinoka *et al.* (Shinoka *et al.*, 1995; Shinoka *et al.*, 1996). They fabricated a single leaflet made of PGLA woven mesh sandwiched between two nonwoven PGA meshes. The leaflet was seeded with myofibroblasts and then with endothelial cells; thereafter, the leaflet was implanted in an ovine model at the pulmonary valve position. Their results after six weeks demonstrated cellular distribution, new tissue formation, elastin and collagen production and mechanical properties similar to the native leaflet. However, infections and inflammatory responses

in animals were observed. The histological analysis showed that the leaflet was immalleable to function due to the high initial stiffness and thickness of composite PLA/PGA polymers.

Sodian *et al* in 2000 (Sodian *et al.*, 2000) choose polyhydroxyoctanoate (PHO) to be part of composite valve scaffold. Four different materials were used to fabricate the valve scaffold: nonporous film of PHO was used in the wall sandwiched between two layers of nonwoven PGA, the leaflet made out of single layer of porous PHO, polydioxanone sutures used to suture the leaflet to the wall. Histological analysis showed organized tissue formation and significant amount of collagen. However, formation of elastin was absent. After 24 weeks, degradation analysis showed that the scaffold was still in the conduit and did not degrade, which suggests longer degradation time than PGA. This might lead to tissue reaction in the future. Another limitation of this study is that it was implanted at low pressure profile.

Another study by Sodian *et al* in 2000 (Sodian *et al.*, 2000), incorporated the use of PHO with PGA to fabricate trileaflet scaffold. Scaffold was seeded with myofibroblasts and endothelial cells and implanted in ovine model for 17 weeks. All valves performed properly upon opening and closing. Although smooth blood flow was observed and collagen and GAGs were deposited, elastin was absent. Additionally, there was no formation of endothelial layer which could limit the durability of this scaffold.

Poly-4-hydroxybutyrate (P4HB) was evaluated as a composite scaffold with PGA by Mol and colleagues in 2006 (Mol *et al.*, 2006; Schmidt *et al.*, 2006). Trileaflet scaffold was fabricated using the composite material and seeded with myofibroblasts and

endothelial cells, and then cultured in a bioreactor for 14 days, and then implanted in ovine model for 20 weeks. The scaffolds showed uniformly and organized formation of new tissue characterized by the formation of collagen and a loose layer of elastin and GAGs. However the valves showed mild to moderate stenosis at 20 weeks *in vivo* with partial formation of endothelial cell at the leaflet surface.

### 3.4.2 Static and Dynamic Culturing of Scaffolds

TEHV bioreactors are used in which the *in vivo* biomechanical and biochemical conditions are mimicked *in vitro* to produce a functional tissue development (Barron *et al.*, 2003; Freed *et al.*, 2006). These conditions include: the opening and the closing behavior of the valve at 1Hz frequency, flow rate, pressure and shear stress.

Barron *et al* (Barron *et al.*, 2003) suggested that culturing tissue-engineered heart valves in an initial low shear stress with exposure the developing tissue to physical stimulus is advantageous for initial tissue development. The design and the use of bioreactors in tissue-engineered heart valves greatly vary depending on the application and the desired goals. Heart valve bioreactors are used *in vitro* before implantation to improve cell seeding efficiency, cell proliferation and penetration within the scaffold, the production of ECM components and the mechanical properties of the scaffold to withstand the real hemodynamic environment *in vivo* (Unsworth and Lelkes, 1998; Hoerstrup *et al.*, 2000; Gulbins *et al.*, 2005; Mol *et al.*, 2006; Sodian *et al.*, 2006).

The effect of time and flow rate of tissue-engineered heart valves constructs that are cultured in a bioreactor is still not fully understood. To better understand this major effect, Mol and colleagues (Mol *et al.*, 2006) cultured polyglycolic acid (PGA) heart valves scaffolds coated with Poly-4hydroxybutyrate (P4HB) in two different diastolic

pulse duplicator (DPD) bioreactors for 4 weeks. The first set of scaffolds was cultured in dynamic bioreactor by varying the pressure from 5-30 mmHg. The second set was cultured in a static bioreactor under constant flow rate (4ml/min). To mimic the opening and the closing of the aortic heart valve, they applied a dynamic pressure gradient over the valve (1Hz). After four weeks, their results showed that the valve constructs that were cultured in dynamic bioreactor have significantly higher GAGs production and improved mechanical properties in the radial direction only than the static bioreactor or control cultured flasks, whereas the collagen production increased significantly with the use of dynamic bioreactor to be comparable to the native valve, but was lower than the static bioreactor. The effect of the culturing time was also one of the major goals for this study. They realized that the collagen and GAGs production increased over the time up to four weeks and were stable thereafter. The effect of culturing time significantly improved the biomechanical properties to be comparable to the native aortic valve in the radial direction only again in the radial direction but not in the circumferential direction. The opening of the valve was optimal, while the closing of the valve was suboptimal where the valve did not form a tight sealing. The absence of elastin formation proved by histology analysis of scaffolds after four weeks of culturing in a dynamic bioreactor was a major cause of tissue creep. So, even though this study is considered as one of the most comprehensive studies conducted recently to fully understand the effect of the bioreactor on many tissue properties, still more comprehensive studies are needed in this field to optimize the most advantageous culture time and pressure for new tissue formation *in vitro* before implantation.



Few studies have been conducted so far to optimize the optimal flow/pressure profile that helps the formation of neo-tissue. To address the problem of low flow rate profile, Lichtenberg and colleagues (Lichtenberg *et al.*, 2006) in 2005 seeded decellularized ovine pulmonary heart valves with endothelial cells under simulated physiological conditions for two days. The initial flow was 0.1L/min, and then gradually increased 0.3L/min/day up to 2L/min with a cycle rate of 60beats/min as a way to mimic the fetal development of the heart valves, with keeping pH, gases levels (CO<sub>2</sub> and O<sub>2</sub>), glucose, and lactate at constant natural levels. Their results demonstrated that a monolayer of endothelial cells covered the inner valve surface after seven days for eight constructs that were cultured in a dynamic bioreactor. The biomechanical properties revealed comparable values to the native valve tissue in both radial and circumferential directions. The production of ECM components (collagen, elastin, and GAGs) was comparable to the native valve. Stable cell-matrix connection was achieved by an initial low pressure with a gradual increase. This study was the first to demonstrate that a biological scaffold showed evidence of sufficient stability under high flow rate. This study also proved the importance of continuous adjustment of the physiological parameters and the bioreactors design according to the type of scaffolds (synthetic or biological), and cell type and/or source to improve heart valve results. Despite the fact that this study was the first study to have analogous results to the native valve tissue in all aspects, long-term animal studies should convey comparable results to be able to move this success to clinical human studies in the near future.

In some previous studies, specifically with synthetic scaffolds, it was found that tissue-engineered heart valves had inadequate mechanical strength or functional

performance (Hoerstrup *et al.*, 2002; Tang *et al.*, 2005) . A hypothesis has been proposed by Hoerstrup and colleagues (Hoerstrup *et al.*, 2002) that growing tissue constructs in a biomimetic bioreactor would produce more mature heart valve constructs with more favorable performance *in vivo*. So, to evaluate the effect of bioreactor on tissue formation of scaffolds conditioned *in vitro* before implantation, Hoerstrup and his colleagues (Hoerstrup *et al.*, 2000) grew PGA scaffolds coated with P4HB seeded with endothelial cells *in vitro* by culturing them in a diastolic pulse duplicator for 14 days by varying the pressure-flow rate from 30mmHg (70ml/min) up to 55mmHg (125ml/min), and then implanted them at the pulmonary valve in six animal models for 20 weeks as proposed previously in literature for complete remodeling. Their results for scaffolds before implantation showed synchronous opening and closing of the valves in the bioreactor under low pressure (35mmHg) and high pressure (>150mmHg). Tissue analysis after 14 days of culturing in the bioreactor showed dense fibrous tissue near to the surface of the leaflet, while it was loose near to the central core compared to loose and poorly organized tissue in the static control. They also demonstrated that the amount of collagen, GAGs, and DNA were higher than the control at day 14 of culturing and comparable to the native heart valve values, while the elastin was not detectable in any leaflets. Suture retention strength was significantly higher when compared to the static control. *In vivo* studies at 16 and 20 weeks showed that the leaflet had a loose spongy layer on the ventricular side (inflow), while a fibrous layer was formed on the arterial flow (outflow) side. Collagen in the fibrous layer and GAGs in the central core were detectable at 20 weeks, where elastin was only detectable near the inflow surface after 6 weeks. Mechanical testing showed a comparable stress-strain behavior and

values between the tissue-engineered valves and the native one. Despite all of those promising results, regurgitation was present at 16 and 20 weeks due to the noncoaptation of valve as a result of scaffold shrinkage during of scaffold degradation. This issue can be compensated by optimizing the design of the scaffold to initially increase the coaptive area of the leaflets and by optimizing the ideal time between the implantation and the degradation of the scaffold. These results are just preliminary results and should be extended more in terms of the number of implanted valves and the implantation time.

## CHAPTER FOUR

### ADVANCES IN BONE MARROW- DERIVED MESENCHYMAL STEM CELLS FOR CARDIOVASCULAR TISSUE ENGINEERING

#### 4.1 Isolation of Mesenchymal Stem Cells (MSCs) From Bone Marrow

Human mesenchymal stem cells (hMSCs) were discovered by Friedenstein in 1970's (Miao *et al.*, 2006). hMSCs are present in adult bone marrow are believed to be multipotents cells (Pittenger *et al.*, 1999). hMSCs have the ability to replicate as undifferentiated cells and differentiate to various mesenchymal tissue lineages such as bone, cartilage, fat, tendon, muscle and marrow stroma (Rebelatto *et al.*, 2008). Upon isolation and culturing, MSCs displayed a stable phenotype and grew as a monolayer in vitro. Several studies have shown that MSCs possess the ability to exclusively differentiate upon induction into adipogenic, osteogenic and chondrogenic lineages (Pittenger *et al.*, 1999; Sutherland *et al.*, 2005; Rebelatto *et al.*, 2008).

#### 4.2 Bone Marrow MSCs in Tissue-Engineered Heart Valves Applications

MSCs can be easily isolated from the bone marrow in animals and humans. Possible locations in humans and animals are iliac crest, femur and sternum. MSCs can be phenotypically converted into endothelial cells (EC) in vitro (Song *et al.*, 2007). MSCs can also provide a source for fibroblasts/ myofibroblasts and smooth muscle cells (SMC) (Song *et al.*, 2007; Kurpinski *et al.*, 2010; Song *et al.*, 2010). Recent research efforts investigated the potential of bone marrow MSCs to differentiate when seeded on synthetic heart valve scaffolds (Sutherland *et al.*, 2005). MSCs isolated from bone

marrow were seeded PGA/PLLA nonwoven meshes semilunar heart valve scaffolds and statically cultured for 4 weeks and then implanted at the pulmonary position into sheep for 8 months. At the end of the study, MSCs showed the ability to differentiate into SMC, EC and fibroblasts. The results also showed that histological structure similar to the native heart valve was obtained.

Another research effort investigated the seeding of MSCs isolated from bone marrow on PGA/ P4HB composite heart valve scaffolds (Perry *et al.*, 2003). Scaffolds were cultured for 1 week statically and then transferred to pulse duplicator bioreactor for 2 weeks. The preliminary results showed patchy surface confluency of cells and deep cellular material. However, the study did not perform immunohistochemistry to determine the type of the cells covered and penetrated the surface. Biomechanical testing showed that the leaflets had a comparable stiffness to the native heart valve.

#### **4.3 Effect of Mechanical stimulations on Bone Marrow-Derived MSCs Differentiation and Proliferations**

In addition to the biochemical stimulations that control MSCs proliferation and differentiation, biomechanical stimulations (i.e. dynamic culturing) are believed to be important for controlling MSCs behavior. Several studies have shown previously that culturing heart valves in a dynamic environment has greatly influenced cell proliferation and ECM deposition (Hoerstrup *et al.*, 2002). However, optimal dynamic conditions are still unknown and need further investigations.

Recently, a study revealed that cyclic flexure and laminar flow accelerates the tissue formation of MSCs seeded that are on scaffold (Engelmayer *et al.*, 2006). The Study aimed to determine the appropriate mechanical stimuli for MSCs cultivation. The

independent and coupled effects of two main physiological mechanical stimuli that affect the heart valves function were studied-Cyclic flexure and laminar flow (i.e. shear stress). MSCs were isolated from sheep bone marrow and seeded onto rectangular strips of nonwoven 50:50 blend PGA/PLLA and statically cultured for 4 days. After the static culture, the scaffolds were loaded into flex-stretch-flow bioreactor. 4 groups were studied; static, cyclic flexure laminar and flex-flow and incubated for 1 and 3 weeks. The results showed that by 3 weeks, flex-flow group showed a dramatic accelerated tissue formation compared to all other groups. The new tissue formation was determined by higher collagen formation and scaffold stiffness.

#### **4.4 Effect of Scaffold Matrix Components on Bone Marrow-Derived MSCs Differentiation and Proliferation**

A recent study showed that scaffold matrix greatly influences the behavior of seeded MSCs on heart valve leaflets (Iop *et al.*, 2009). Human bone marrow MSCs were isolated and seeded statically on decellularized porcine and human heart valve leaflets in culture plates for 30 days. The cells were seeded onto fibrosa or ventricularis leaflets. The results showed that both human and porcine valves showed no histopathological features. On the contrary, both valves reconstructed endothelium lining and fibroblasts, myofibroblasts and SMCs were presents as in the corresponding valve. Also the results revealed that porcine and human valves behaved differently where human valve showed more spreading and differentiation indicating that the matrix-cell source influenced the behavior of the MSCs. Also, with respect to the human valve, the results showed also that MSC spreading, differentiations, enhanced cell survivals and colonization were higher in the ventricularis than the fibrosa. This

suggests that MSC phenotypic conversion is influenced in vitro by the anisotropic properties of the heart valve.

The signal transduction of the cell-matrix interaction has been shown recently to influence the differentiation of MSCs into SMCs (Suzuki *et al.*, 2010). MSCs cultured on dishes that were coated with laminin, collagen IV and fibronectin for 7 days. Also MSCs were seeded on biodegradable scaffold coated with laminin and implanted into rat subcutaneous space. Results showed that MSCs numbers increased on collagen dishes. Dishes coated with laminin showed higher expression of  $\alpha$ -smooth muscle actin and calponin than other culture dishes. In vivo studies showed that fully differentiated MSCs into SMCs were confirmed by the expression of smooth muscle marker (SM2) within 2 weeks.

## CHAPTER FIVE

### REINFORCING CHITOSAN-BASED HEART VALVE SCAFFOLD USING CHITOSAN FIBERS

#### 5.1 Introduction

In tissue engineering, scaffolds serve as a biological and mechanical support for cell growth and functionality. Appropriate selection of cells and scaffold is required to produce an effective tissue engineered construct. Recent studies have demonstrated a strong correlation between scaffold strength and/or stiffness and cell behavior (Dikovsky *et al.*, 2008; Dado and Levenberg, 2009). It has also been shown that scaffold stiffness influences the differentiation of mesenchymal stem cells (MSCs) to specialized cell types (Engler *et al.*, 2004; Engler *et al.*, 2006). However, attaining appropriate mechanical properties in scaffolds is still a challenge in general, and in heart valve scaffolds in particular (Hoerstrup *et al.*, 2000).

Natural polymers such as collagen and fibrin have been investigated as potential scaffolds for cardiovascular tissue engineering due to the high strength they impart (Ikari *et al.*, 2000; Ye *et al.*, 2000; Lewus and Nauman, 2005; Sarkar *et al.*, 2007). However, collagen-based scaffold were very weak and required a Dacron mesh to provide initial strength to prevent rupture at very low pressure of <10 mmHg (Weinberg and Bell, 1986). With incorporating two Dacron meshes, burst pressure increased up to 180 mmHg but usually failed through the development of pinhole leak. Fibrin gel was used to fabricate a trileaflet heart valve and seeded with myofibroblasts (Jockenhoevel



*et al.*, 2001). Despite that the mechanical integrity of fibrin gel model was enough to withstand the suturing; it was insufficient for direct implantation.

Chitosan is a natural polymer that has low to moderate mechanical properties that limit its use in load-bearing tissue engineering applications such as heart valves and large blood vessel constructs. In contrast to natural polymers, synthetic polymers have more controllable mechanical properties (Flanagan and Pandit, 2003). However, high initial mechanical properties for some synthetic polymers such as polyglycolic acid (PGA) have been proved to be immalleable to function as a flexible valve leaflet structure (Shinoka *et al.*, 1995). This inflexibility in valve structure prevents proper opening and tight closing of engineered valve leaflets (Shinoka *et al.*, 1995; Shinoka *et al.*, 1996). Hence, controlling the mechanical properties of scaffolds independent of changes in scaffold chemistry, degradation rate and biocompatibility is still a significant challenge.

The reinforcement of weak scaffolds with fibers through natural or synthetic fibers has been investigated previously (Weinberg and Bell, 1986; Li *et al.*, 2006; Li *et al.*, 2006). It was shown that increasing the number of Dacron meshes used to reinforce collagen gel improved the burst strength of the scaffold (Weinberg and Bell, 1986). Li and colleagues (Li *et al.*, 2006) used chitin fibers to reinforce collagen-based scaffolds and demonstrated improvement in the mechanical properties of the reinforced scaffold. Recently, the same group investigated the use of chitin fibers to reinforce poly (L-Lactic Acid) (PLLA) scaffolds (Li *et al.*, 2009). They showed that reinforced scaffolds had better cell attachment, proliferation, differentiation and mineralization compared to unmodified PLLA scaffolds. Wang and colleagues produced a nano-fibrous PLLA

scaffold through a thermally-induced phase separation method (Wang *et al.*, 2009). The scaffold was then reinforced with chitosan fibers dispersed within the solution ultrasonically. Although, this study utilized chitosan fibers as a reinforcement method, detailed investigation on the effects of mechanical properties of fibers or fiber dimensions have not been explored. Moreover, the study has evaluated the compressive modulus for dry chitosan samples only. A more realistic approach would be to evaluate the mechanical properties of the scaffold in the wet state since wet scaffolds are known to behave differently due to the lower mechanical properties caused by swelling. Moreover, fiber dimensions and mechanical properties should be studied first to understand their effect on fiber-reinforced scaffold.

This study seeks to fabricate a mechanically viable chitosan-based tissue engineered heart valve construct. In an attempt to improve the mechanical properties of the chitosan-based scaffold, the effectiveness of reinforcing the chitosan scaffold with chitosan fibers was investigated. The main goal of this study is to evaluate the effectiveness of fiber-reinforced approach to improve the mechanical properties of chitosan-based scaffolds. The working hypothesis is that ***embedding chitosan fibers within a chitosan heart valve scaffold would improve its mechanical properties.*** In this study, effects of fiber length, fiber/scaffold mass ratio and heparin modification of fibers on the mechanical properties of porous chitosan scaffolds were investigated.

## 5.2 Experimental Work

### 5.2.1 Materials and Methods

Heparin sodium USP (average molecular weight 10-12 KDa) was purchased from Celsus Laboratories (Cincinnati, OH). High molecular weight and medium

molecular weight (HMW& MMW) chitosan from crab shells (MW of 450 KDa and 190-310 KDa respectively, 75-85% degree of deacetylation) and 1-ethyl-3-(3-dimethylaminopropyl)-carbodiimide (EDC) were purchased from Sigma-Aldrich (St. Louis, MO). All other chemicals and solvents were of analytical reagent grade.

### **5.2.2 Formation of Chitosan Fibers Using Gel Extrusion Technique**

Chitosan fibers were formed by gel extrusion technique. Briefly, high molecular weight (HMW) chitosan was dissolved in 0.2 M acetic acid and stirred for 6 hours to form a 1.5 wt% solution. Due to hardware limitation, a 26-gauge Teflon catheter was used to extrude the solution. The solution was then extruded through the 26-gauge (internal diameter 0.45 mm) Teflon catheter directly into 10 wt% ammonia solution using a syringe pump at a rate of 85 ml/hr as shown in Figure 3. Fibers were left for 15 minutes in the ammonia solution to neutralize. After neutralization, hydrogel chitosan fibers were then air-dried under tension at room temperature.

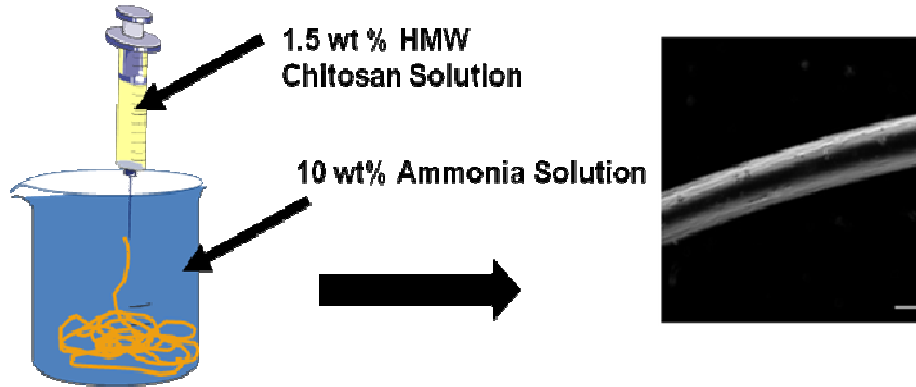


Figure 3: Formation of chitosan fibers using gel extrusion technique (left) and Phase contrast image of hydrogel chitosan fibers with average diameter of  $\sim 325\mu\text{m}$ . Scale bar is  $250\mu\text{m}$ . Average diameter was calculated from 40 measurements.

### 5.2.3 Formation of Chitosan-Based Heart Valve.

Unigraphics NX computer aided design software (Siemens Aktiengesellschaft, Munich, Germany) was used to generate a model of a heart valve prosthesis based on published physiological measurements by Mano Thubrikar and others (Thubrikar, 1990; Jockenhoevel *et al.*, 2001) . The model consisted of a hollow cylinder containing three valve leaflets in the closed and open leaflets positions (Figure 4 A). The valve model was converted to a model of a negative mold and the mold was fabricated in silicone elastomer using a commercial rapid prototyping service. Porous chitosan heart valve scaffolds were fabricated by filling the silicone trileaflet mold with 6 ml of 2 wt% medium molecular weight (MMW) chitosan dissolved in 1 vol% acetic acid. Freezing was initiated by application of liquid nitrogen to the ventricular side of the mold leaflet surface for 5 minutes followed by immersion of the entire mold in a dry ice-isopropanol bath for 3 hours. Freezing with liquid nitrogen produces smaller pore size compared to freezing in dry ice isopropanol. With this freezing approach, aortic side will have bigger pore size

allowing the cells to be entrapped at the ventricular side which has smaller pore size. The frozen structure was then lyophilized overnight and the ventricular side of porous chitosan scaffold is shown in Figure 4 B and the aortic side is shown in Figure 4 C. Pore sizes were determined by analysis of SEM images of dry scaffolds using Sigma Scan Pro image analysis software (SPSS Inc., Chicago, IL).

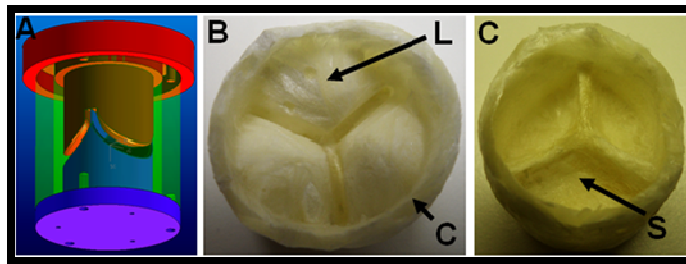


Figure 4: (A) Unigraphics® image of trileaflet heart valve mold, (B) Ventricular view of porous chitosan trileaflet heart valve scaffold showing the leaflet (L) and the cylinder (C) and (C) Aortic view of trileaflet heart valve scaffold showing the sinus (S)

#### 5.2.4 Formation of Fiber-Reinforced Chitosan-Based Disc Scaffold

Chitosan disc scaffolds were formed by transferring 9 ml of chitosan solution into 35 mm Petri dishes, freezing in a dry ice-isopropanol bath at  $-70^{\circ}\text{C}$  for 3 hours and then lyophilizing overnight. Fiber-reinforced disc scaffolds were formed by first embedding chitosan fibers (2 mm or 10 mm in length) homogeneously in the chitosan solution at four different fiber/scaffold mass ratios (0, 0.2, 0.3 and 0.4 on a dry weight basis) prior to freezing.

### **5.2.5 Formation of Fiber-Reinforced Chitosan-Based Heart Valve Scaffold.**

Similarly to fiber-reinforced disc scaffold, fiber-reinforced heart valve scaffolds were formed by distributing some fibers in the mold. Due to the electrostatic charges, chitosan fibers were held in place after being distributed within the silicon mold. Chitosan solution was then added gradually to the mold with distributing more fibers while filling the mold. Embedded chitosan fibers were of 2 mm length and at a fiber/scaffold mass ratio of 1.0. As the leaflet is considered the most functional part within the valve scaffold, 0.4 fiber/scaffold mass ratio were used to reinforce the leaflet and the remaining fibers were used to reinforce the sinus and the cylinder of the valve.

### **5.2.6 Covalent Immobilization of Heparin onto Chitosan Fibers and Formation of Reinforced Scaffolds with Chitosan-Heparin Fibers.**

Chitosan fibers were generated using the gel extrusion technique described above in section 5.2.2.1. After neutralizing in ammonia solution for 15 minutes, chitosan fibers were immersed overnight in a pre-activated heparin solution. Briefly, heparin at 0.6 chitosan/heparin mass ratio was dissolved in phosphate buffered saline (PBS) and activated by adding a 10 fold molar excess of EDC (1:1 mass ratio). Chitosan fibers were immersed in the pre-activated heparin solution and the reaction was allowed to take place for 24 hours. Heparin-derivatized chitosan fibers were then dried under tension at room temperature. Heparin-derivatized fibers were characterized by measuring the fiber diameters before and after hydration in PBS solution for 15 minutes.

### **5.2.7 Mechanical Testing of Fibers and Fiber-Reinforced Scaffolds.**

After rehydration, mechanical properties of individual fibers were determined in the wet state using uniaxial tensile testing on a MTS Bionix 100 testing machine, at a constant strain rate of  $1 \text{ min}^{-1}$ . After lyophilization, scaffolds were initially neutralized with 2 wt% ammonia solution for 10 minutes then washed 4 times with PBS. Rectangular samples (7 x 2 x 15 mm) were cut from disc scaffolds and tested in the wet state. Mechanical testing was done as for fibers. Maximum stress, breaking strain and modulus of elasticity at 2% (fibers) and 20% (scaffolds) strain were determined from the stress-strain plots.

### **5.2.8 Statistical Analysis.**

Statistical comparisons of data were performed using Student's t-test with a 95% confidence limit. Data are presented as mean  $\pm$  standard deviation. Differences with  $p < 0.05$  were considered significant.

## **5.3 Results**

### **5.3.1 Porosity and Mechanical Properties of Heart Valve Scaffolds and Chitosan Fibers.**

Table 1 shows pore sizes of heart valve scaffolds at different locations. Local freezing conditions yielded different pore sizes at different locations within the scaffold that were adequate for cell penetration upon seeding. The aortic side had a larger pore size of  $130 \mu\text{m}$  compared to the ventricular side that had a mean pore size of  $54 \mu\text{m}$ .

The outer surface of the valve cylinder had a smaller pore size (70  $\mu\text{m}$ ) than the inner surface (115  $\mu\text{m}$ ).

Measurements of chitosan fibers after rehydration showed an average diameter of 320  $\mu\text{m}$  (Figure 3). Mechanical testing demonstrated that chitosan fibers had higher mechanical properties compared to chitosan-based valve scaffolds as shown in Table 2. Scaffold tensile strength was 58 kPa and stiffness was 70 kPa. These values are lower than the values of both human pulmonary and aortic valve strength and stiffness in the radial and the circumferential directions (Stradins *et al.*, 2004) as shown in Table 3.

Table 1: Pore size of heart valve scaffold at different locations

<b>Location</b>	<b>Leaflet-Aortic Side (<math>\mu\text{m}</math>)</b>	<b>Leaflet-Ventricular Side (<math>\mu\text{m}</math>)</b>	<b>Cylinder-Inner side (<math>\mu\text{m}</math>)</b>	<b>Cylinder-Outer side (<math>\mu\text{m}</math>)</b>
<b>Mean <math>\pm</math> SD</b>	130 $\pm$ 73	54 $\pm$ 45	115 $\pm$ 60	70 $\pm$ 39
<b>Median</b>	104	32	101	63
<b>Minimum Value</b>	38	15	37	23
<b>Maximum Value</b>	308	161	352	200

Table 2: Mechanical properties of chitosan fibers and chitosan based scaffolds

<b>Mechanical Aspect</b>	<b>Chitosan Fibers (n=10)</b>	<b>Chitosan Scaffold (n=7)</b>
<b>Tensile Strength (kPa)</b>	750 $\pm$ 80	58 $\pm$ 28
<b>Maximum Strain (%)</b>	20 $\pm$ 4	90 $\pm$ 30
<b>Modulus of Elasticity (kPa)</b>	3500 $\pm$ 780	70 $\pm$ 10



Table 3: Mechanical properties of chitosan based heart valve scaffold compared to human pulmonary and aortic valves

<b>Mechanical Aspects</b>	<b>Chitosan-Based Heart Valve Scaffold (n=7)</b>	<b>Human Pulmonary Valve (Radial/Circumferential Direction)</b>	<b>Human Aortic Valve (Radial/Circumferential Direction)</b>
<b>Ultimate Stress (KPa)</b>	58±28	290±60 / 2,780±1,050	320±40 / 1740±290
<b>Ultimate Strain (%)</b>	90±10	30±4 / 19.4±3.91	24±4 / 18.35±7.61
<b>Modulus of Elasticity (KPa)</b>	70±10	1320±930 / 16,050±2,020	1950±150 / 15,340±3,480

### 5.3.2 Effect of Fiber Length and Fibers/Scaffold Mass Ratio on Scaffold Mechanical Properties

Local and overall mechanical properties of fiber-reinforced scaffolds can be influenced by fiber content, fiber length, fiber mechanical properties and fiber distribution. Thus, the effects of varying fiber/scaffold mass ratio and fiber length and mechanical properties were studied in order to characterize the response of overall scaffold properties to these parameters. Representative stress-strain curves for a reinforced scaffold (2 mm fibers at 0.4 fiber/scaffold mass ratio) and an unmodified

chitosan scaffold are shown in Figure 5. Scaffold reinforced with fibers at 0.4 fiber/scaffold mass ratio has higher strength, elasticity and stiffness compared to unmodified scaffold.

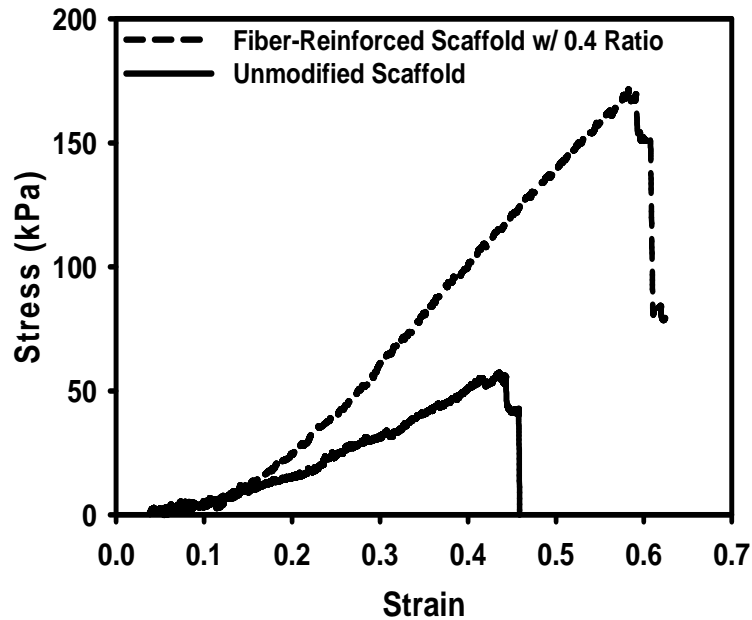


Figure 5: Stress-strain curve of reinforced scaffold at 0.4 fiber/scaffold mass ratio and unmodified chitosan based scaffold. Reinforced scaffold had a higher strength and strain values compared to unmodified scaffolds.

Scaffolds reinforced with 2 mm fibers showed significant improvement in strength and stiffness (Figure 6 A, B) as fiber/scaffold mass ratio increased. A 3-fold improvement in scaffold strength (to 139 kPa) and stiffness (to 0.36 MPa) were achieved at the 0.4 mass ratio.

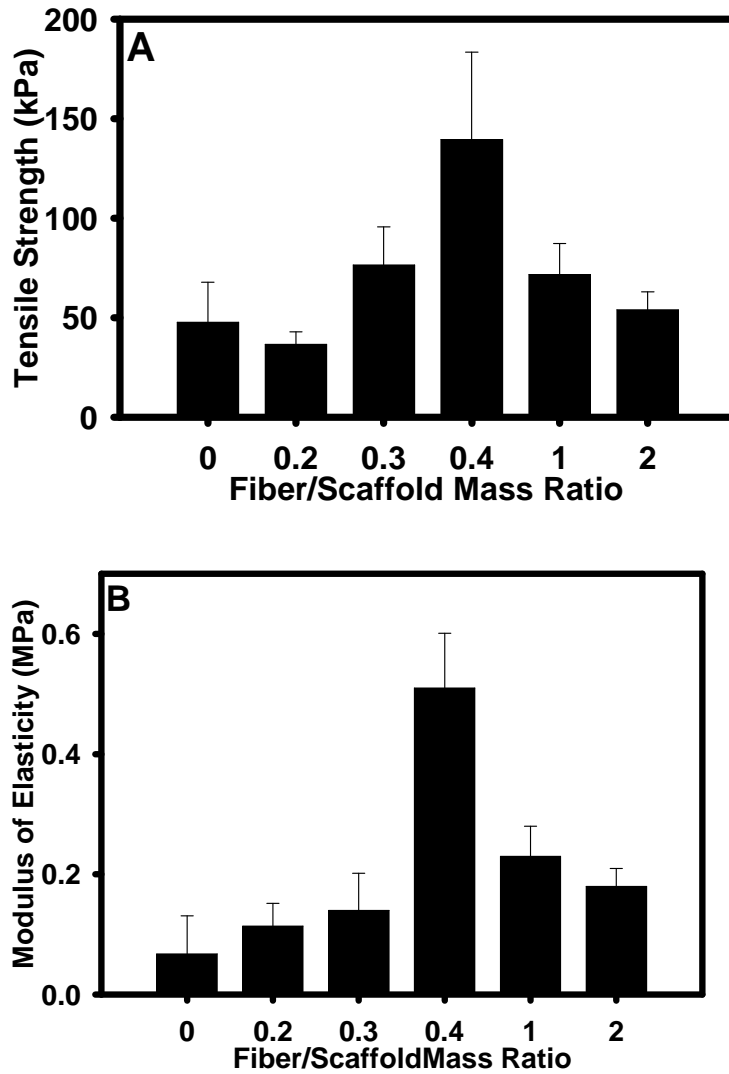


Figure 6: Effect of fiber/scaffold mass ratio on scaffold (A) Strength and (B) Stiffness.

(n=7), all values were statistically different from unmodified scaffold.

Reinforced scaffolds with longer (10 mm) fibers showed lower strength and stiffness values (comparable to control) when compared to reinforced scaffold with the shorter (2 mm) fibers (Figure 7 A, B). Since fiber properties were independent of length, the higher scaffold mechanical properties obtained with shorter fibers were believed to be due to differences in fiber alignment and the homogenous distribution within the

scaffold, and possibly a reduced effect of fiber defects with shorter fibers. We also suggest that with shorter fiber, the defects are less than those found in the longer fibers. These defects are weak points within the fiber structure and do not provide any mechanical support to the scaffold.

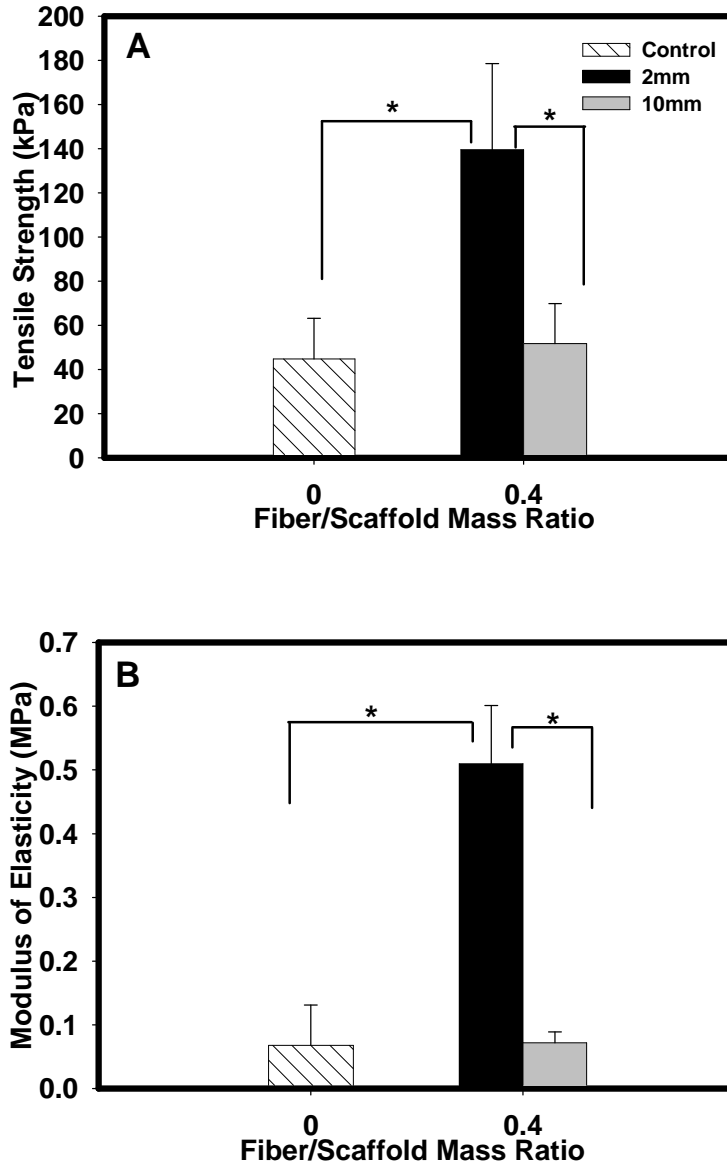


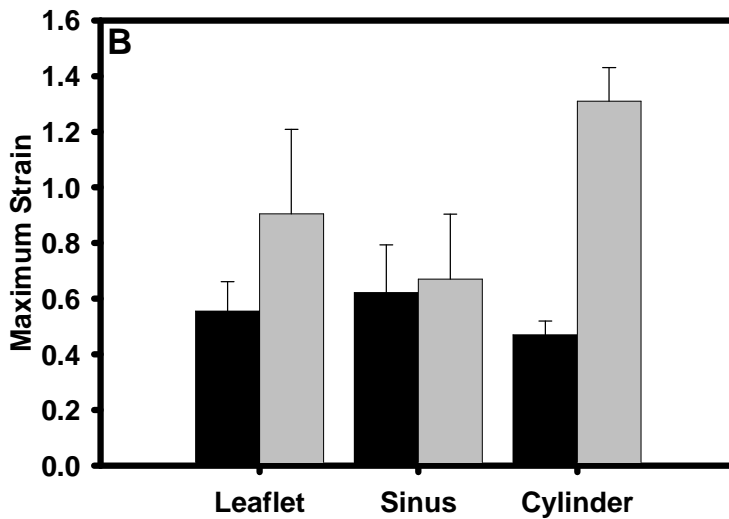
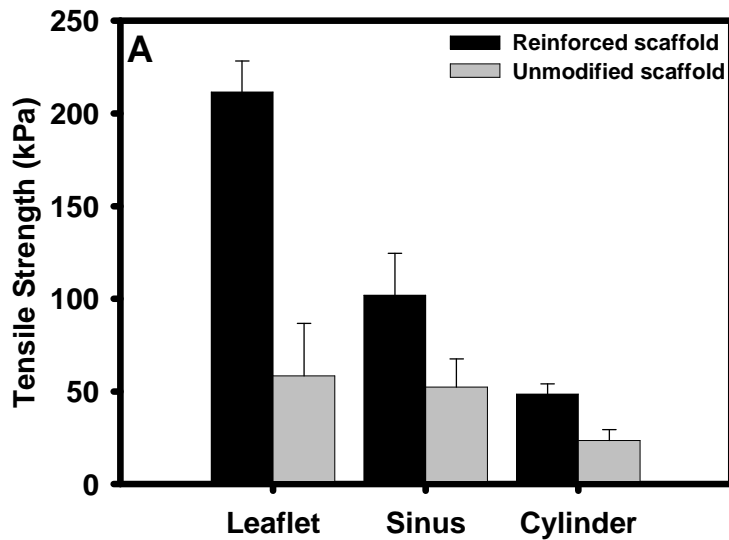
Figure 7: Effect of fibers length on chitosan (A) strength and (B) stiffness. \* indicate a statistical difference ( $p < 0.05$ ). (n=7)

### 5.3.3 Effect of Fiber Reinforcement on Chitosan-Based Heart Valve Scaffolds

In order to examine the effectiveness of fibers on improving scaffold properties in more complex geometries, fiber-reinforced heart valve scaffolds were fabricated at a fiber/scaffold mass ratio of 1.0. Reinforced heart valve scaffolds showed significant improvements in strength and stiffness at the leaflet, sinus and cylinder as shown in Figure 8. At the leaflet, a 4-fold improvement in strength from 50 to 220 kPa was achieved (Figure 8 A) along with a 6-fold improvement in stiffness from 0.07 to 0.4 MPa (Figure 8 C). Sinus strength and stiffness improved 2-fold. Likewise, a 2-fold improvement in strength and stiffness was achieved at the cylinder. The improvements correlated with a reduction in maximum strain (Figure 8 B). The major reduction occurred at the leaflet and cylinder. Leaflet maximum strain was reduced from 0.9 to 0.58 while cylinder maximum strain reduced from 1.3 to 0.25. Different fibers mass fractions were distributed according to the importance of structure in the valve. More fibers mass fraction was given to leaflet, which is the major component of the valve, followed by the sinus, which is a crucial part of the valve and important for valve function, and the least was for the cylinder. The only statically differences in strength, elasticity and stiffness values for the unmodified scaffolds were between the leaflet and the cylinder or sinus due to the pore size variations of the scaffold. There was no statistical difference in strength, elasticity and stiffness values for the unmodified scaffold between the cylinder and the sinus.

Table 4 shows mechanical properties of reinforced heart valve scaffolds compared to human pulmonary and aortic valves. Leaflet strength (220 kPa) was near comparable to the radial properties of the human pulmonary (290 kPa) and aortic (320

kPa) heart valves. Minimum leaflet stiffness (260 kPa) was near comparable to the minimum value of the pulmonary valve (390 kPa). Reinforced scaffold had also a near comparable elasticity values to both human valves. However, the improved properties of the valve scaffold are still lower than the properties of the aortic and pulmonary valves in the circumferential direction.



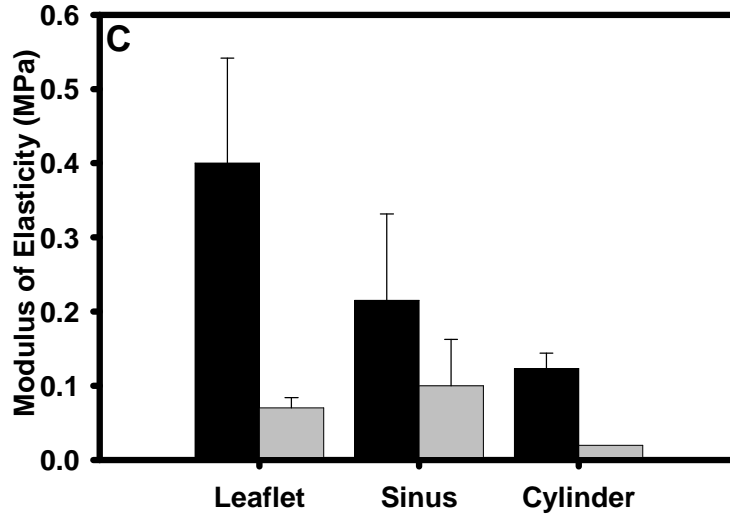


Figure 8: Reinforced heart valve scaffold with 2mm fibers length at 1.0 fiber/scaffold mass ratio showing (A) Strength, (B) Maximum Strain and (C) Modulus of elasticity. Values were statistically different at each location between the two conditions ( $p < 0.05$ ).

#### 5.3.4 Partial Dissolution of Chitosan Fibers within Chitosan Scaffold

Partial fibers dissolution occurred to the embedded chitosan fibers due to the acidic nature of chitosan solution forming the scaffold. Although, both phase contrast and SME images (Figure 9 A, B) showed that fibers were present within the matrix; lack of fibers in some areas with the scaffold suggested the partial dissolution of fibers. We further confirmed the fibers dissolution by immersing chitosan fibers in 1 vol% acetic acid concentration. Complete fibers dissolution by losing fiber structure and forming hydrogels within half an hour of immersion was observed. However, fibers dissolution was minimized in the experiments through quick freezing of scaffold after fibers embedding. Based on these findings, it was proposed that further improvement of scaffold mechanical properties can be achieved if fibers dissolution is prevented. The working hypothesis for this experiment is that *immobilizing heparin onto chitosan*

*fibers would prevent dissolution of chitosan fibers and further improve scaffold mechanical properties.* The following section will provide more details on the effect of heparin covalent crosslinking onto chitosan fibers on the fibers mechanical properties.

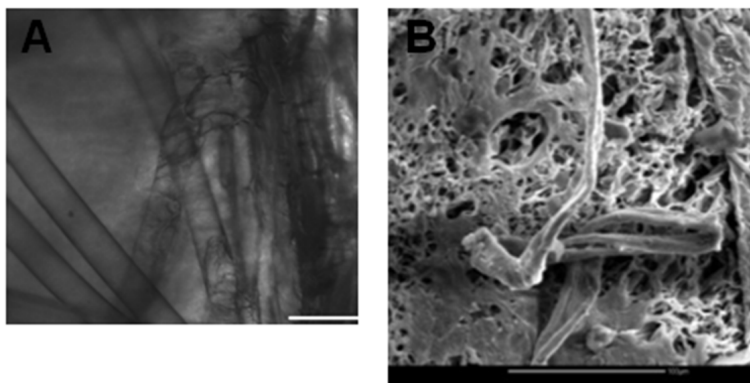


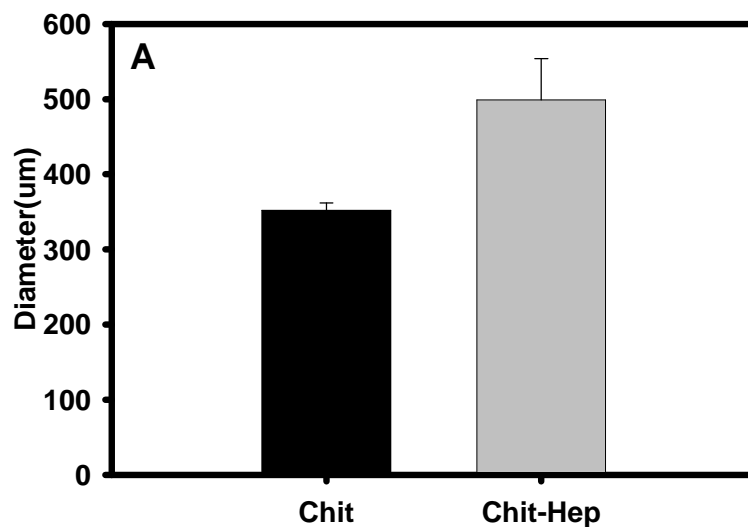
Figure 9: Reinforced scaffolds with chitosan fibers. (Left) phase contrast image of transverse section of scaffold showing the embedded chitosan scaffold were present within the matrix, scale bar 250µm and (Right) transverse section SEM image shows porous chitosan scaffold with fibers embedded, scale bar is 100 microns

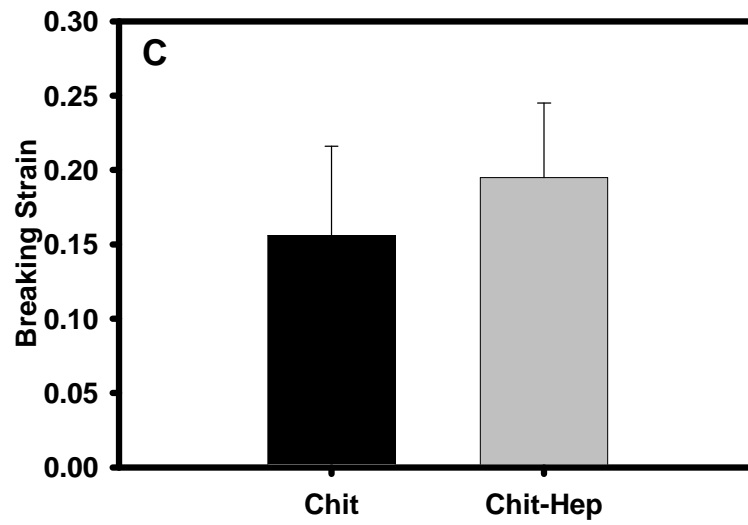
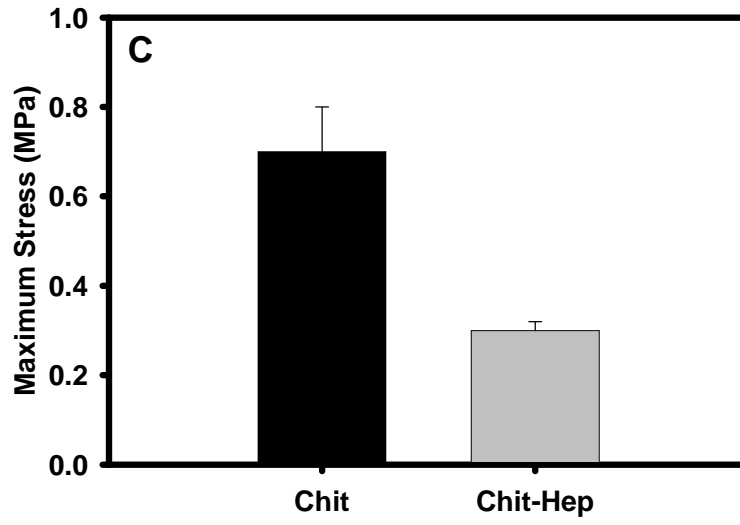
### 5.3.5 Effect of Heparin Immobilization on Chitosan Fibers Mechanical Properties

Since observations indicated that chitosan fibers embedded in a chitosan solution exhibited swelling and loss of defined structure, crosslinking was considered as a method of stabilizing fibers in the acidic solution environment. Heparin can function as a multi-valent crosslinker for chitosan materials by using carbodiimide chemistry to generate intermolecular amide linkages. Heparin can also contribute useful biological properties to a biomaterial. It was hypothesized that preventing fiber dissolution via



crosslinking would further improve scaffold mechanical properties. Covalent immobilization of chitosan fibers with heparin produced a significant increase in fiber diameter from 325  $\mu\text{m}$  to 500  $\mu\text{m}$  due to fibers swelling (Figure 10 A). Heparin-chitosan fibers had lower strength and stiffness values when compared to unmodified chitosan fibers. Fiber strength decreased from 0.7 MPa to 0.3 MPa after immobilization (Figure 10 B), while a slight improvement in breaking strain from 0.15 to 0.2 resulted from heparin immobilization (Figure 10 C). Fiber stiffness (Figure 10 D) was also reduced from 3.6 MPa to 1.6 MPa. A dissolution study of heparin-chitosan fibers showed that fibers did not dissolve for up to 24 hours when immersed in acidic solution.





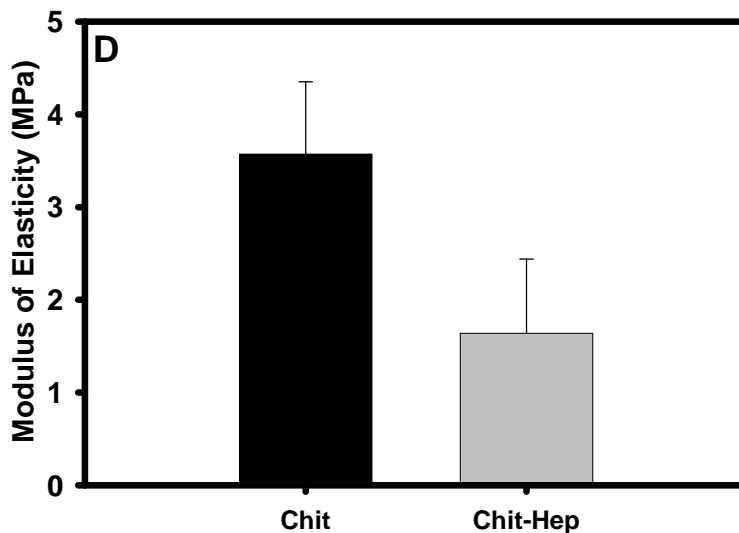


Figure 10: Effect of crosslinking of chitosan fibers with heparin on fibers (A) diameters, (B) strength, (C) elasticity and (D) stiffness. (n=10)

### 5.3.6 Effects of Fiber Crosslinking and fiber mechanical properties on Scaffold Mechanical Properties

Despite the reduced mechanical properties of the heparin-immobilized fibers, scaffolds reinforced with heparin-chitosan fibers showed a significant improvement in strength and stiffness as fiber/scaffold mass ratio increased (Figure 11). At a 0.4 fiber/scaffold mass ratio, strength improved 2-fold from 40 to 80 kPa (Figure 11 A). Likewise stiffness also improved 2-fold from 0.08 to 0.16 MPa (Figure 11 B). This improvement confirmed our hypothesis that improvement can be achieved even with fibers that have below optimal mechanical properties. Moreover, these finding suggested that the mechanical properties of fibers can greatly influence the mechanical properties of the reinforced scaffold.

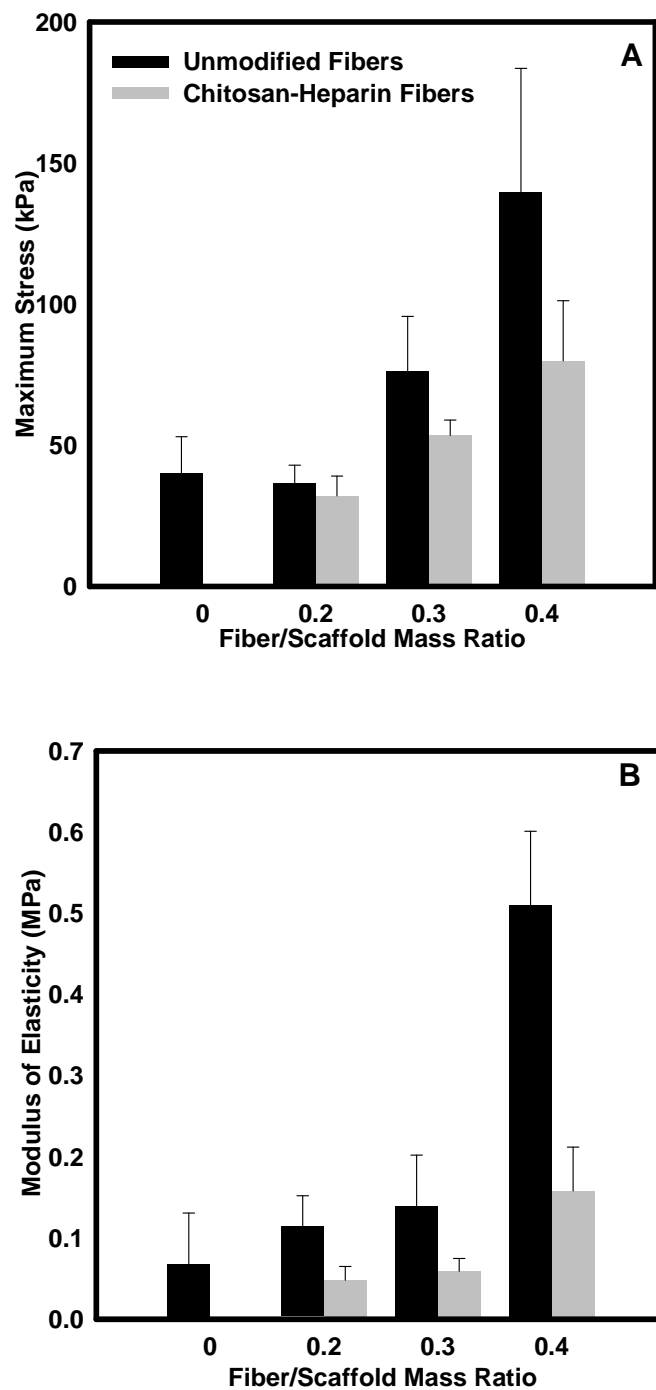


Figure 11: Effects of chitosan fiber and modified heparin fiber mechanical properties on scaffold (A) tensile strength and (B) modulus of elasticity. Error bars indicate standard deviation from 7 samples. Values at each mass ratio for the two conditions were statistically different except for tensile strength at a ratio of 0.2.

## 5.4 Discussion

While chitosan is being widely studied as an implant material for regenerative medicine and tissue engineering, relatively low mechanical properties have limited its application in load-bearing situations. On the other hand, recent results hint that low stiffness may actually play a role in defining materials with favorable tissue responses and high biocompatibility (Engler *et al.*, 2006; Dikovsky *et al.*, 2008; Dado and Levenberg, 2009; Suzuki *et al.*, 2010). Thus, maintaining low surface stiffness while increasing bulk strength and stiffness may be a key to improve chitosan's broad utility while maintaining its desirable biological properties.

The composite approach employed in this study allows the inclusion of higher strength chitosan fibers which favorably increase the overall material properties, while retaining the low stiffness of the embedding chitosan matrix. It is the embedding matrix which provides the majority of the scaffold contact area, and thus determines the cell and tissue response.

Fabrication of scaffolds from chitosan solutions using the freeze-drying technique is a diffusion-limited process that can be expected to generate a relatively low crystallinity matrix. This amorphous structure yields substantially lower mechanical properties than those obtained using slower evaporative methods or strong bases, both of which generate chitosan films with higher crystallinity (Suh and Matthew, 2000). As with other polymeric materials, forming chitosan fibers by extrusion produced a material with higher strength and stiffness. These property increases are direct result of two phenomena. First the extrusion introduces a degree of molecular alignment due to flow. Secondly, the extrusion into a base both immobilized the molecular organization by

gelation, and also compacted the molecular structure and increased crystallinity by rapid extraction of protons from the cationic polymer. The net effect of increased molecular alignment and crystallinity yields to higher mechanical properties (Notin *et al.*, 2006). Chitosan fibers produced using this technique had smooth surfaces consistent with previous reports (Tuzlakoglu *et al.*, 2004).

The mechanical properties of chitosan fibers produced by gelation techniques have been studied previously. However, properties have varied widely depending on: chitosan degree of deacetylation and molecular weight, concentration in solution, solvent type, fiber diameter and hydration state, coagulation solvent type, and pH (Hirano and Midorikawa, 1998; Knaul *et al.*, 1999; Lee *et al.*, 2007). This wide range of variable parameters hindered direct comparison. However, the strength of our fibers was comparable to those values of chitosan fiber produced by wet spinning under the same condition by Notin and colleagues (Notin *et al.*, 2006).

The high mechanical properties of chitosan fibers exceeded those of the native valve tissue which may involve introducing material with less desirable biological properties if used alone to fabricate a non-woven mesh scaffold (Stradins *et al.*, 2004). The reinforced scaffold showed a continuous improvement in strength and stiffness up to at least a 0.4 fiber/scaffold mass ratio. With higher mass ratios, scaffold strength and stiffness decreased, a finding that is consistent with Wang *et al* (Wang *et al.*, 2009). Wang *et al* similarly demonstrated a maximum in compressive modulus up to a 0.4 fiber/scaffold mass ratio when chitosan fibers were used to reinforce PLLA nanofibrous scaffolds. Above 0.4 ratio, compressive modulus decreased.

Fiber length was also shown to greatly affect the mechanical properties of our scaffolds. Shorter fibers may be expected to provide a more homogenous distribution throughout the scaffold due to the ease with which they can redistribute during the solution freezing process. Furthermore, shorter fibers are more likely to align with the pore walls and thus contribute more of their strength to the pore wall in which they are embedded. Additionally, defects generated in fibers during formation can adversely affect the mechanical properties of longer fibers, since each fiber may have several defects. Such defects within a long fiber can adversely affect scaffold properties some distance away from the actual defect site. Shorter fibers will intrinsically have fewer defects per fiber and cannot transmit the effects of a defect to distant locations. In addition to the effect of short fibers on scaffold mechanical properties, we also believe that producing chitosan fibers with small diameter will improve their mechanical properties. Despite that we did not explicitly investigate that effect of reducing fiber diameter on fiber mechanical properties; however, we still have shown the covalent immobilization of chitosan fibers with heparin increased fiber diameters. This increase in diameter correlated to an increase in fiber strength and stiffness as shown in Figure 10. These results support the fact that the reduction in fiber diameters will improve the fiber mechanical properties. This improvement in fiber mechanical properties will improve the overall scaffold properties

Reinforcing actual heart valve scaffolds with this method improved strength and stiffness and reduced scaffold elasticity. The improved strength and elasticity values were comparable to the radial directions of native aortic and pulmonary valves. The fiber-reinforcement significantly improved valve scaffold stiffness but not to a closer

stiffness value of the native valves. The percentage of improvement was found to vary with location in these structured scaffolds. In addition to the differences in fiber/ scaffold mass ratio, the variation with location was likely due to differences in fiber alignment with the local scaffold plane. Since the 2 mm fibers were randomly oriented in the chitosan solution, the degree of fiber alignment achieved in particular scaffold region would be expected to vary with the thickness of the scaffold region, as well as the freezing conditions and the resultant porosity and pore orientation of that region. Since the valve leaflets were the thinnest scaffold component, they exhibited the greatest fiber alignment with the local plane and hence the greatest percentage improvement in properties. Changes in fiber distribution during mold assembly and loading may also have played a role. Moreover, quantifying the orientation of the fibers would effectively explain the effect of fiber orientation on scaffold mechanical properties.

Covalent crosslinking of chitosan hydrogels produces a permanent network structure that resists dissolution at the low pH conditions at which chitosan is normally soluble (Berger *et al.*, 2004). Heparin was specifically chosen as a crosslinking agent due to its useful biological properties including growth factor and matrix protein binding (Lindahl and Hook, 1978). Previously, Uygun *et al.* (Uygun *et al.*, 2009) showed that among six glycosaminoglycans (GAGs) studied, MSC growth rate was highest on immobilized heparin. Given the known swelling of chitosan fibers when mixed into an acidic solution, it was hypothesized that covalent crosslinking of chitosan fibers with heparin would minimize fiber swelling and strength loss during reinforced scaffold preparation. Additionally, literature suggested that crosslinking different forms of hydrogels with heparin by soaking may result in a highly crosslinked surface (Mi *et al.*,



1997). This surface crosslinking ultimately inhibits the crosslinker from diffusion to the core of the hydrogel. This may explain the increase in fibers diameter upon crosslinking. (Mi *et al.*, 1997; Shu *et al.*, 2001).

Covalent and ionic immobilization of GAGs on chitosan substrates or fibers have been investigated previously (Madihally *et al.*, 1999; Madihally and Matthew, 1999; Cho *et al.*, 2008), however, insufficient information was provided regarding the mechanical properties of immobilized constructs. In this study we showed that immobilization of chitosan fibers with heparin reduced their strength and stiffness. We observed similar trend for other GAGs such as dermatan sulfate and chondroitin 4-sulfate (data are not shown). Since the crosslinking occurs with chitosan amino groups that would normally be involved in hydrogen bonding, the reduction in fiber mechanical properties may be due to reductions in chitosan crystallinity caused by the elimination of some inter-chain hydrogen bonds. This phenomenon would also account for the increase in fiber diameter as the reduced crystallinity and physical crosslinking would result in increased swelling of the hydrated fiber matrix. Moreover, from a stress point of view, the increase in fibers diameters resulted in a larger cross-sectional area. This increase in cross-sectional area decreases the stress. Fan *et al* recently showed that chitosan scaffold stiffness decreased when crosslinked with galactosylated hyaluronan, a finding that is consistent with our results (Fan *et al.*, 2010). Despite this reduction in fiber mechanical properties, the heparin-modified fibers still improved the mechanical properties of the reinforced scaffolds, but to a lesser extent to the unmodified fibers. This confirms that the mechanical property improvements are directly correlated to the mechanical

properties of the embedded fibers and are not simply the result of an effective increase in chitosan solution concentration.

## **5.5 Conclusions and Future Work**

In this chapter, the feasibility of improving the mechanical properties of chitosan scaffolds by embedding chitosan fibers within the scaffold has been demonstrated. The ability to control the degree of mechanical property improvement was shown by adjusting three major factors; the fiber/scaffold mass ratio, fiber length and fiber mechanical properties. The methods described here broaden the range of chitosan scaffold mechanical properties and thereby increase the usefulness of this biomaterial.

It was also shown that embedded chitosan fibers improved scaffold mechanical properties; however, further improvement is needed. Scaffold mechanical properties can be further improved through the improvement in fiber mechanical properties as it was shown that fiber mechanical properties greatly affect the degree of scaffold improvement. The next chapter will discuss different chemical and physical treatments that were used to increase fiber mechanical properties. Fiber distribution within the scaffold should be quantified to better evaluate the effect of fibers on scaffold. Moreover, achieving a better fiber distribution and alignment similar to the collagen and the fibrin fibers within the native valve leaflet is also believed to further improve the scaffold mechanical properties specifically in the circumferential direction.

## CHAPTER SIX

### IMPROVING CHITOSAN FIBER MECHANICAL PROPERTIES THROUGH PHYSICAL AND CHEMICAL TREATMENTS

#### 6.1 Introduction

Chitosan, the principal derivative of chitin, is a linear polysaccharide that is considered the second most abundant natural polymers after cellulose (Madhally *et al.*, 1999; Suh and Matthew, 2000). Due to its attractive biocompatibility, low toxicity and biodegradability properties, currently chitosan is widely investigated as potential biomaterials for different biomedical and bioengineering applications.

One of the main concerns with using chitosan hydrogel is the low to moderate mechanical properties of its scaffold, fibers or cast membranes (Wei *et al.*, 1992). Several approaches have been proposed to improve its mechanical properties using physical treatments or chemical modifications.

Chemical modification attained a great attention from researchers than physical treatments due to the variety and the wide possibilities that can be done through the numerous amino and hydroxyl side groups. In general, chemical modifications, intended to improve the mechanical properties of chitosan fibers, usually applied after fibers are formed and dried. However, recent studies showed that chemical modification may result in reducing mechanical properties of fibers (Hirano *et al.*, 1999). In contrast, another study showed that mechanical properties of chitosan fibers can be improved through immersion in a separate solutions of phosphate and phthalate ions (Knaul *et al.*, 1999). When chitosan fibers crosslinked with epichlorohydrin, mechanical properties of

wet fibers significantly improved as reaction time and temperature increase (Wei *et al.*, 1992).

Physical treatments to improve mechanical properties of chitosan membranes through annealing showed an improvement in membranes ductility (Kolhe and Kannan, 2003). However, studies which were performed to evaluate the effect of either chemical modifications or physical treatments on the mechanical properties of chitosan fibers in particular are insufficient and inconclusive.

Chitosan fibers have been used in different tissue engineering applications to reinforce scaffolds (Li *et al.*, 2006; Li *et al.*, 2009; Wang *et al.*, 2009). Recently, chitosan fibers have been introduced as a reinforcement method to improve scaffold mechanical properties (Wang *et al.*, 2009). In the previous chapter, the utility of chitosan fibers to reinforce chitosan-based scaffold was demonstrated. It was also shown that the mechanical properties of chitosan fibers influence the degree of scaffold improvement. Scaffold reinforced with stronger fibers were shown to have higher strength and stiffness values compared to scaffold reinforced with weaker fibers. The working hypothesis for this study is that ***improving the mechanical properties of chitosan fibers will further improve chitosan based heart valve scaffold.*** The scope of this chapter focuses on improving the mechanical properties of chitosan fibers through various chemical or physical treatments. This improvement in fiber mechanical properties will produce to a heart valve scaffold with more improved mechanical properties in the radial and the circumferential directions. As it was mentioned in the previous chapter, the fabrication of chitosan fibers involves three main parameters which control fiber mechanical properties and these parameters are: (1) the acetic acid

concentration which is used to dissolve the chitosan, (2) the pH of coagulation bath solution that is used to form the hydrogel fibers and (3) the drying temperature (i.e. annealing). The main aim of this study is to evaluate the effect of these three parameters on fiber mechanical properties.

## **6.2 Experimental Work**

### **6.2.1 Materials and Methods**

High molecular weight (HMW) chitosan from crab shells with molecular weight of 450 KDa with 75-85% degree of deacetylation was purchased from Sigma-Aldrich (St. Louis, MO). All other chemicals and solvents were of analytical reagent grade.

### **6.2.2 Fabrication of Chitosan Fibers Using Polymer Fiber Extrusion Technique**

Chitosan fibers were produced using polymer fiber extrusion technique as mentioned in the previous chapter. Briefly, powder of polymer was dissolved in certain concentration of a low pH acid solution and then extruded directly into a coagulation bath contains high pH basic through a Teflon catheter. After neutralizing, fibers are dried under tension at room temperature.

In this experiment, chitosan solution was prepared by dissolving 1.5 wt. % HMW chitosan powder in different volume concentrations of acetic acid (AA) (1, 2, 3 and 6 vol%). Chitosan solution was then extruded directly into two different weight concentrations of ammonia solution (10 and 25 wt%) through 26 gauge (0.45mm diameter) Teflon catheter. Fibers were then dried (i.e. annealed) under tension at different temperatures in a lab oven (40, 90, 140 and 195 °C) for 15 minutes and then

cooled down slowly at a rate of  $1\text{C min}^{-1}$ . For all experiments, chitosan solution was extruded through a syringe pump at a constant rate of  $85\text{ ml.hr}^{-1}$ . Chitosan fibers made of 1.5 wt% chitosan dissolved in 1 vol% of AA and extruded in 10 vol% ammonia solution and dried under tension at room temperature were used as a control for all experiments. To further improve chitosan fiber mechanical properties, the effect of multiple parameters were combined and evaluated.

### **6.2.3 Measurement of Fiber Diameters**

After drying under tension at room temperature, fibers, which were prepared by varying AA concentration, ammonia solution concentration and drying temperatures, were fully rehydrated in phosphate buffer saline (PBS). Phase contrast images of wet fibers produced by different conditions were captured using Nikon DIAPHOT 300 microscopy controlled by HPS-SCSI software (Hamamatsu Corporation, NY, USA). Diameters were measured using sigma scan pro image analysis software (SPSS Inc., Chicago, IL) and the average was calculated for each condition from 40 measurements.

### **6.2.4 X-Ray Diffraction (XRD) Analysis of Fiber Microstructure**

Crystallinity of wet chitosan fibers produced by different conditions were evaluated using rigaku smart lab model X-diffractometer in which a high intensity monochromatic Ni-filtered  $\text{Cu } K_{\alpha}$  radiation was generated at 40 kV and 200 mA. Scanning was done at  $3\text{ degrees min}^{-1}$  with a step size of 0.25. Graphs of intensity versus 2-theta were plotted for ammonia concentration and annealing experiments. For annealing experiment, more analysis was conducted by plotting the peak height ratio of crystalline to amorphous peaks against the temperature. Height peaks was evaluated

by averaging the intensity of  $\pm 5$  degrees around the corresponding crystalline or amorphous peak.

### 6.2.5 Evaluating the Mechanical Properties of Chitosan Fibers

For each experiment, mechanical testing was conducted on wet fibers (n=15) using 100N Bionex monotonic tensile testing machine. Fiber diameters were fed manually to a user interface software TestPad v 1.0 when mechanical testing was conducted. Fibers were mechanically tested by setting gauge length to 20mm and speed to 20mm/min. Maximum stress, breaking strain and modulus of elasticity at a strain rate of 2% were evaluated for all samples and average values were plotted against each investigated condition.

### 6.2.6 Statistical Analysis

Statistical analysis of data on fiber diameters and mechanical properties was performed using one way student's t-test with a 95% confidence limit. Data were presented as mean  $\pm$  SD.

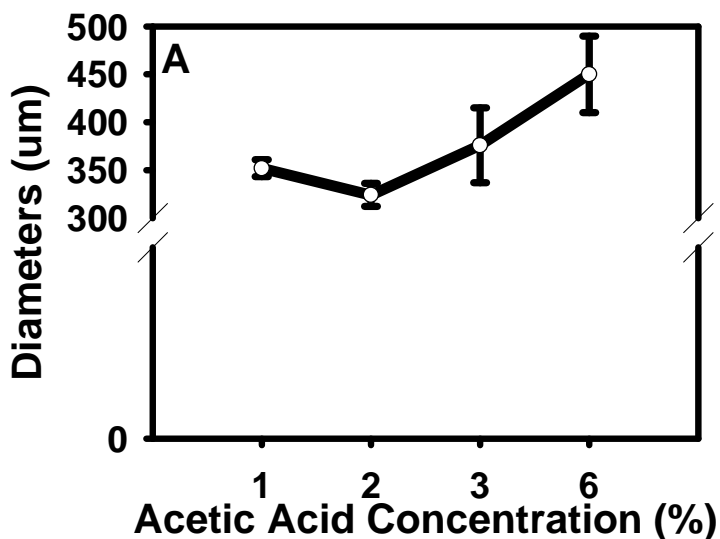
## 6.3 Results

### 6.3.1 Effect of Acetic Acid Concentration on Chitosan Fibers Mechanical Properties

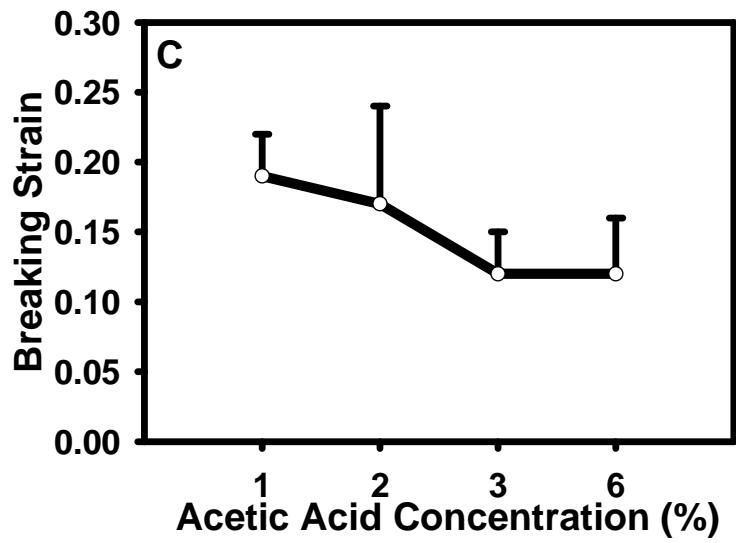
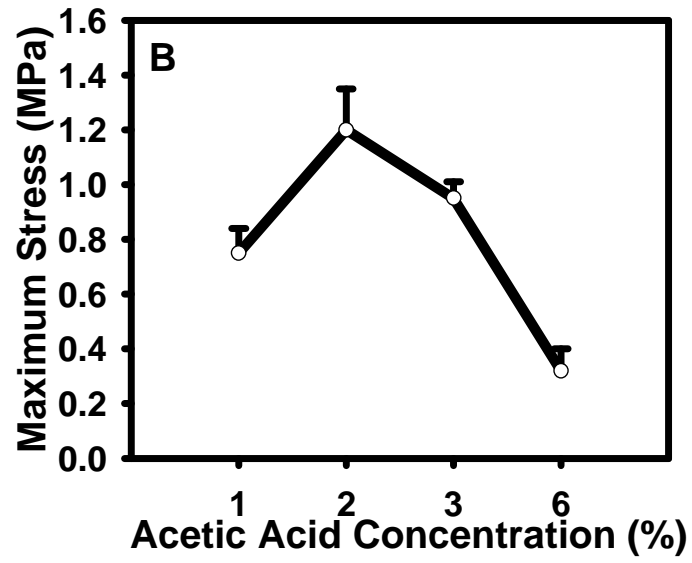
The working hypothesis for this experiment is that ***increasing the concentration of acetic acid to a certain value in chitosan solution will form chitosan fibers with improved microstructure and mechanical properties.*** Increasing acetic acid

concentration increased fibers diameters as shown in Figure 12 A, however a slight decrease was observed in fibers diameters at 2 vol% AA.

Mechanical properties of fibers showed approximately 2fold improvement in fibers strength from 0.7 to 1.2 MPa when 2 vol% of AA was used (Figure12 B). As the concentration of AA increases beyond 2 vol%, strength of fibers decreased gradually to be around 0.9 MPa at 3 vol % of AA. However, when 6 vol % of AA was used to dissolve the chitosan, fibers strength decreased by 2fold from 0.7 to 0.3 MPa (Figure12 B). Increasing AA concentration resulted in decreasing the fibers elasticity slightly and was significant when AA concentration exceeded 2 vol% (Figure 12 C). Fibers stiffness improved by 2fold from 3.5 to 7 MPa as the AA concentration increased up to 3 vol% and decreased thereafter to be 0.3 MPa (Figure 12 D).







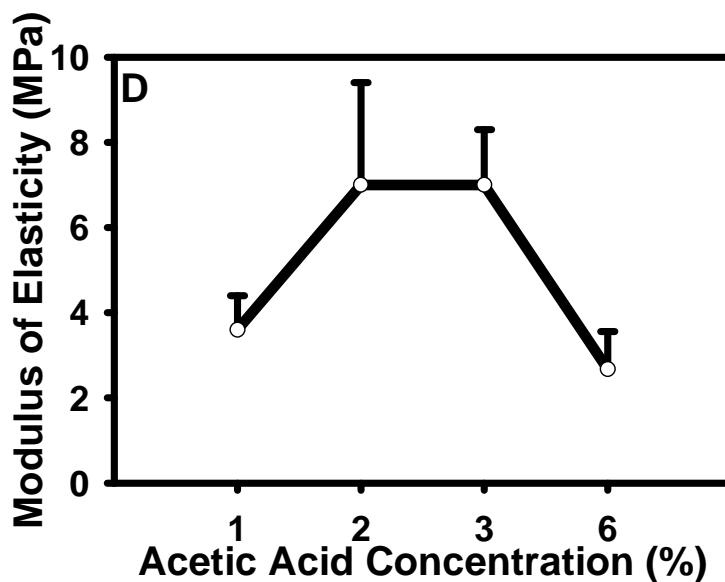
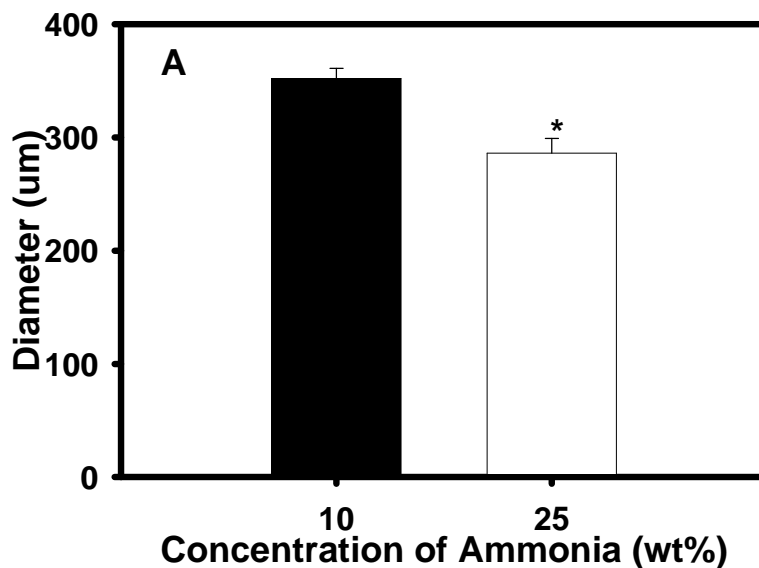


Figure 12: Effect of acetic acid (AA) concentration on chitosan fibers (A) diameters, (B) strength, (C) elasticity and (D) stiffness.

### 6.3.2 Effect of Coagulation Bath pH of Ammonia Solution on Chitosan Fibers Mechanical Properties

Coagulation bath that contains strong base is usually used to produce hydrogel polymer fibers. It was hypothesized that ***increasing the pH of the coagulation bath will cause a more organized fiber microstructure and improve the mechanical properties of chitosan fibers.*** To do so, the concentration of ammonia solution in the coagulation bath from 10 wt% up to 25 wt% was increased. Results showed that chitosan solution extruded in 25 wt% ammonia solution resulted in reducing chitosan fiber diameters from 352 to 286  $\mu\text{m}$  as shown in Figure 13 A. This reduction in fiber diameters suggests formation of fibers with more crystalline structure and improved mechanical properties. To further confirm these findings, XRD test was conducted. XRD spectra of wet chitosan fibers showed 2 dissimilar peaks as shown in Figure 13 B (Lee

*et al.*, 2004). The first peak is a sharp and intense peak at  $2\theta=21^\circ$  which represents the crystalline region. The second peak is less intense and broader than the first peak at  $2\theta=27^\circ$  which represents the amorphous region (Uygun *et al.*, 2010). With higher ammonia concentration, the crystalline peak is higher compared to the lower ammonia concentration. Additionally, the peaks height ratio of crystalline/amorphous peaks (i.e.  $2\theta_{21}/2\theta_{27}$ ) was higher for fibers coagulated in 25 wt% ammonia solution. This confirms that the crystalline fraction is the principal structure in the fibers which were extruded in higher ammonia solution. This crystalline structure (i.e. compact structure) makes the fibers more hydrophobic and resisting swelling upon hydration, a phenomena that explains the reduction in fiber diameter. Moreover, this crystalline structure suggests improvement in fiber mechanical properties. The XRD spectra shown in Figure13 B confirmed this hypothesis and showed a higher crystalline ( $2\theta=20^\circ$ ) to amorphous peak ( $2\theta=27^\circ$ ) for fibers extruded in higher ammonia solution.



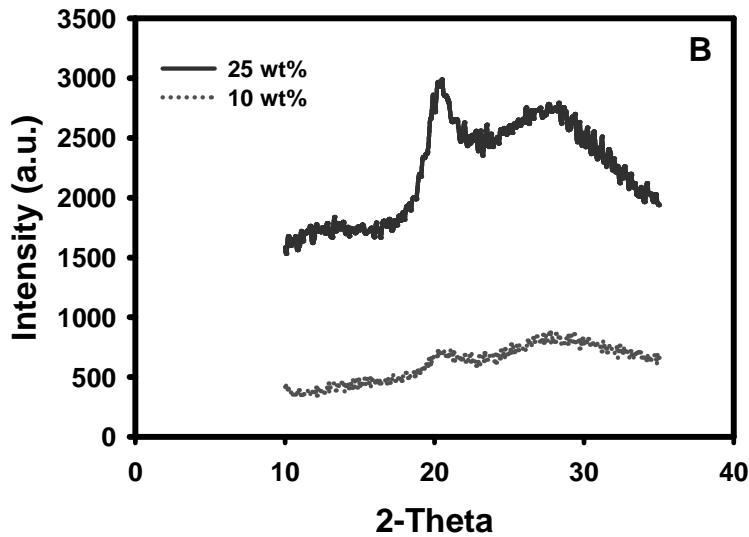
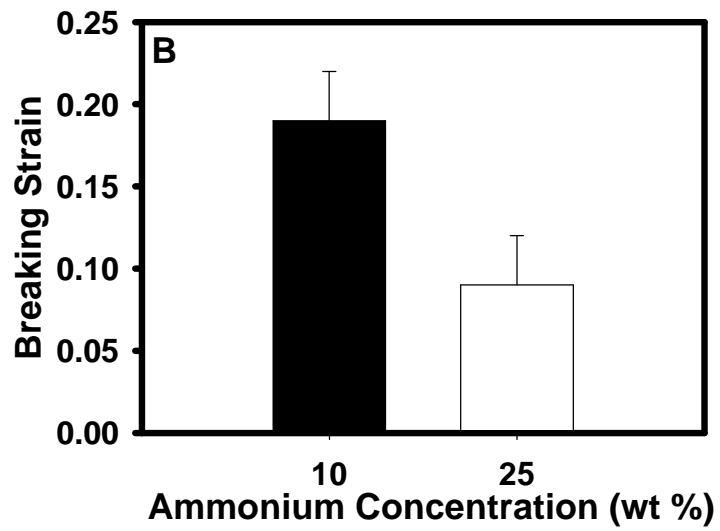
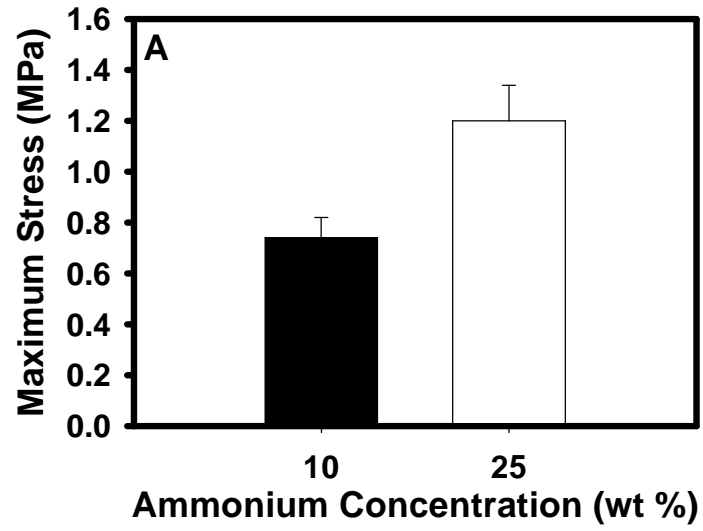


Figure 13: Effect of coagulation bath of ammonia solution, (A) chitosan fibers diameters and (B) XRD spectra of chitosan fibers extruded in 10 or 25 wt% ammonia solutions. (\*  $p < 0.05$ )

Mechanical testing results further confirmed our as fiber strength improved by 2fold from 0.7 to 1.2 MPa as shown in Figure 14 A when higher concentration of ammonia solution was used. Fiber elasticity decreased by 2fold from 0.2 to 0.09 when chitosan extruded in higher concentration of ammonia solution as shown in Figure 14 B. Extruding chitosan solution in higher ammonia concentration resulted in a significant improvement in fibers stiffness with 4fold increase from 3.5 to 13 MPa as shown in Figure 14 C. The mechanical results confirmed our hypothesis that with higher ammonia concentration, the crystalline fraction is dominant in fibers microstructure.



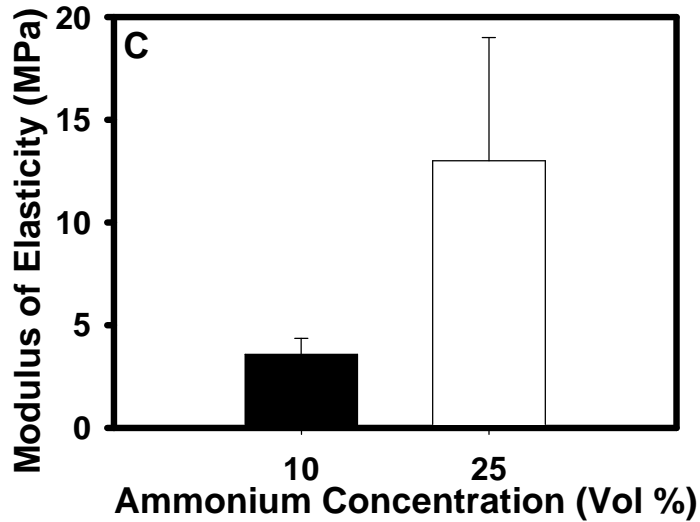


Figure 14: Effect of coagulation bath ammonia solution on chitosan fibers mechanical properties, (A) fiber strength, (B) fiber elasticity and (C) fiber stiffness.

### 6.3.3 Effect of Drying Temperature on Chitosan Fibers Mechanical Properties

Drying fibers under tension at high temperature helps in reforming the microstructure of fibers. It was hypothesized that ***annealing of chitosan fibers (drying temperature) will form more organized microstructure and improve fibers mechanical properties***. Different temperatures were studied as drying temperatures and results were compared to fibers dried at room temperature.

Measurement of diameters revealed a reduction in fibers diameters as drying temperature increased. The reduction in fiber dimension was mostly significant after 90°C as shown in Figure 15. This reduction in fibers diameters suggested that fibers are hydrophobic and resist swelling due to the crystalline microstructure.

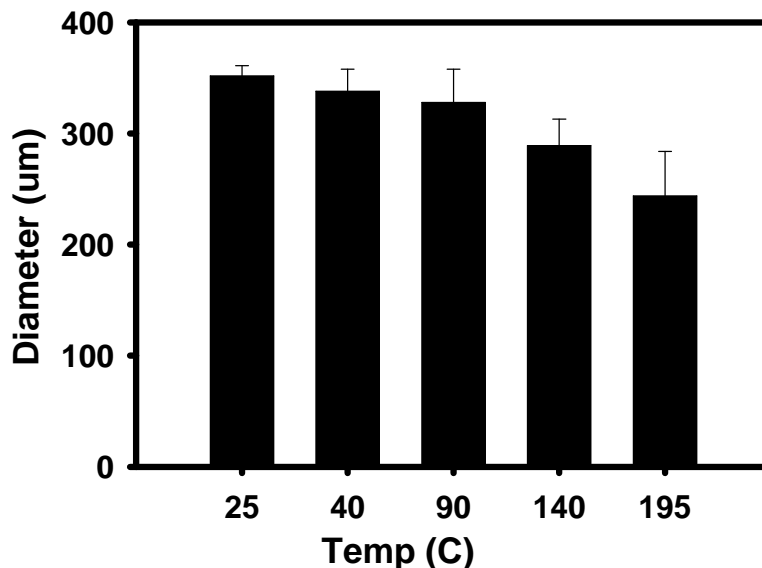


Figure 15: Effect of drying temperature on chitosan fiber diameters

XRD spectra of chitosan fibers annealed at different temperatures shown in Figure 16 A revealed distinct peaks: two amorphous peaks were present at  $2\theta=9^\circ$  and  $27^\circ$  and crystalline peak at  $2\theta=21^\circ$ . Chitosan fibers that were dried at room temperature had a broader and less sharp crystalline peak. Also, the second amorphous peak was much broader compared to the same peak in different annealing temperatures. This suggests a less organized microstructure and lower mechanical properties. Figure 16 B shows the height ratio of the crystalline peak to the second amorphous peak ( $2\theta_{21} / 2\theta_{27}$ ). The height ratio increased as the annealing temperature increased indicating that the microstructure is moving toward the crystalline structure. The increase in the crystalline structure causes an improvement in mechanical properties due to the organized structure. A significant increase in the height ratio at 40C was observed which is due to the phase transition that chitosan was undergoing around this temperature (Goycoolea *et al.*, 2007).

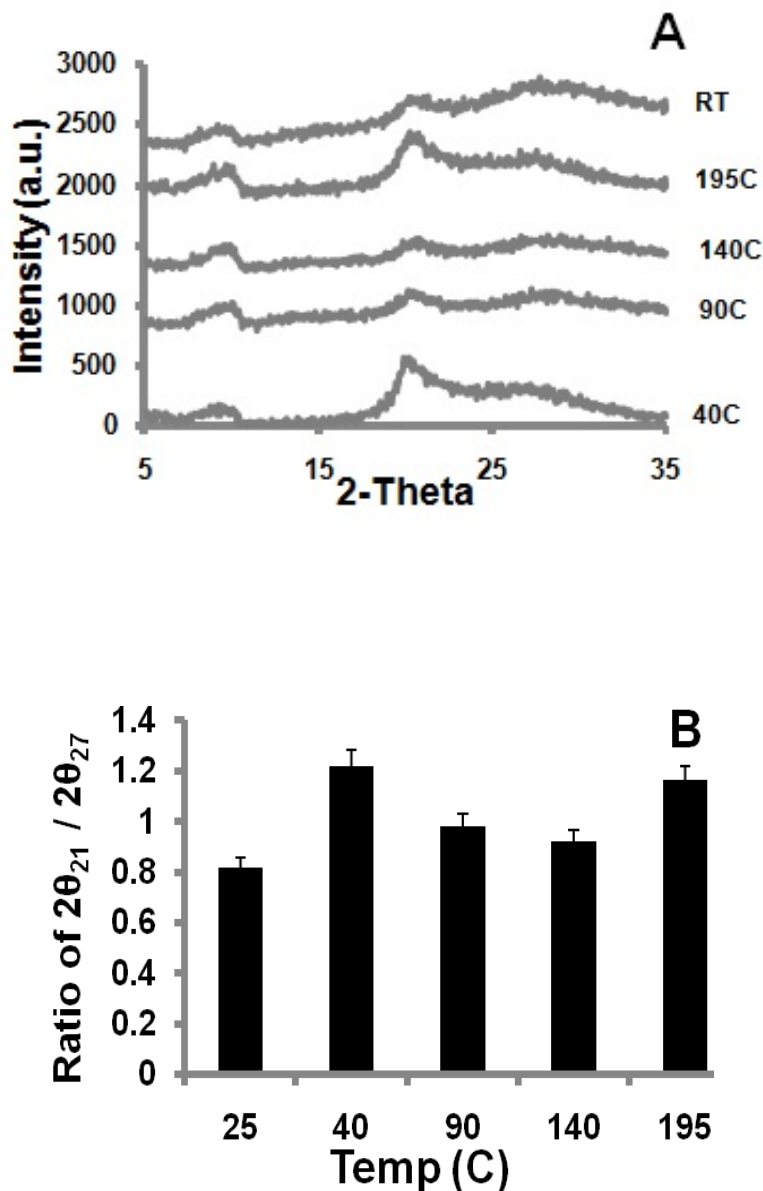
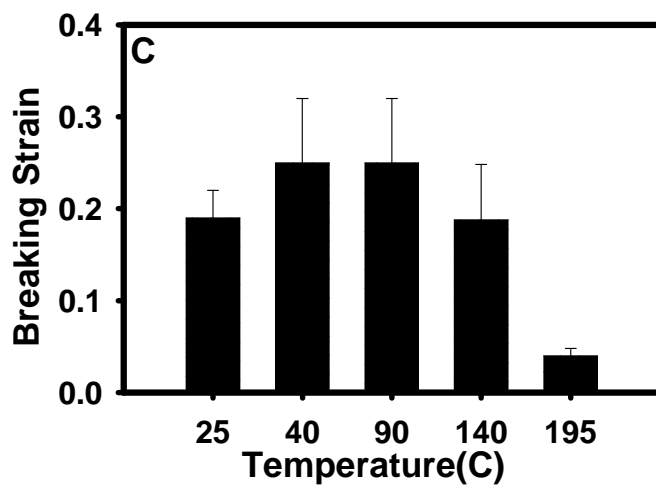
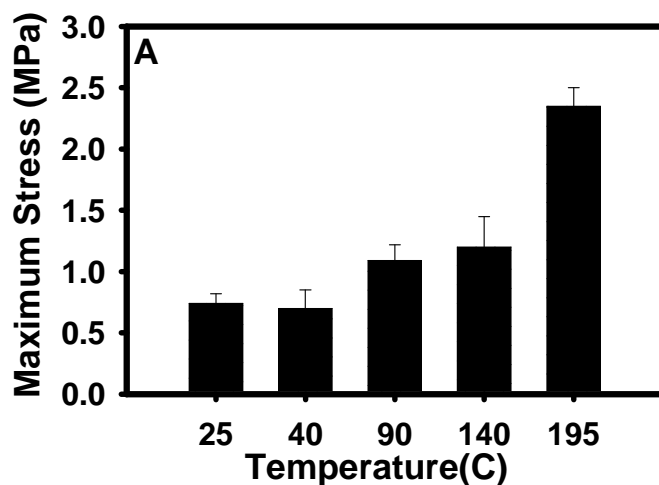


Figure 16: XRD spectra of chitosan fibers annealed at different temperature (A) and height ratio of crystalline to amorphous peaks (B)

Mechanical properties of annealed fibers showed that fibers strength improved as temperature increases as shown in Figure17 A. A significant 3fold improvement of fibers strength was obtained at 195°C. Fibers elasticity slightly improved when temperature increased up to 90°C and then decreased thereafter to be the minimum at



195°C as shown in Figure 17 B. Fibers stiffness improved with increasing the temperature to be significant after 90°C with 8fold improvement in fibers stiffness at 195°C as shown in Figure 15 C). The improvement in annealed fibers mechanical properties was consistent with the XRD results which showed that increasing temperatures produces fibers with more crystalline structure.



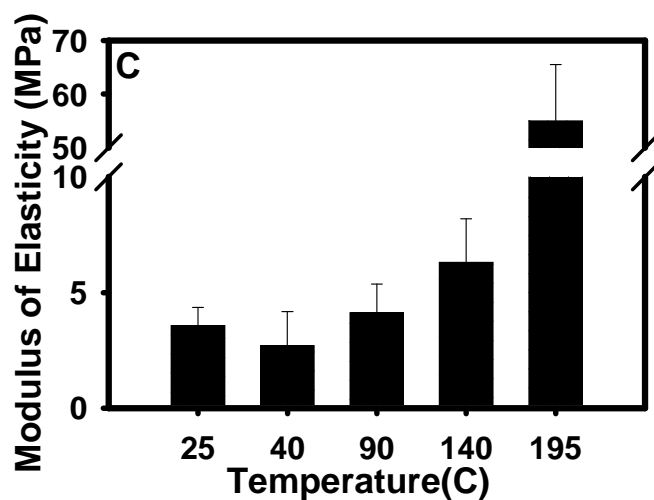


Figure 17: Effect of annealing temperature on (A) chitosan fibers strength, (B) fibers elasticity and (C) fibers stiffness.

#### 6.3.4 Effect of Combined Parameters on the Mechanical Properties of Chitosan Fibers

As it was shown in the proceeding sections in this chapter, individual parameters improved fiber mechanical properties. In this study, the aim is to combine these individual parameters to seek further improvement in fiber mechanical properties. Figure 18 shows representative stress-strain curves of chitosan fibers with different parameters combination.

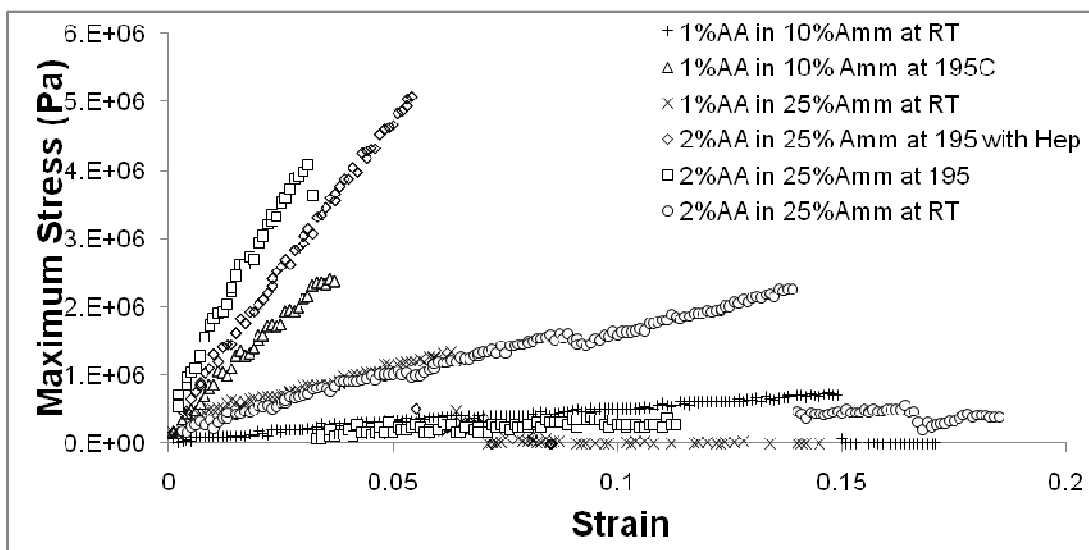
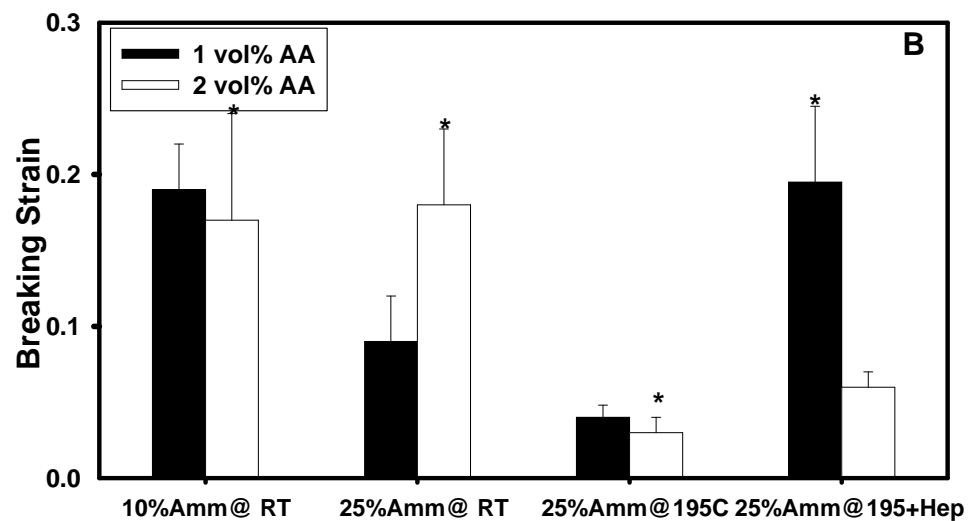
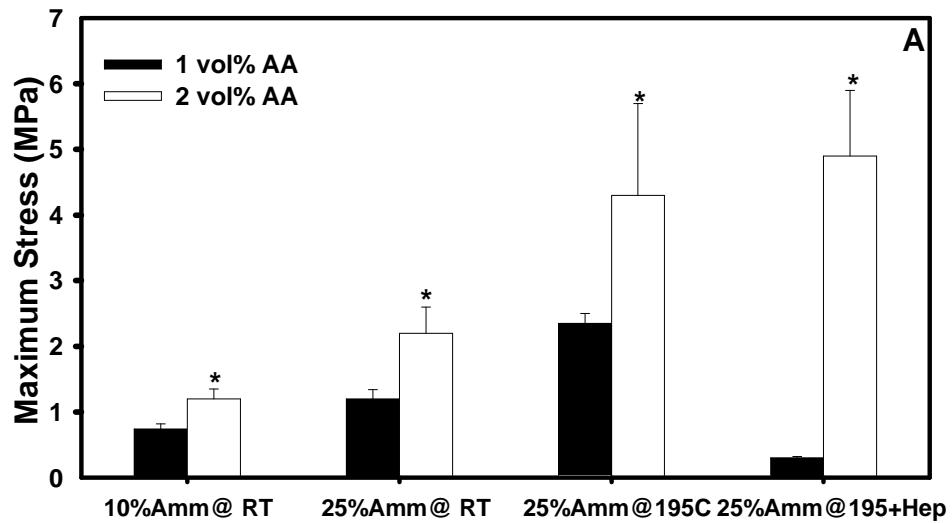


Figure 18: Representative Stress-Strain curve of different chitosan fibers formed with combined parameters

Figure 19 shows the effect of single parameters on chitosan fibers mechanical properties and the effect of combined parameters. When fibers formed by dissolving chitosan solution in 2 wt% AA and extruded in 25 vol% ammonia solution, fibers strength improved 3-fold compared to control fibers (Figure 19 A). Further improvement in fibers strength was achieved when annealing was combined from 0.07 MPa to 0.42 MPa. A further improvement up to 7-fold from 0.07 MPa to 0.5 MPa was achieved when fibers immobilized with heparin. Fibers elasticity decreased when one parameter was investigated (Figure 19 B). When 2 parameters were combined, fibers elasticity was comparable to the control. However, when 3 parameters or more were combined, fibers elasticity decreased significantly. In general, fiber elasticity was either comparable to control fibers elasticity or less. Fibers stiffness improved with all parameters that were

investigated (Figure 19 C). The improvement in fibers stiffness was always significant when fibers are annealed at 195C.



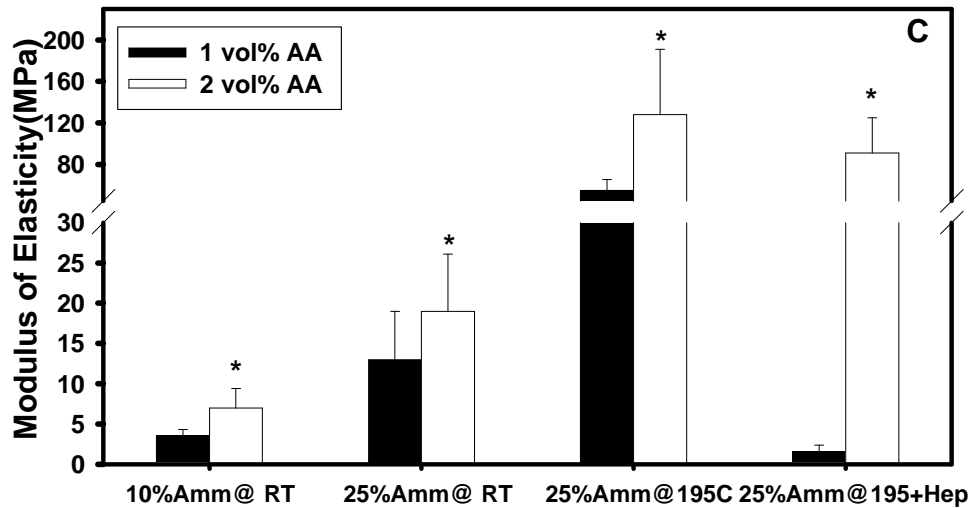


Figure 19: Effect of combing parameters on (A) fiber strength, (B) fiber elasticity and (C) fiber stiffness

#### 6.4 Discussion

Chitosan dissolves slowly in acidic pH solution, swells in neutral solution and precipitates in basic solutions.

When 2 vol% of acetic acid was used to dissolve the chitosan, a reduction in fiber diameter occurred. This reduction in fiber diameter can be explained by the complete dissolving of the chitosan particles within the solution. A complete dissolving will result in forming chitosan fibers with more crystalline structure. However, when acetic acid concentration was increased, fiber diameters were increased. The excess amount of acetic acid causes polymer protonation for the chitosan. This protonation and increase in hydrogen bonding tends to form a loosely-packed and extended structure. This extended structure is more hydrophilic and amorphous. This explanation was confirmed by the mechanical properties results. The results showed that the strength increased when 2 vol% of acetic acid was used and then decreased as the acetic acid

concentration decreased. Moreover, the elasticity of the fibers decreased significantly after 2 vol% of acetic acid.

Lee and colleagues showed that increasing sodium acetate concentration in NaOH coagulation bath increases fibers tenacity and modulus of elasticity as coagulation solution's pH increases (Lee *et al.*, 2007). This finding was consistent with our findings that increasing the concentration of ammonia solution (i.e. increasing the pH) improved fiber mechanical properties.

Most of mechanical properties and XRD peaks changes (Figures 13 and 14) occurred around 90C. Several quite different glass transition temperatures of chitosan have been reported (150C, 161C and 203C) (Scandola *et al.*, 1991; Sakurai *et al.*, 2000; Ahn *et al.*, 2001). A recent study attempted to determine the glass transition temperature ( $T_g$ ) of chitosan films using four methods including differential scanning calorimetry (DSC)(Dong *et al.*, 2004). It has been reported that the first heating run showed an endothermic peak around 100 °C while the second heating run confirmed the  $T_g$  to be between (140-150 °C)(Dong *et al.*, 2004). The first temperature (100 °C) attributes to absorbance of moisture and the reformation of the microstructure of chitosan fibers. In our experiment, the decrease in fiber diameters starts to be significant and to occur around 90C which confirms the reforming of the microstructure. Additionally, major changes in fibers strength, elasticity and stiffness started to occur around that temperature also. However, the crystalline structure was dominant in fibers microstructure around the chitosan  $T_g$  which was confirmed by the significant reduction in fibers diameters and the improvement in fibers strength and stiffness. Phase transition of chitosan has been reported to occur around 30 °C (Goycoolea *et al.*, 2007).

In our experiment, we observed major microstructural changes confirmed by the XRD spectra results shown in Figure 16. Below this temperature, chitosan hydrogel is swollen, hydrated and hydrophilic, while above it, the hydrogel becomes dehydrated and hydrophobic. These theories explain the bigger diameter of chitosan fiber before 40 °C and the reduction in their diameters as temperature increase beyond 40 °C. Around this temperature, chitosan is believed to form glasses before crystallize. This phenomenon may explain the high crystalline/ amorphous ratio obtained at 40 °C in Figure 16 B but the low strength and stiffness values shown in Figure 17.

When individual parameters were combined, significant improvement in fiber strength and stiffness were achieved. This improvement is a result of forming chitosan fibers with more crystalline structure which resist swelling.

Physical and chemical treatments which were used to improve chitosan fibers mechanical properties did not affect fiber biocompatibility and supported cell attachment and proliferation in a short term culture. In Chapter eight, detailed evaluation of fiber biocompatibility with mesenchymal stem cells will be introduced.

## **6.5 Conclusions and Future Work**

Chemical modification was shown previously to improve fibers mechanical properties but caused structural changes and potentially result in adverse toxicity effects which hinder the use of these modified fibers in tissue engineering applications. Improving chitosan fibers produced through polymer fiber extrusion technique was demonstrated through physical treatments avoiding any potential major structural changes or toxicity effects. These findings should expand the use of chitosan fibers with

improved mechanical properties in numerous tissue engineering applications. Despite that the effect of these mechanically improved fibers was not evaluated on scaffold mechanical properties, it is still expected that these improved fibers will provide additional strength and stiffness to the scaffold.



## CHAPTER SEVEN

# ISOLATION, CHARACTERIZATION AND PROLIFERATION OF OVINE BONE MARROW- DERIVED MESENCHYMAL STEM CELLS: POTENTIAL SOURCE FOR CARDIOVASCULAR TISSUE ENGINEERING

## 7.1 Introduction

### 7.1.1 Bone Marrow-Derived Mesenchymal Stem Cells (MSC)

Human mesenchymal stem cells (hMSCs), which are present in adult bone marrow, are believed to be multipotential cells (Pittenger *et al.*, 1999). MSCs are a rare population of adult bone marrow (0.001-0.01%) and their number decreases with age (Rao and Mattson, 2001). Isolating these cells from peripheral blood and cord blood is hard due to limited number of cells (Miao *et al.*, 2006). hMSCs have the ability to replicate as undifferentiated cells and differentiate to various mesenchymal tissue lineages such as bone, cartilage, fat, tendon, muscle and marrow stroma (Rebelatto *et al.*, 2008). The ability of a population of mesenchymal stem cells within the bone marrow to differentiate into bone and cartilage was first suggested by Friedenstein nearly 40 years ago (Miao *et al.*, 2006) Upon isolating and culturing, MSCs display a stable phenotype and grow as a monolayer *in vitro*. Several studies have shown that MSCs possess the ability to exclusively differentiate upon induction into adipogenic, osteogenic and chondrogenic lineages (Pittenger *et al.*, 1999; Sutherland *et al.*, 2005; Rebelatto *et al.*, 2008). MSCs gained a great attention from researchers around the world mainly because of their therapeutic potential for tissue or organ repair.

### 7.1.2 Characterization of Bone Marrow-Derived Mesenchymal Stem Cells

Characterization of multipotency property of MSCs can be demonstrated by three ways: First, MSCs must be plastic-adhesive and have self-renewal properties when maintained in standard culture conditions. Second, MSCs must express CD105, CD73 and CD90, and lack the expression of CD45, CD34, CD14 or CD11b, CD79 $\alpha$  or CD19 and HLA-DR surface molecules. Third, MSCs must differentiate into adipocytes (fat), osteoblasts (bone), and chondroblasts (cartilage) *in vitro* using lineage-specific inducing media (De Ugarte *et al.*, 2003). However, most recent studies have demonstrated that MSCs differentiation potential may vary depending on the source (Rebelatto *et al.*, 2008) and the culture medium supplements (Chase *et al.*, 2010).

### 7.1.3 Bone Marrow MSCs in Tissue-Engineered Heart Valves Applications

Despite that MSCs can be easily isolated from the bone marrow in animals and humans, low cells number is still a major limitation for broad study of these cells. Possible locations in humans and animals are the iliac crest, femur, sternum, fetal blood and liver, cord blood and in some cases, in adult peripheral blood (Miao *et al.*, 2006). MSCs can be phenotypically converted into endothelial cells (EC) *in vitro* by culturing with 50 ng/ml of vascular endothelial growth factor (VEGF) (Song *et al.*, 2007). MSCs can also provide a source for fibroblasts/ myofibroblasts and smooth muscle cells (SMC) (Song *et al.*, 2007; Kurpinski *et al.*, 2010; Song *et al.*, 2010). Recent research efforts have investigated the potential of bone marrow MSCs to differentiate when seeded on synthetic heart valve scaffolds (Sutherland *et al.*, 2005). MSCs isolated from bone marrow were seeded PGA/PLLA nonwoven meshes semilunar heart valve

scaffolds and statically cultured for 4 weeks and then implanted at the pulmonary valve position into sheep for 8 months. At the end of the study, MSCs showed the ability to differentiate into SMC, EC and fibroblasts. The results also showed that histological structure similar to the native heart valve was obtained.

Another research effort investigated seeding MSCs isolated from bone marrow on PGA/P4HB composite heart valve scaffolds (Perry *et al.*, 2003). Scaffolds were cultured for 1 week statically and then transferred to a pulse duplicator bioreactor for 2 weeks. The preliminary results showed patchy surface confluency of cells and deep cellular material. However, the study did not perform immunohistochemistry studies to determine the type of the cells which covered and penetrated the surface. Biomechanical testing showed that the leaflets had a comparable stiffness to the native heart valve.

## **7.2 Experimental Work**

### **7.2.1 Isolation of Ovine Bone Marrow Mesenchymal Stem Cells**

The protocol developed by DeUgarte and Hedrick for isolating mesenchymal stem cells from sheep bone marrow was followed with some modification (De Ugarte *et al.*, 2003). Briefly, Sheep femur bones were collected 4-6 hours after slaughtering from Saad slaughterhouse, Eastern Market, MI. Femur bones were cut at the epiphyses from both sides and the bone marrow was extracted as a whole and then cut into small pieces. 10 ml of DMEM medium added to the bone marrow pieces and then vortexed for 3 minutes. The mixture was then passed through a 100 $\mu$ m filter. The remaining bone marrow washed 3 times with medium and the washing medium collected and

centrifuged for 10 minutes at 2500 rpm. The supernatant was then aspirated and cells were resuspended in DMEM culture medium supplemented with 10% FBS, 250 µg/ml amphotericin B (Fungizone) and 0.01 mg/ml Gentamicin. Cells seeded at 2 million cells/cm<sup>2</sup> and cultured, labeled passage zero, maintained at 37°C in 5% CO<sub>2</sub> in air. The first medium change was done on day 5 of culture after MSCs started to attach. When cells reached 70% confluency on day 15 of culture, cells were passaged using Trypsin-EDTA. Briefly, cells were washed 2 times with warm PBS for 5 minutes each and then Trypsin was added to the plates and incubated for 10 minutes in the incubator. Trypsin neutralization was achieved by adding fresh DMEM medium supplemented with FBS to the plates. Cells were collected and centrifuged for 10 minutes at 2500 rpm and then the supernatant was aspirated and cells were resuspended in medium and cultured, labeled passage 1, at low density of 2000 cells/cm<sup>2</sup>.

### **7.2.2 Cryopreservation of Sheep Bone Marrow Mesenchymal Stem Cells**

MSCs were cryopreserved by deep-freezing in liquid nitrogen after the first passage until further use. Freezing medium consists of DMEM supplemented with 30% FBS and 5% Dimethylsulfoxide (DMSO). Cells were detached from the plate surface as mentioned before. Freezing medium was added to the cells pallet. Cells were distributed in freezing vials at 500,000 cells/vial and froze for 3 hours in 100% isopropanol dry ice and then stored in liquid nitrogen.

### **7.2.3 Characterization of Bone Marrow-Derived Mesenchymal Stem Cells (MSCs)**

To characterize the isolated MSCs, a differentiation into chondrogenesis, adipogenesis, and osteogenesis lineages was conducted. Passage 6 frozen vial was

cultured in DMEM culture medium supplemented with 10% FBS, 250 µg/ml amphotericin B (Fungizone) and 0.01 mg/ml Gentamicin. When cells reached 80% confluency, differentiation experiment was conducted on 2-D dish cultures for the three lineages. For each lineage, two-duplicate cultures were used and two cultures were used as a control.

### **Differentiation of MSCs into Adipocytes**

After culturing MSCs for a week in a normal culture medium, adipogenic differentiation was induced by culturing cells for 3 weeks in adipogenic medium consisting of DMEM culture medium supplemented with 15% FBS, 0.5 mM isobutylmethylxanthine, 1 µM dexamethasone, 5 µg/ml insulin and 60 µM indomethacin. To demonstrate that the MSCs differentiated into adipocytes, Oil Red O staining was used to visualize lipid-rich vacuoles. Briefly, cells were fixed for 60 minutes at room temperature in 4% formaldehyde and then washed with 70% ethanol. Cells were incubated in 2% (w/v) oil red O reagent for 5 minutes at room temperature. Excess stain was removed by washing with 70% ethanol followed by several washes with distilled water. Counter stained for 2 minutes was then applied using hematoxylin and Eosin Staining (HE) to stain the nucleus.

### **Differentiation of MSCs into Osteocytes**

Osteogenic differentiation was induced after 1 week of culturing in normal culture medium. Cultured cells were induced for 3 weeks of culturing using DMEM culture medium supplemented with 15% FBS, 0.1 µM dexamethasone, 100 µM ascorbate-2-

phosphates and 10 mM  $\beta$ -glycerophosphate. The deposition of minerals in experimental cultures was demonstrated by von Kossa staining.

### **Differentiation of MSCs into Chondrocytes**

Chondrogenic differentiation was induced after 1 week of cell culture in normal culture medium. Cells were detached using Trypsin and then centrifuged at 300g for 10 minutes in a 15-ml polypropylene tube to form pellet. Chondrogenic differentiation medium consists of DMEM high glucose (HG) supplemented with 1% FBS, 0.5  $\mu$ g/ml insulin, 10 ng/ml TGF $\beta$ -1, 50  $\mu$ M ascorbate-2-phosphate, and 1% ABAM. Medium was gently overlaid to avoid detaching the cell nodules. Cultures were maintained in chondrogenic medium for 2 weeks prior to analysis. Safranin O staining was used to visualize the deposition of proteoglycans where Masson's Trichrome staining was used to visualize the deposition of collagen type II within the nodules.

### **7.2.4 MSCs Differentiation into Smooth Muscle Cells (SMC)**

Differentiation of MSCs into SMC started immediately at day one of culture by inducing the differentiation by specific SMC differentiation medium. Differentiation medium consists of DMEM-HG supplemented with 30% FBS, 1 ng/ml TGF $\beta$ -1 and 30  $\mu$ M ascorbate-2-phosphates, while control cells were grown in DMEM-HG supplemented only with 10% FBS. Differentiation properties were analyzed after one week of inducing the differentiation.  $\alpha$ -smooth muscle actin ( $\alpha$ -SMAActin) staining was used to confirm the differentiation of MSCs into SMC using primary antibody, mouse anti  $\alpha$ -smooth muscle actin clone 1A4-Fluorescein isothiocyanate (FITC) (Sigma) according to the manufacturer protocol. Briefly, cultured MSCs were fixed by incubating

with 4% formaldehyde solution for 10 minutes at room temperature. The cells were then washed twice with PBS. The fixed cells were then permeabilized by incubating in 0.2% Triton X-100 in PBS for 1-1.5 minutes at room temperature and gently rinsed with PBS four times. Cells were then incubated with blocking solution of 5% non-fat dry milk in PBS for 30 minutes. Later on, the blocking solution was aspirated off, and the surfaces were washed with PBS four times. The cells were then stained with primary antibody, mouse anti  $\alpha$ -smooth muscle actin clone 1A4-Fluorescein isothiocyanate (FITC) (Sigma) at a dilution of 1:250, for 2-3 hrs at room temperature in the dark. To the existing antibody staining solution, 300  $\mu$ L of 300 nm DAPI (counter-stain) solution was added and incubation was continued for another 5 minutes. Later on, the staining solution was removed and surfaces were washed 5 times with PBS over 30 minutes in dark. After that, the stained cells were observed under the fluorescence microscope.

Alamar blue assay (Molecular Probes, Invitrogen, CA) was used to evaluate MSCs proliferation in growth and differentiation mediums according to the manufacturer protocol. Briefly, alamar blue solution was diluted at 1:10 volume ratio in fresh DMEM-HG culture medium and the mixture was then incubated with cells for 4 hours. Absorbance was read using Perkin Elmer spectrophotometer at 570 nm and normalized to absorbance readings at 600 nm.

### **7.2.5 Effect of Serum Concentration on MSCs Proliferation and Attachment**

Serum concentration in culture medium almost affects the proliferation of any cell type due to the components contained in it. To assess the effect of serum concentration on MSCs proliferation, MSCs at cell density of 10,000 cells/cm<sup>2</sup> were cultured in DMEM-HG culture medium supplemented with different concentration of fetal bovine serum

(FBS). FBS concentrations were 1, 2.5, 5, 7.5, 10, and 30%. MSCs cultured in culture medium without any FBS were used as a control. Additionally, the effect of different concentrations of FBS in culture medium were compared to proliferation of MSCs cultured in differentiation medium which contains 30% FBS, 1 ng/ml of TGF- $\beta$ 1 and 30  $\mu$ M of ascorbic acid. MSCs were marinated in cultures for 5 days and Alamar blue assay was used to measure the proliferation rate at day 1, 3 and 5 of culture.

### **7.2.6 Effect of Immobilized GAGs on MSCs Proliferation and Attachment**

The aim of this study was to evaluate the effect of different immobilized GAGs on chitosan membranes on MSCs proliferation. Heparan Sulfate (MW 10-12 KDa), Heparin sodium (MW 10-12 KDa) were both purchased from Celsus laboratories, Chondroitin-4-Sulfate sodium salt from bovine trachea (MW 20-30 KDa) purchased from Sigma Aldrich and hyaluronic acid sodium salt (MW 1600-1800 KDa) purchased from BioChemika-Fluka were covalently immobilized on chitosan membranes as described in literature (Uygun et al., 2009). Briefly, chitosan solution was air dried in 24 well plate for overnight. Pre-activated GAGs solution at 1:1 chitosan to GAGs mass ratio was added to the dry membranes and allowed to react overnight. Pre-activated solution was prepared by mixing equal volume of EDC solution prepared at a concentration such that the molar ratio of EDC to GAGs carboxyls in the reaction mixture was 10:1. Membranes were then washed with PBS and sterilized with 80% ethanol. MSC of passage 6 were seeded on different GAGs-Chitosan membranes at 60,000 cells/cm<sup>2</sup>. Cultures were maintained in DMEM-HG culture medium supplemented with 1% ABAM and 10% FBS for 8 days. Phase contrast Images at day 1 and day 3 were taken to observe any morphological changes in the cultures of different immobilized GAGs. Alamar blue

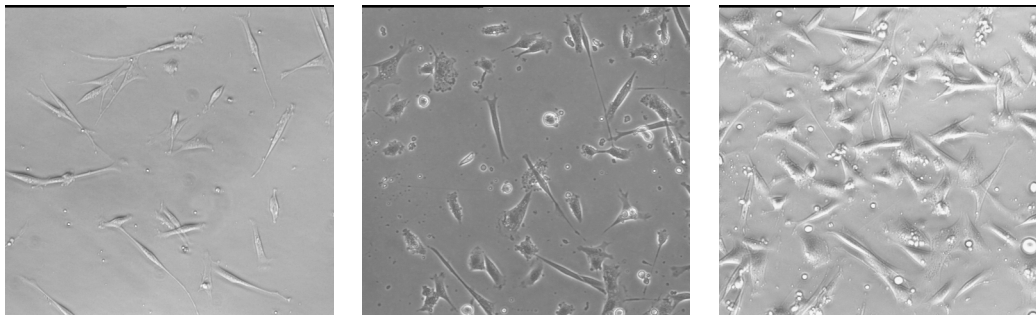


(Invitrogen, CA) assay was used according to the manufacturer protocol to quantify MSC proliferation.

### 7.3 Results

#### 7.3.1 Isolation of Ovine Bone Marrow-Derived MSCs

MSCs isolated from sheep bone marrow attached well to plastic culture plates as shown in Figure 20. Cultured MSCs formed a monolayer and had a bipolar to polygonal fibroblast-like shape. During MSCs culturing, cell proliferation potential increased as the culture time increased.



**Passage Zero, Day8**

**Passage Zero, Day13**

**Passage Zero, Day15**

Figure 20: Cell attachment and morphology of MSCs at passage 0 during isolation,

Objective is 10X

Subculturing until passage 6 was reached easily to magnify the number of available MSCs from the same batch for future experiments. Figure 21 shows MSCs of different passages cultured and grown. Phase contrast images show that subculturing

did not affect the proliferation potential or the adhesion capacity of MSCs up to passage 4.

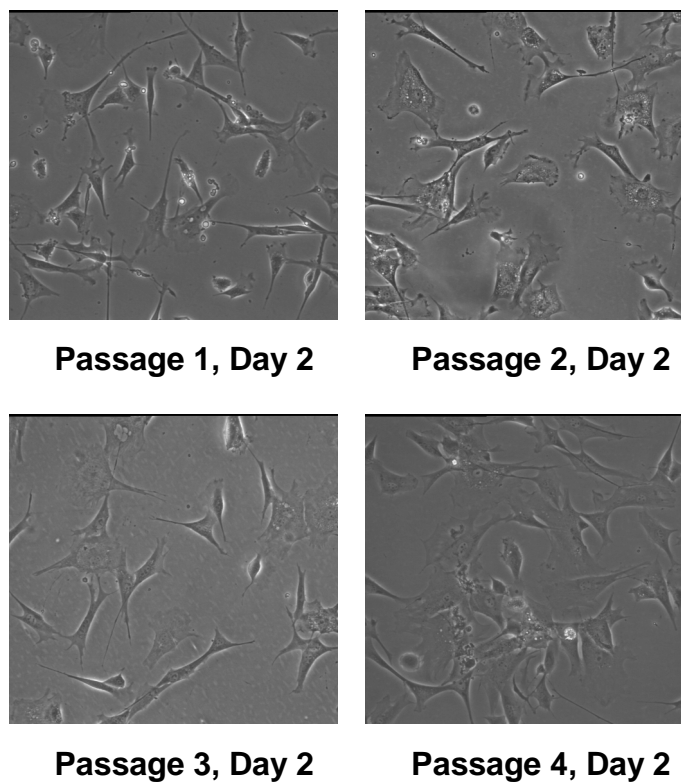


Figure 21: Subculturing of MSCs up to passage 4, objective is 10X

## 7.3.2 Characterization of MSCs

### 7.3.2.1 MSCs Differentiation into Adipocytes

Figure 22 shows phase contrast microscopy images for control and experimental cultures captured at different time points. Day 6 shows the beginning of formation of oil drops in the experimental cultures indicating the starting of MSCs differentiation into adipocytes. The formation of oil drops continued to form as the culture days increased.

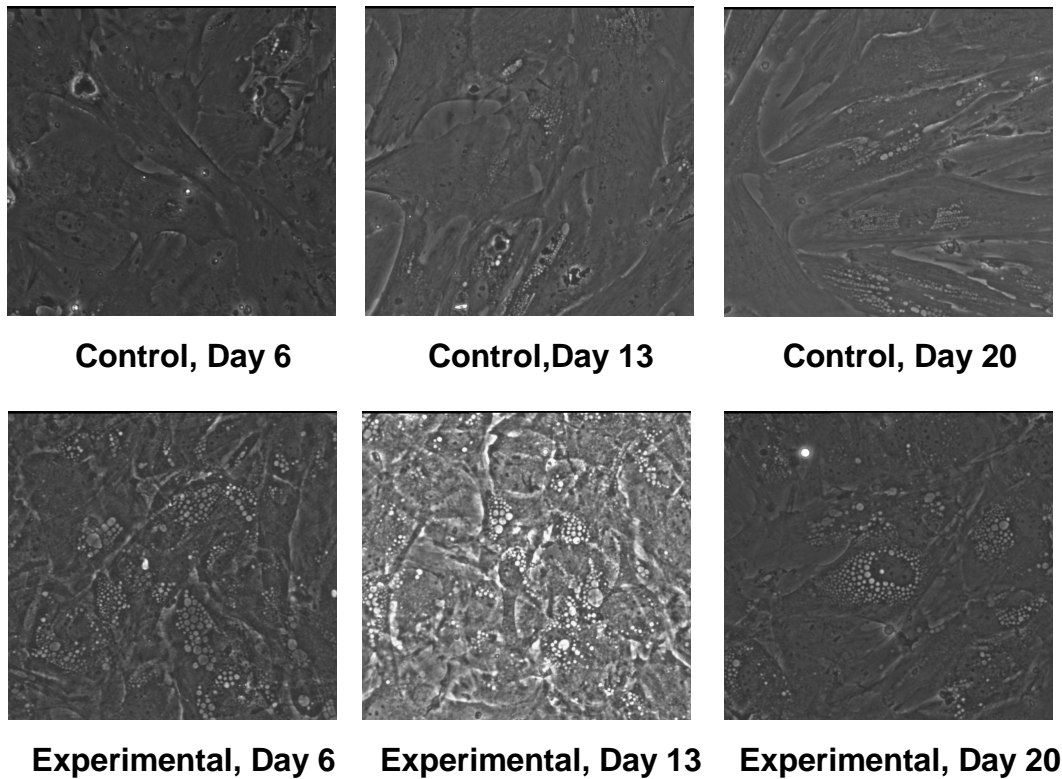


Figure 22: MSCs differentiation into adipocytes. Formation of oil vacuoles indicating MSCs differentiation into adipocytes at Day 20, Objective 20X

Adipogenic differentiation was shown by changes in cell morphology which was then followed by formation of lipids vacuoles during the culture period as seen in Figure 22. However, Oil Red O- stain results did not show that cells stained with oil red stain despite that the oil droplets were clearly visible with phase contrast microscopy images. This can be due to the high passage of MSCs that were used (passage 6). Literature suggested that a lower passage (<3) should be used to differentiate MSCs to adipocytes (Rebelatto *et al.*, 2008).

### 7.3.2.2 MSCs Differentiation into Osteocytes

MSCs cultured with osteogenic medium formed colonies as seen in figure 23 at day 13. The cellular morphology changed from fibroblast-like cells to a cuboidal form as starting at day 6 of culture and more obvious at day 13 of culture.

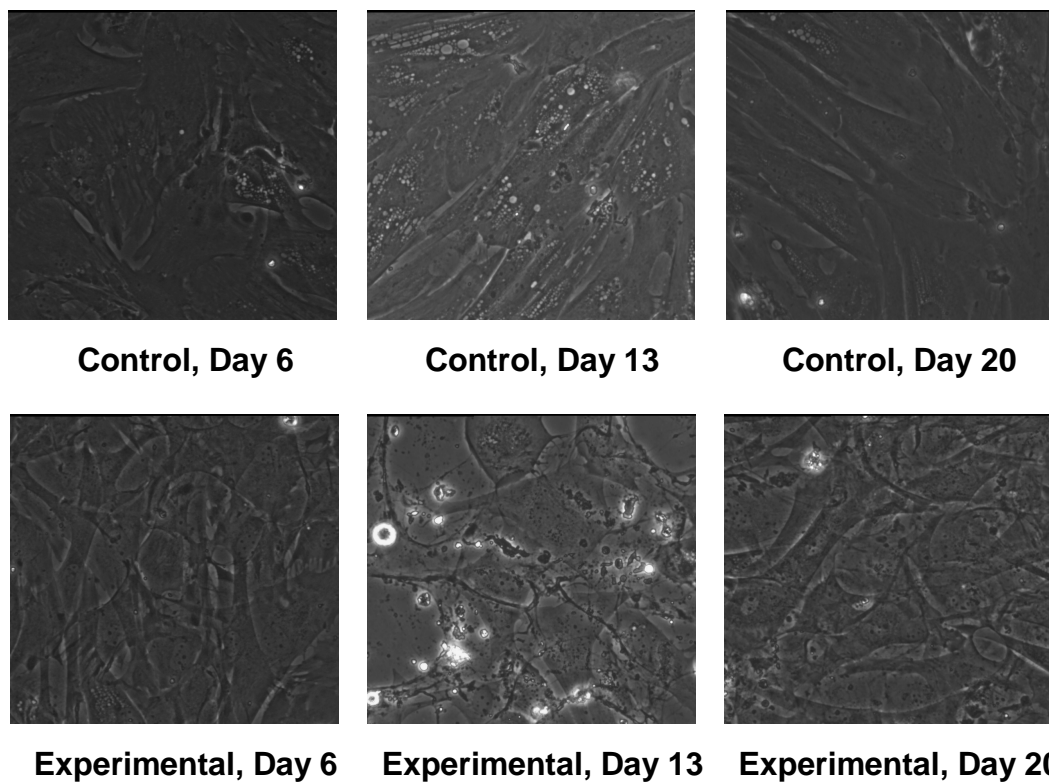


Figure 23: Morphological changes in MSCs during their differentiation into osteocytes,  
Objective 20X

Figure 24 shows that calcium deposition was present in the experimental cultures and not in the control cultures. Safranin O was used as a counter stain. Figure 24 shows the tissue culture plates for control and experimental cultures. Experimental

cultures showed higher amount of nodule formation within the culture. Stain confirms that MSCs differentiated into osteocytes lineage.

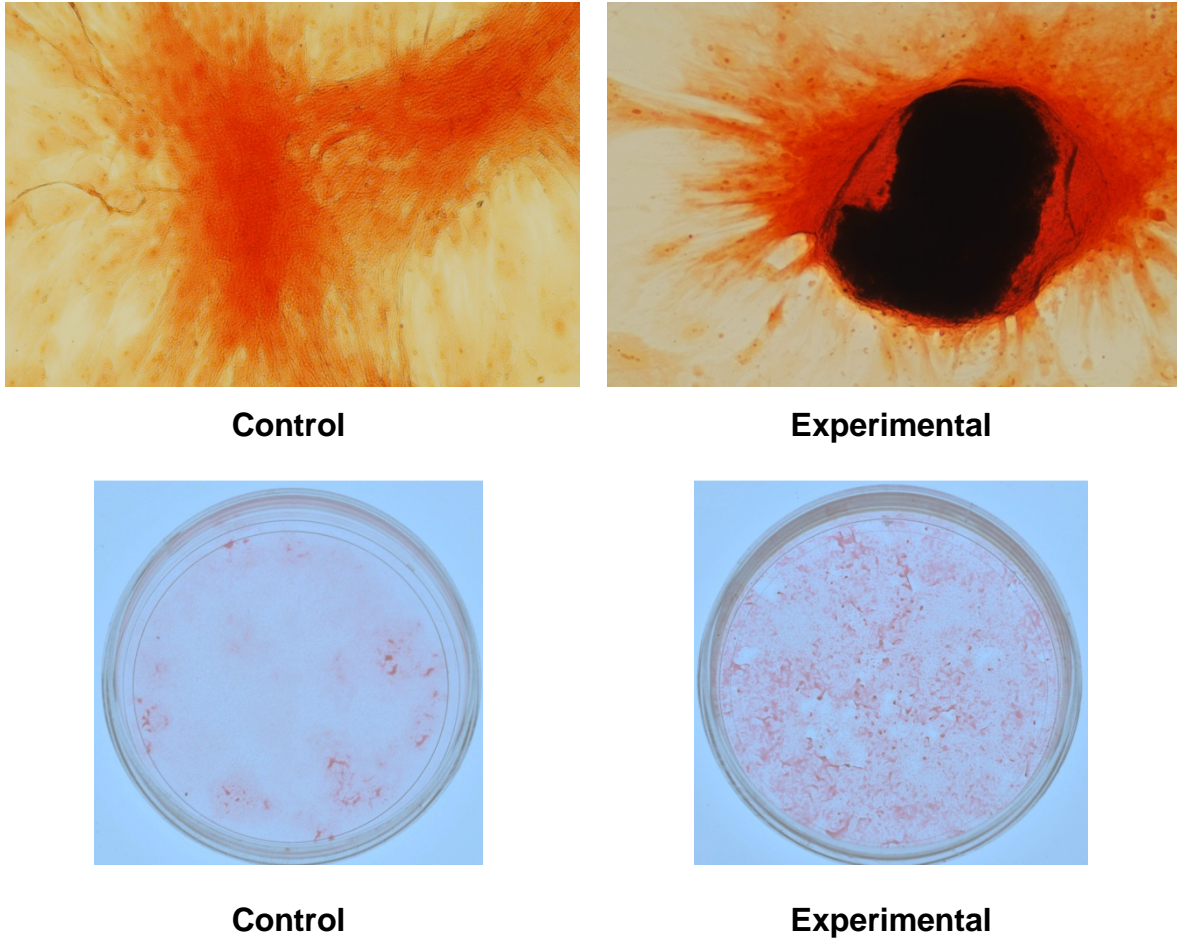
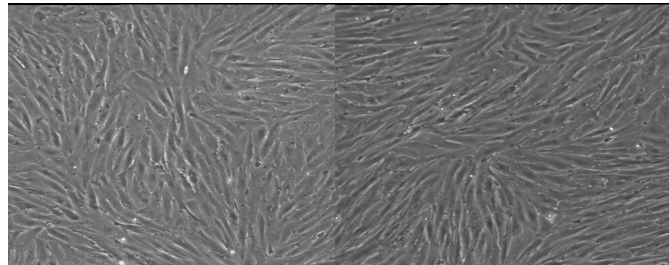


Figure 24: Von Kossa and safranin-O staining at higher magnification, upper panel, and the whole culture plate, lower panel

### 7.3.2.3 MSCs Differentiation into Chondrocytes

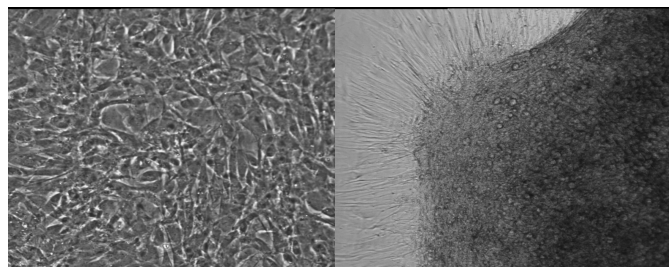
Figure 25 shows the morphological changes of control and experimental cells. As the culture goes on, cells in experimental cultures have polygonal shape and start to

form multiple layers before detachment which are indications of MSCs differentiation into chondrocytes.



**Control, Day 13**

**Control, Day 20**



**Experimental, Day**

**13**

**Experimental, Day**

**20**

Figure 25: Morphological changes of MSCs during their differentiation into Chondrocytes, Objective 4X

Figure 26 shows H&E staining that was used to visualize the cells distribution and morphology within the pellet. Higher magnification of the pellet shows cells stained blue. Safranin-O staining was used to visualize the deposition of protoglycans within the pellet. Mason's Trichrome staining was used to confirm the presence of collagen type II

which stained blue. These results confirmed the differentiation of MSCs into chondrocytes.

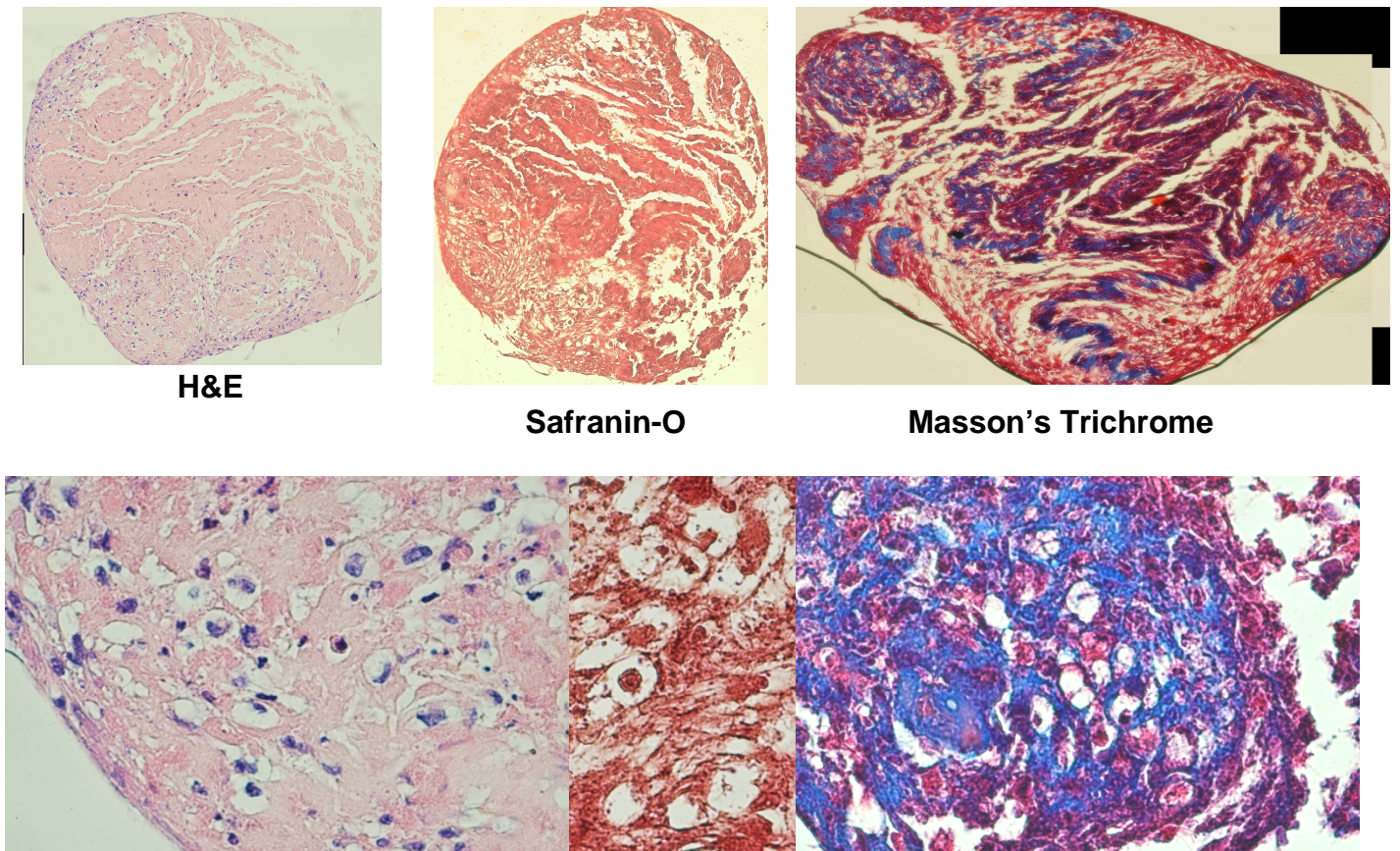


Figure 26: H&E, Safranin-O and Masson's Trichrome staining confirm the differentiation of MSCs into chondrocytes

#### 7.3.4 Differentiation of MSCs into Smooth Muscle Cells (SMC)

MSCs differentiation into SMC was induced with higher concentration of FBS and the addition of TGF- $\beta$ 1 and ascorbic acid to the culture medium. Figure 27 shows that there was no morphological difference of MSCs cultured in growth medium (referred as control) and MSCs cultured in differentiation medium (referred as experimental).

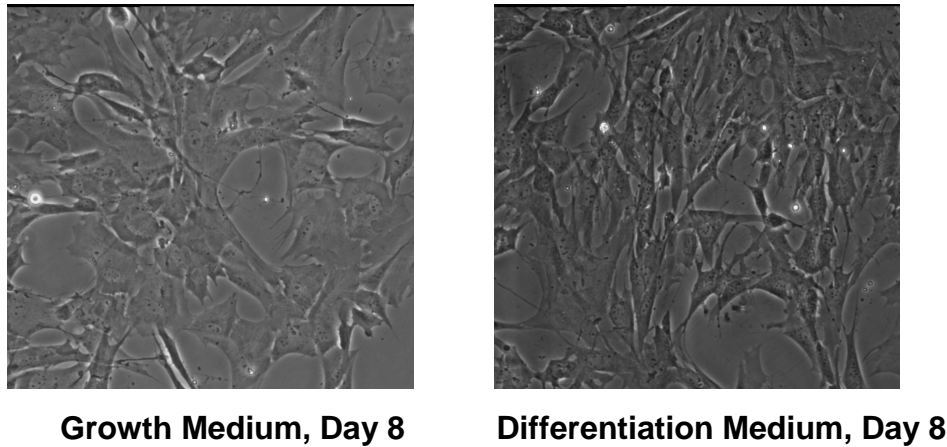
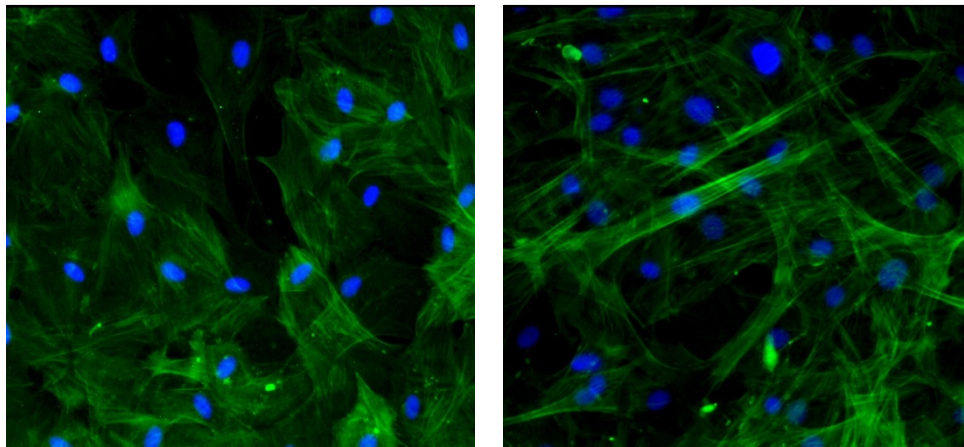


Figure 27: Morphological changes of MSCs during differentiation into SMCs, Objective 10X

Staining results for  $\alpha$ -SMAActin showed that both MSCs cultured in growth medium and differentiation medium stained for SMC marker. The amount of actin protein produced by MSCs cultured in growth medium or differentiation medium using western blot analysis was quantified. Results, as shown in Figure 29, demonstrated that there was no statistical difference between the amount of actin protein produced by MSCs cultured in both mediums. Two possible mechanisms might explain why MSCs cultured in growth medium stained positive with  $\alpha$ -SMAActin: first, is the effect of transforming growth factor-  $\beta$ 1 (TGF- $\beta$ 1). It has been suggested in literature that 1 ng/ml of TGF- $\beta$ 1 is sufficient to induce the differentiation of MSCs into SMCs (Narita *et al.*, 2008). Normally, traditional FBS can contain 16 ng/ml of TGF- $\beta$ 1, so growth medium which contains 10% FBS may have 1.6 ng/ml of TGF- $\beta$ 1 that was sufficient to induce the differentiation. The second mechanism is that some MSCs are believed to be



pericytes (Caplan, 2008). To test the validity of this hypothesis, freshly isolated MSCs of passage 0 were cultured in DMEM without FBS for one day and stained with  $\alpha$ -SMAActin. As shown in Figure 29, MSCs showed expression of  $\alpha$ -SMAActin which might indicate that these cells have similar synthetic characteristics to SMC. The two mechanisms will be discussed in detail in the discussion section in this chapter.



**Growth Medium, Day 8**

**Differentiation Medium, Day 8**

Figure 28:  $\alpha$ -SMAActin staining confirms that both MSCs cultured in growth medium or differentiation medium differentiated into SMC, Objective 20X

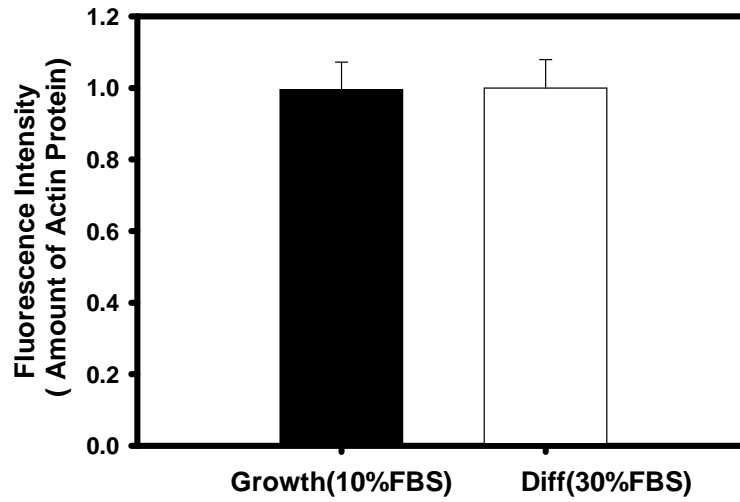


Figure 29: Amount of Actin production in MSC cultured in growth medium or differentiation medium

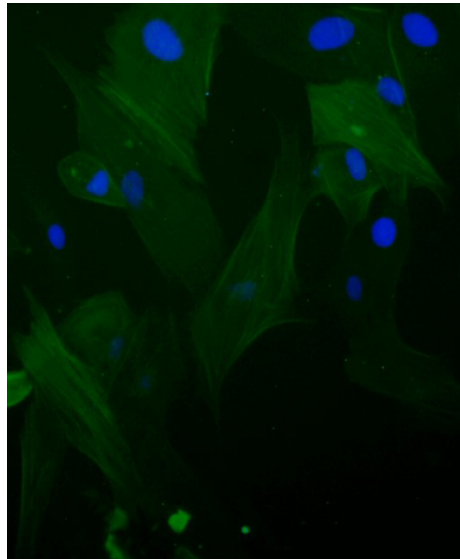


Figure 30:  $\alpha$ -SMA Actin staining of MSC of Passage 0 cultured in DMEM culture medium without FBS for 1 day, Objective 20X

MSCs proliferation was evaluated for cells cultured in both mediums for 5 days. In both cultures, results showed that MSCs demonstrated the same growth rate.

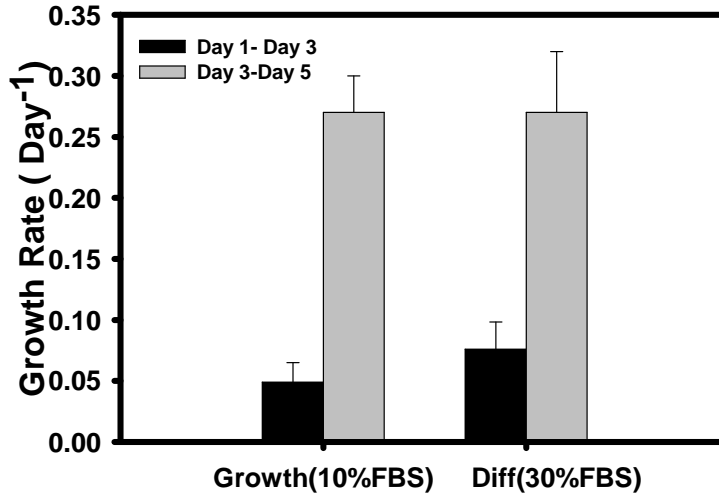


Figure 31: Growth rate of MSC cultured for 5 days in growth medium or differentiation medium

### 7.3.5 Effect of Serum Concentration on MSCs Proliferation and Attachment

MSCs cultured with different concentration of FBS showed an immediate attachment on tissue culture plates as seen in Figure 32. After one day of culture in different serum concentrations, MSCs attached to the surfaces and spread. It's likely that MSCs has high adhesion capacity as they well adhered to the tissue culture plate when they even cultured in a culture medium without any FBS. There was no clear morphological changes of MSCs cultured in different concentration of FBS. However, MSCs showed a different proliferation rate with changing the concentration of the FBS in the culture medium. The growth rate of MSCs decreased after day 3 when cultured without FBS in the medium. It's likely that MSCs proliferation was hindered by that fact that the culture medium does not have the necessary growth factors for proliferation

such as transforming growth factor- $\beta$ 1 (TGF- $\beta$ 1), human platelet-derived growth factor-BB (PDGF-BB) and basic fibroblast growth factor (bFGF). MSCs cultured in high serum medium (< 10% FBS) showed higher growth rate compared to the same population cultured in low serum medium, however, the difference is not remarkable for the same period of culture. It's necessary to mention again here that there was no statistical difference between the growth rate of MSCs cultured in 10% FBS (growth medium) and differentiation medium. This was consists with the results demonstrated in Figure 31 above.

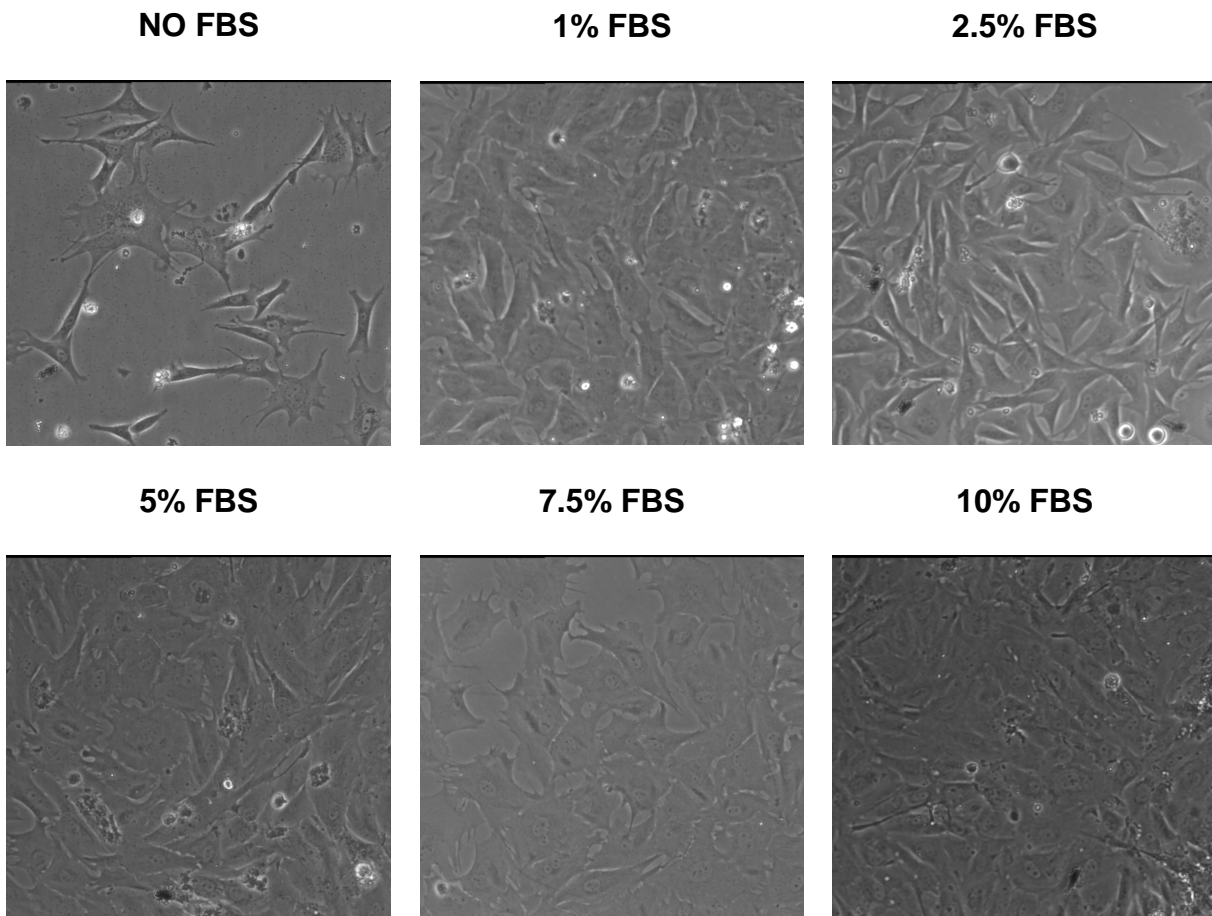


Figure 32: Effect of serum concentration in culture medium on MSCs attachment and spreading, Objective 10X

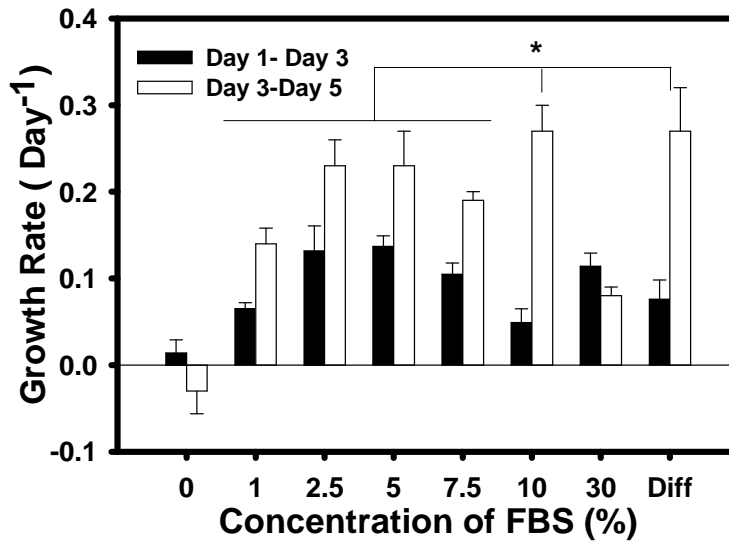
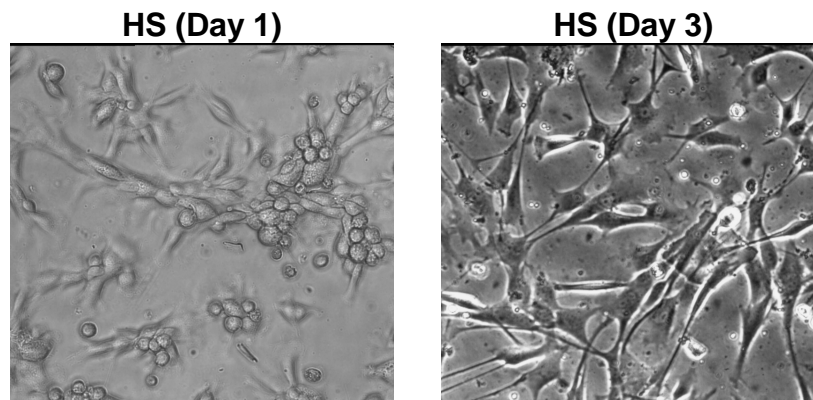


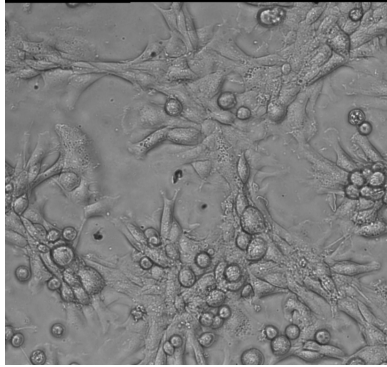
Figure 33: Effect of Serum concentration on MSCs proliferation for 5 days culture.

### 7.3.6 MSCs Proliferation GAG-Chitosan Membranes

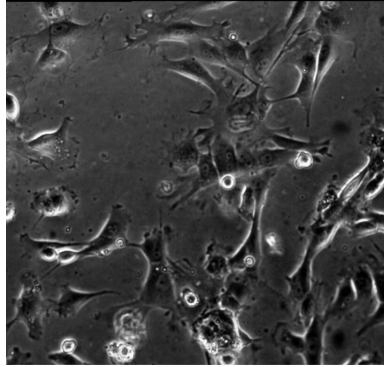
As it appears in Figure 34, all GAGs supported MSC attachment and spreading from day 1 except on chondroitin-4-sulfate (C4S) surfaces. Upon attachment, MSCs were elongated and showed spindle shape morphology. MSCs continued to spread and proliferate throughout the culture period including C4S surfaces. MSCs cultured on chitosan membranes showed immediate cell attachment and spreading from the first day of culture.



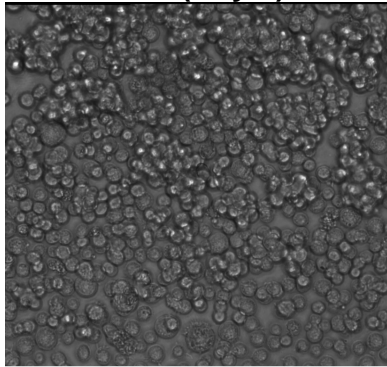
**Hep (Day 1)**



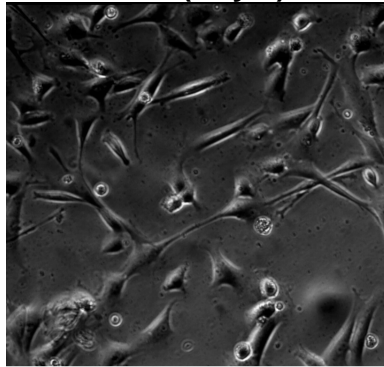
**Hep (Day 3)**



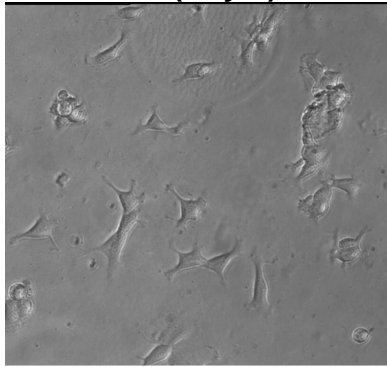
**C4S (Day 1)**



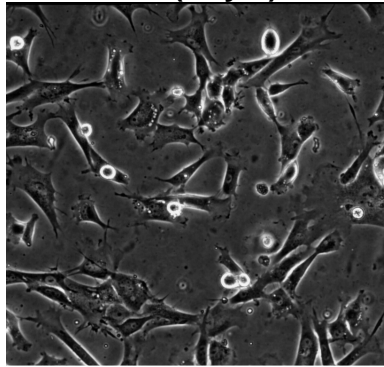
**C4S (Day 3)**



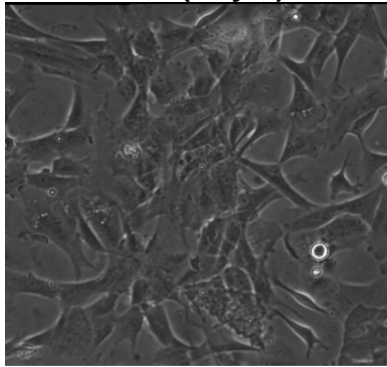
**HA (Day 1)**



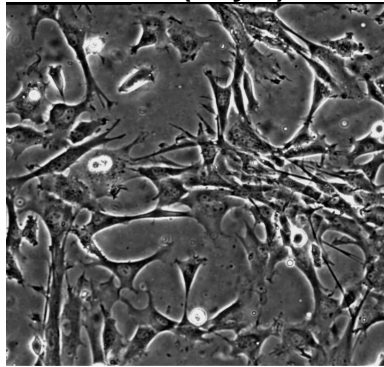
**HA (Day 3)**



**Chit (Day 1)**



**Chit (Day 3)**



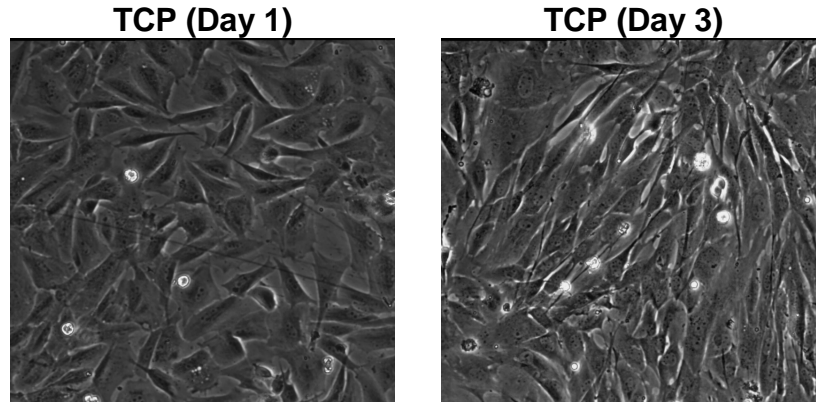


Figure 34: Cell morphology of MSC cultured on different immobilized GAGs, HS (Heparan Sulfate), Hep (Heparin Sodium), C4S (Chondroitin-4-Sulfate), HA (hyaluronic Acid), Chit (Chitosan) and TCP (Tissue Culture Plate). Objective is 10X.

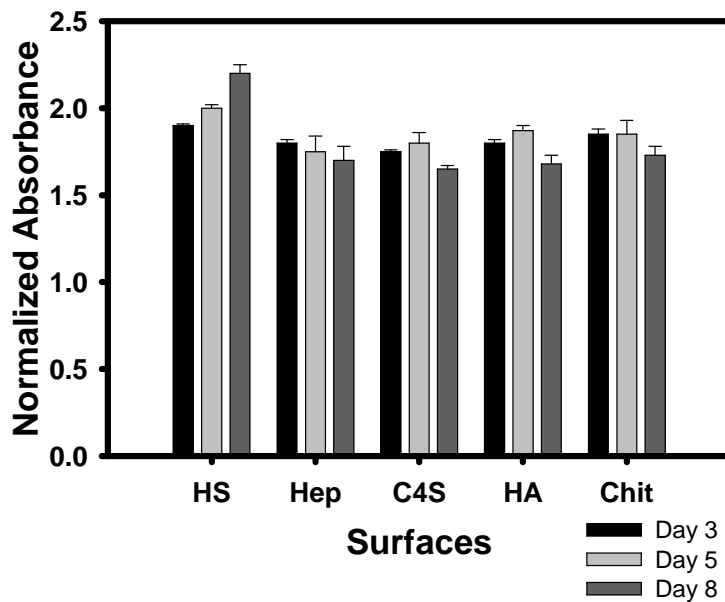


Figure 35: Effect of different immobilized GAGs on MSC proliferation for 8 days in static culture.

## 7.4 Discussion

In this study, isolation and characterization of ovine bone marrow-derived mesenchymal stem cell were demonstrated. Despite the limitation with the number of MSC that can be isolated from the bone marrow, yet MSCs were isolated in a sufficient number to conduct the experiments outlined in this chapter and in the following chapter. As there is no definitive marker to characterize MSCs, usually, MSCs are characterized by their adhesion capacity and the multipotency ability to differentiate into adipocytes, chondrocytes and osteocytes. Isolated cells were confirmed to be MSCs using inducing differentiation medium into the three main lineages. Induced cells showed the ability to differentiate into the desired population within 3 weeks at maximum.

The differentiation of MSCs into smooth muscle like cells was demonstrated in this chapter. MSCs stained positive for  $\alpha$ -SMAactin marker, an early differentiation marker for smooth muscle cells (SMC). However, it is necessary to mention that MSCs cultured in either the differentiation medium which contains 30% FBS and 1ng/ml of TGF- $\beta$ 1 or the growth medium which contains 10% FBS showed positive expression of  $\alpha$ -SMAactin. These findings suggest two mechanisms that might control the differentiation of MSCs into SMC. The first mechanism is controlled by TGF- $\beta$ 1 concentration in the culture medium. TGF- $\beta$ 1 has been shown previously to induce the differentiation of neural crest stem cells into SMC (Shah *et al.*, 1996; Chen and Lechleider, 2004), embryonic stem cells into SMC (Sinha *et al.*, 2004) and adipose tissue derived stem cells into SMC (Jeon *et al.*, 2006). Narita and colleagues studies the effect of TGF- $\beta$ 1 on MSCs differentiation into SMC (Narita *et al.*, 2008). In their study, it was shown that increasing the concentration of TGF- $\beta$ 1 in the culture medium from 0.1



ng/ml up to 10 ng/ml significantly increased the expression level of smooth muscle specific genes ( $\alpha$ -SMAActin, Calponin and SM22). Also, it was concluded in this study that 1ng/ml of TGF- $\beta$ 1 is enough to induce the differentiation of MSCs into SMC. Actin protein expression shown in Figure 29 in this chapter demonstrated that both MSCs cultured in growth medium or differentiation was almost the same. The reason behind this similarity in protein expression level is due to the FBS. It has been well documented in the literature that 1 ml of FBS contains up to 16 ng/ml of TGF- $\beta$ 1 (Danielpour, 1993; Lucia *et al.*, 1998). In the growth culture medium which contains 10% FBS, the concentration of TGF- $\beta$ 1 can be as high as 1.6 ng/ml. It was well documented in literature that 1 ng/ml of TGF- $\beta$ 1 is sufficient to induce the differentiation of MSCs into SMC and increase the gene expression of SMC specific markers (Narita *et al.*, 2008). This might explain why MSCs cultured in 10% FBS stained positive for  $\alpha$ -SMAActin. It was also shown that concentrations higher than 1 ng/ml of TGF- $\beta$ 1 did not upregulate the gene expression for all SMC specific markers (Narita *et al.*, 2008). This might explain why there was no difference in actin protein production in both cultures.

The growth rate of MSC did not change when cultured in growth medium or differentiation medium. It has been shown before that TGF- $\beta$ 1 provides no significant enhancement of cell proliferation on its own (Chase *et al.*, 2010). This might explain why growth rates were not statistically significant.

The second mechanism is that some MSCs are now believed to be pericytes, the cells that cover the outermost layer of small blood vessels, as MSCs express cell markers similar to the pericytes (Caplan, 2008). Moreover, this relationship between MSCs and pericytes was further confirmed by the ability of pericytes to express the

surface cell markers CD146+, CD34-, CD45-, CD56- and by the subsequent in vitro differentiation of pericytes into osteogenic, chondrogenic, adipogenic and myogenic lineage, which are hallmarks for MSC identity (Caplan, 2007). However, MSCs differ from pericytes as the latter lack the ability to differentiate into hematopoietic or neural phenotypes in vitro (Kiel *et al.*, 2005). In Figure 31, it was shown that MSC of passage 0 stained positive for  $\alpha$ -SMAActin after culturing for one day in culture medium without FBS. This might support that MSCs are pericytes and have similar phenotype to SMC. Ball and colleagues showed that cultured MSCs had some similar characteristics of synthetic state vascular smooth muscle cells (SMC) (Ball *et al.*, 2004).

The proliferation assay results of MSCs cultured in different concentrations of FBS demonstrated that MSCs proliferation increased with increasing FBS concentration in the medium, however, the difference in the proliferation rate was not remarkable. Despite that serum does possess a proliferative effect on most cells including MSCs; it also contains a number of some components which vary from one lot to another. Moreover, serum components are not even fully known or characterized. As a result, the use of relatively high concentration of FBS (<10%) in MSCs cultures will definitely provide inconsistent results in MSCs proliferation and differentiation. Chase and colleagues recently developed a novel serum-free medium for the expansion of human mesenchymal stem cells (Chase *et al.*, 2010). DMEM culture medium was only supplemented with a combination of TGF- $\beta$ 1, bFGF and recombinant human platelet-derived growth factor-BB (PDGF-BB). Results showed a significant propagation with retained phenotypic, differentiation and colony forming potential of human MSCs. Moreover, Invitrogen has released a reduced serum (2% FBS) with growth supplements

for MSCs expansion named MesenPRO RS™. According to the product sheet of MesenPRO RS™ found on the manufacturer website, the new culture medium has shown 35-45% improvement in MSCs expansion over 4 days of culture compared to classical culture medium (DMEM supplemented with 10% FBS). The new culture medium is also capable of maintaining the gene expression profile of MSCs and multipotentiality.

Immobilized GAGs on Chitosan membranes supported MSCs attachment, spreading and proliferation as shown in Figure 34 and Figure 35. MSCs cultured on immobilized heparan sulfate surfaces showed slightly higher proliferation rate compared to other GAGs for the 8 day culture. As heparan sulfate is a highly sulfated GAG, it's likely that heparan sulfate has relatively more available ligands for MSC to attach compared to the other immobilized GAGs. Heparan sulfate is known to act as a low affinity receptor for variety of ligands including growth factors. It was also shown on heparan sulfate that the variety in the conformation and the orientation of heparan sulfate functional groups allows it to employ different modes of bindings with individual proteins or protein complex (Gallagher, 2001). Moreover, it has been shown that heparan sulfate is involved in multiple cell signaling pathways (Turnbull *et al.*, 2001). This might explain why the proliferation rate on immobilized heparan sulfate was the highest during the 8 day culture among all studied GAGs. However, before making a definitive conclusion on the effect of GAGs on MSCs proliferation and differentiation, the effect of serum in culture medium should be fully understood or an alternative serum free culture medium should be used to avoid any inconsistency of results.

It is also worth mentioning that MSCs isolated from ovine bone marrow have a high adhesion capacity to surfaces in contrast to MSCs isolated from rat bone marrow. It was shown in Figure 34 that MSCs attached and spread well on chitosan membranes while rat bone marrow MSCs showed minimal cell attachment and proliferation when cultured on chitosan membranes (Uygun *et al.*, 2009).

## 7.5 Conclusions and Future Work

Two mechanisms have been proposed to explain why MSCs have similar characteristics to vascular smooth muscle cells. The ill-defined and highly variable nature of traditional serum not only limits the understanding of these mechanisms, but also MSCs proliferation and multipotentiality. Serum free medium is a practical alternative for classical culture medium. The use of serum free medium will provide better understanding of MSCs differentiation into specific cell lineages or the effect of a tested material or additive.

For the preliminary results introduced in this chapter, it was demonstrated that MSCs can be isolated from ovine bone marrow and grown in vitro to sufficient numbers despite the limitation with MSCs number in bone marrow.

GAGs supported MSCs attachment and proliferation and are potential candidates to be immobilized on chitosan-based scaffolds for improving MSCs proliferation and potentially their differentiation into a mature tissue. However, other parameters should be evaluated before deciding on potential GAG such as the deposition of extracellular matrix proteins in tissues. Also, the effect of GAGs on MSCs differentiation into endothelial cells (EC) should be evaluated to better decide on one GAG that will support MSCs proliferation and differentiation in cardiovascular tissue engineering application.

## CHAPTER EIGHT

### EFFECT OF STIFFNESS OF MECHANICALLY IMPROVED CHITOSAN FIBERS ON BONE MARROW- DERIVED MESENCHYMAL STEM CELLS ATTACHMENT, VIABILITY AND PROLIFERATION

#### 8.1 Introduction

One of the key challenges in stem cells research is to understand how to direct the differentiation of these cells toward to the desired tissue. Engler and colleagues pointed out an important factor that regulates stem cells differentiation and determines their fate: the elasticity of the substrate (Engler *et al.*, 2006). In his research study, Engler identified that changing the stiffness of the substrate can direct the differentiation of human mesenchymal stem cells into neuronal, muscle or bone lineages.

Although, the complex interaction between soluble and extracellular matrix molecules which direct the differentiation of MSC has been studied extensively, the physical properties of the matrix such as elasticity or stiffness did not gain sufficient attention in stem cells research (Discher *et al.*, 2005; Vogel and Sheetz, 2006). The concept behind cell-matrix interaction is that cells use actomyosin contractility for two-way interaction with the matrix (Even-Ram *et al.*, 2006). The contraction of the cell at integrin-based adhesions will be resisted by the matrix. This resistance will be followed by the accumulation of additional molecules at these sites. This process results in a balance of tension force at the cell-matrix interface. Ultimately, the inhibition of myosin will disrupt this cellular response to the matrix. It's believed that cellular force-sensing results in various intracellular signaling (Even-Ram *et al.*, 2006). Others identified some

increased in intracellular signals molecules such as Rho GTPase and MAP Kinase activity, which can alter the gene expression and embryonic development and even tumor cell progression (Paszek *et al.*, 2005; Ingber, 2006; Vogel and Sheetz, 2006). When MSCs grown on soft, intermediate or hard compliance substrates, the gene expression of phosphorylated form of neurofilament heavy chain was exclusively expressed by MSCs grown on soft compliance substrates, while MSCs grown on intermediate compliance substrates showed specific expression of myoD and finally when MSCs were grown on hard compliance substrates showed exclusive expression of bone CBF $\alpha$ 1 (Engler *et al.*, 2006).

The aim of this chapter is to evaluate the effect of fiber stiffness on MSCs proliferation and attachment. The working hypothesis for this experiment is that ***mechanically improved chitosan fibers will improve attachment and proliferation of mesenchymal stem cells***. In chapter six, mechanical properties of chitosan fibers were significantly improved using different chemical and physical treatments. Depending on the physical or the chemical treatment or both combined, chitosan fibers with different stiffness values were generated. These mechanically modified chitosan fibers with different stiffness values will be used as a substrate for growing MSCs.

## 8.2 Experimental Work

### 8.2.1 Fabrication of Mechanically Improved Chitosan Fibers

Chitosan fibers were produced using gel extrusion technique described previously. Briefly, chitosan solution was prepared by dissolving 1.5 wt% chitosan in 2 vol% of acetic acid. The solution was extruded directly into ammonia solution contains

25 wt% ammonium. Four conditions of fibers were tested: (1) fibers dried at 195 ° C and (2) immobilized with GAGs, (3) fibers dried at room temperature and (4) immobilized with heparin sodium. Fibers were then cut into small length (<2mm) and sterilized with 80% Ethanol and then washed several times with PBS. Fibers were compacted by centrifuging to facilitate the handling as one piece and cell culturing and to achieve better cell to cell contact. A total of 30 mg of fibers for each condition was used.

### **8.2.2 MSC Culturing and Seeding**

MSCs of passage 6 were cultured in DMEM-HG supplemented with 10% FBS and 1% ABAM for 1 week until cells reached 70% confluency. For each condition, 100,000 cells were seeded on fibers and left for 2 hours in the incubator to allow cell attachment. After 2 hours, cultured cells on fibers were incubated with DMEM-HG supplemented with 10% FBS.

### **8.2.3 MSC Attachment and Viability on Chitosan Fibers with Different Stiffness Values**

MSCs viability and attachment was evaluated through live/dead assay using Calcein AM (Molecular Probes, Invitrogen, CA) on day 3 and 5 of cultures by following the manufacturer protocol. Briefly, samples were incubated with DMEM without phenol red supplemented with 10% FBS which was mixed with 5 µl of calcein AM and 5 µl of Ethidium homodimer for 10 minutes at 37 °C. Samples were then washed with PBS and DMEM without phenol red supplemented with 10% FBS was added to the samples. Samples were then visualized under the fluorescent microscopy using blue filter for live

cells and green filter for dead cells. Proliferation of MSCs on fibers was evaluated using Alamar Blue assay (Invitrogen, CA) as mentioned before according to the manufacturer protocol on day 3, 6 and 9 of the culture. Briefly, alamar blue solution was diluted at 1:10 volume ratio in fresh DMEM-HG culture medium and the mixture then incubated with cells for 4 hours. Absorbance at 570 nm was read and normalized to absorbance readings at 600 nm using Perkin Elmer spectrophotometer.

#### **8.2.4 MSCs Cytoskeleton Organization on Mechanically Improved Chitosan**

##### **Fibers**

Cytoskeleton organization in MSCs that were cultured on mechanically improved chitosan fibers were investigated by staining the cells for actin fibers with rhodamine labeled phalloidin (R415, Molecular Probes ,Invitrogen, CA) according to the manufacturer protocol on day 9 of the culture. Briefly, medium were aspirated and fibers were washed twice with pre-warmed PBS. Cells were fixed with 4% paraformaldehyde for 10 minutes and then washed twice with PBS. Cells were then permeabilized with 0.2% Triton X100 in PBS for 5 minutes and then washed twice with PBS. To block nonspecific binding sites, fibers were incubated with 1% BSA in PBS for 30 minutes at room temperature and then washed twice with PBS. Fibers were then incubated with 5  $\mu$ l of rhodamine labeled phalloidin in 200  $\mu$ l PBS for 20 minutes and then washed twice with PBS. Cell Nucleus were counterstained with DAPI for 5 minutes and then washed 3 times with PBS, 5 minutes each. Fibers were then imaged with Nikon fluorescence microscope using ultraviolet (UV) and green filters.



### 8.3 Results

#### 8.3.1 MSCs Viability and Proliferation on Mechanically Improved Chitosan Fibers

Chitosan fibers with different stiffness values are shown in Figure 36. Alamar blue assay yielded different proliferation rate correlating with the stiffness of the fibers. MSCs proliferation increased in proportion to fiber stiffness. As seen in Figure 37, the highest proliferation rate was for the chitosan fibers annealed at 195 °C followed by fibers annealed at 195 °C and immobilized with heparin. For the first five days of the culture, proliferation rate of chitosan fibers dried at room temperature were practically comparable to the fibers that were dried at room temperature and then immobilized with heparin despite the difference in fiber stiffness. Moreover, the effect of heparin immobilization on MSCs proliferation was predominant over fiber stiffness at day 9 of culture for the first two conditions. Similarly, fibers dried at 195 °C were also near-comparable to fibers dried at the same temperature but immobilized with heparin despite the statistical difference in data. Heparin is well known to modulate the growth factor and the binding proteins which ultimately improve cell attachment and proliferation. So, the low stiffness value for fibers dried at room temperatures and immobilized with heparin was compensated with the presence of heparin.

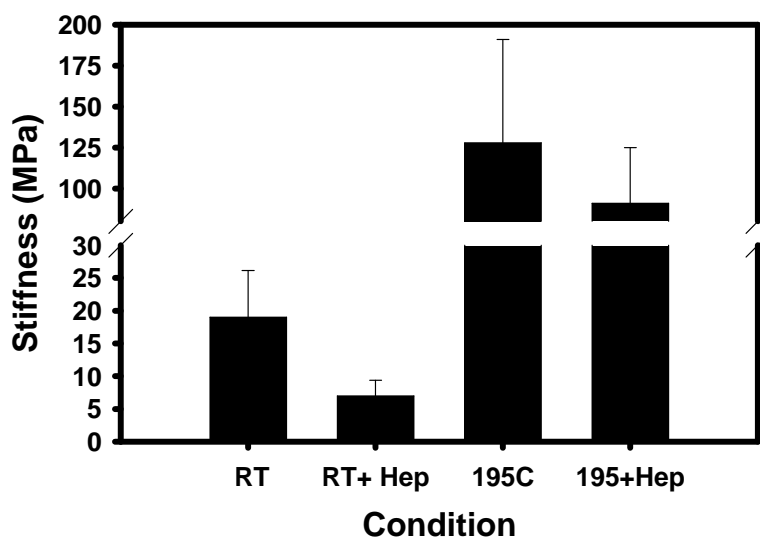


Figure 36: Stiffness for mechanically improved chitosan fiber

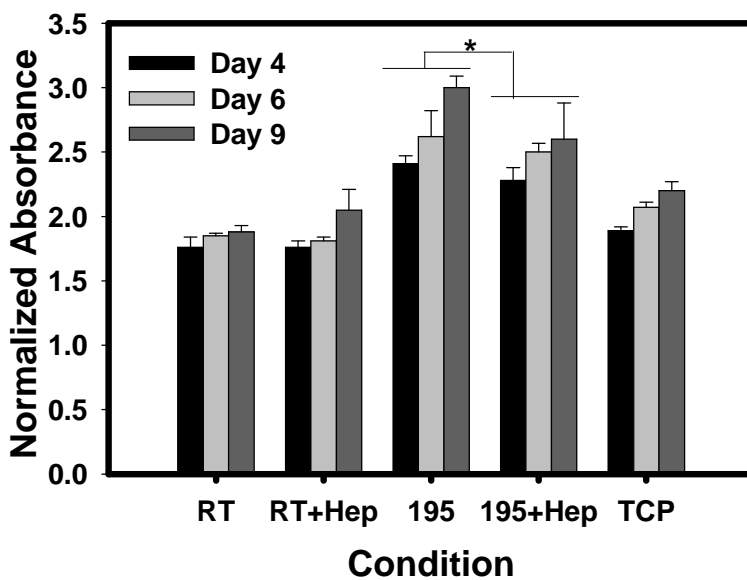


Figure 37: Alamar Blue results of MSC proliferation for 6 days on different fibers with different stiffness values.

Figure 38 shows MSCs viability and attachment on chitosan fibers with different stiffness values. In all cultures, MSCs attached onto all fibers and started to spread from the first days of the culture as demonstrated by the cell elongation and presence of extended cell stress fibers. Moreover, the rate of MSCs viability on all chitosan fibers were high which confirmed by the minimal presence of dead cells stained in red using the ethidium homodimers dye.

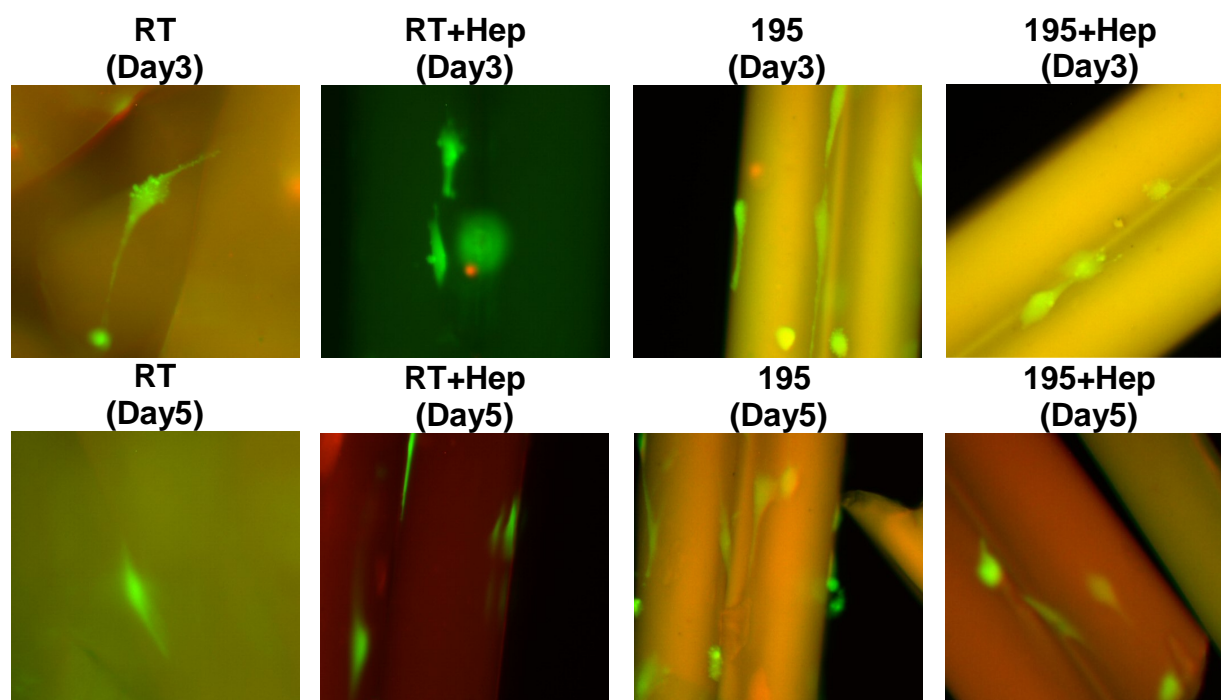


Figure 38: Live/ Dead assay showing MSC attachment and viability on day 3 and 5 of culture for chitosan fibers with different stiffness values, red-dead cells and green-live

cells

### 8.3.2 Cytoskeleton Organization in MSCs Cultured on Mechanically Improved Chitosan Fibers

The extent of cell spreading and cytoskeleton organization in MSCs cultured on mechanically improved chitosan fibers were analyzed by fluorescent staining for actin fibers. Figure 39 shows the actin fibers in MSCs when cultured on chitosan fibers dried at room temperature, chitosan fibers dried at room temperature and immobilized with heparin, chitosan fibers dried at 195 °C and MSCs cultured on a tissue culture plate. Actin fibers present in MSCs cultured on all chitosan fibers were fairly organized indicating a significant degree of cells spreading. Actin fibers seemed to be parallel to the plane of the chitosan fiber, while actin fibers in MSCs cultured on tissue culture plate were relatively disorganized. However, it is also worth mentioning that it was hard to obtain fluorescent images of MSCs cytoskeleton of fibers dried at room temperature and immobilized with heparin due to the fluorescence of the fibers. The arrow in Figure 39 C points to a fluorescent fiber. Additionally, staining nucleus with DAPI was also hard to be shown as fibers were also fluorescent. It's likely that the high crystallinity of chitosan fibers causes fibers to absorb the dye to be fluorescent. It was also clear that chitosan fibers were fluorescent in Figure 38 during the Calcein AM assay which supports they absorbance of chitosan fibers to the fluorescent dye.

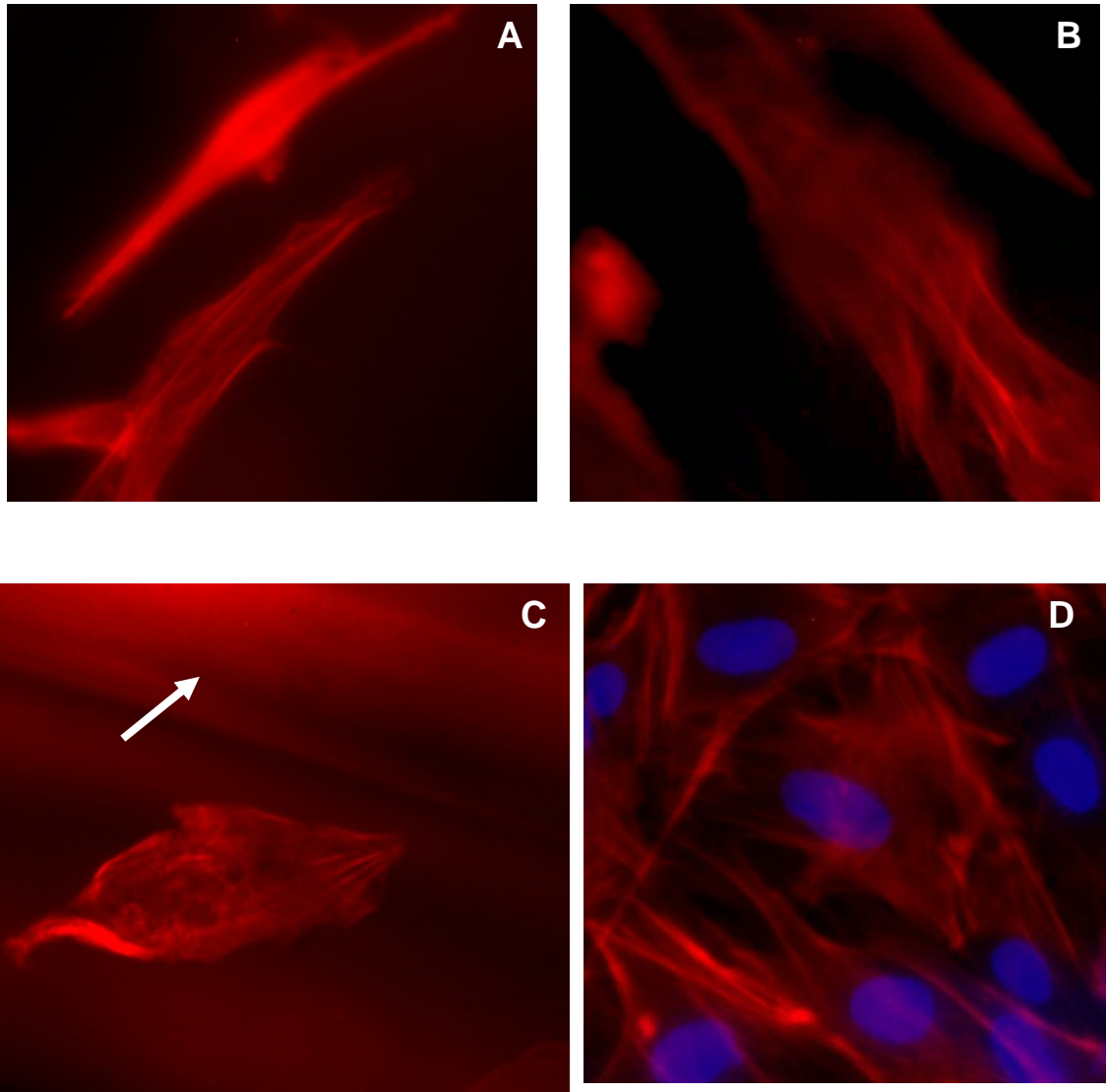


Figure 39: Cytoskeleton organization in MSCs on day 9 of culture when cultured on (A) Fibers dried at RT, (B) fibers dried at RT and Immobilized with Heparin, (C) Fibers annealed at 195 °C, arrow points to fluorescent chitosan fiber and (D) MSCs cultured on Tissue culture plate, red: f-actin, blue: nucleus, Objective 20X.

## 8.4 Discussion

For anchorage dependent cells like MSCs, the adhesion to the culture surface is important for inducing several intracellular processes that control important cellular events such as proliferation, differentiation and cell death. The signal transduction of the cell-matrix interaction has been recently shown to influence the differentiation of MSCs into SMCs (Suzuki *et al.*, 2010). However, in the experiments outlined above, the differentiation of MSCs into SMC was not confirmed with SMC differentiation marker due to the fact that these cells are already differentiated into SMC. As discussed in the previous chapter and confirmed by the results, MSCs showed similar characteristics to SMC when cultured in culture medium supplemented with 10% FBS. So, it is expected that MSCs cultured on fibers possess similar characteristics to SMC.

The main scope of this study was to test the biocompatibility of these mechanically improved chitosan fibers and also to evaluate the effect of fiber stiffness on MSCs proliferation, attachment and cytoskeleton organization. It was demonstrated clearly that mechanically improved chitosan fibers supported MSCs attachment, spreading and viability regardless of fiber stiffness. Moreover, it was feasible to correlate fiber stiffness with cell proliferation. It was shown clearly that fiber with highest stiffness yielded the highest MSCs proliferation. It was demonstrated previously that matrix stiffness determines the fate of MSCs (Engler *et al.*, 2006) and here it was demonstrated that matrix stiffness significantly affects cell proliferation and cytoskeleton organization. It was shown before that increasing chitosan membrane thickness improved serum protein adhesion onto the membranes due to the increase in membrane crystallinity (Uygun *et al.*, 2010). Moreover, it was shown that chitosan

membranes with highest thickness improved MSCs proliferation. In proliferation assay results shown in Figure 37, the proliferation rate correlated to the fibers stiffness which is correlated to the crystallinity of the fibers. As a result, a fiber with high stiffness has an organized crystalline structure and tends to bind more serum proteins which ultimately improve cell attachment and proliferation.

It was also demonstrated that heparin plays a key role in modulating growth factors and binding proteins. Chitosan fibers immobilized with heparin had lower stiffness values compared to unmodified fibers, yet MSCs proliferation was comparable to chitosan fibers with higher stiffness values.

## **8.5 Conclusions and Future Work**

In this chapter, the effect of fiber stiffness on MSCs attachment, cytoskeleton organization and proliferation was clearly demonstrated. Moreover, the biocompatibility of mechanically improved chitosan fibers produced through various chemical and physical treatments were tested and showed that these treatments did not affect fiber biocompatibility. The main purpose of improving the chitosan fibers mechanical properties is to provide additional strength and stiffness to the heart valve scaffold upon using the fiber-reinforcement approach. In addition to this purpose, the results in this chapter showed that improving the scaffold mechanical properties will also improve the cell proliferation within the scaffold to a further extent compared to the unmodified scaffold.

It is recommended to study the effect of fiber stiffness on MSCs differentiation into SMC or potentially to other heart cells by quantifying the amount of specific differentiation protein or gene.

## REFERENCES

- Ahn, J. S., Choi, H. K. and Cho, C. S. 2001. A novel mucoadhesive polymer prepared by template polymerization of acrylic acid in the presence of chitosan. *Biomaterials* 22(9): 923-928.
- Aiedeh, K., Gianasi, E., Orienti, I. and Zecchi, V. 1997. Chitosan microcapsules as controlled release systems for insulin. *J Microencapsul* 14(5): 567-576.
- Akhtar, K. and Ahmed, W. 2008. Profile of congenital heart disease and correlation to risk adjustment for surgery; an echocardiographic study. *J Coll Physicians Surg Pak* 18(6): 334-337.
- Bader, A., Schilling, T., Teebken, O. E., Brandes, G., Herden, T., Steinhoff, G. and Haverich, A. 1998. Tissue engineering of heart valves--human endothelial cell seeding of detergent acellularized porcine valves. *Eur J Cardiothorac Surg* 14(3): 279-284.
- Ball, S. G., Shuttleworth, A. C. and Kielty, C. M. 2004. Direct cell contact influences bone marrow mesenchymal stem cell fate. *International Journal of Biochemistry & Cell Biology* 36(4): 714-727.
- Barron, V., Lyons, E., Stenson-Cox, C., McHugh, P. E. and Pandit, A. 2003. Bioreactors for cardiovascular cell and tissue growth: a review. *Ann Biomed Eng* 31(9): 1017-1030.
- Berger, J., Reist, M., Mayer, J. M., Felt, O., Peppas, N. A. and Gurny, R. 2004. Structure and interactions in covalently and ionically crosslinked chitosan hydrogels for biomedical applications. *Eur J Pharm Biopharm* 57(1): 19-34.



- Caplan, A. I. 2007. Adult mesenchymal stem cells for tissue engineering versus regenerative medicine. *Journal of Cellular Physiology* 213(2): 341-347.
- Caplan, A. I. 2008. All MSCs are pericytes? *Cell Stem Cell* 3(3): 229-230.
- Chase, L. G., Lakshmiathy, U., Solchaga, L. A., Rao, M. S. and Vemuri, M. C. 2010. A novel serum-free medium for the expansion of human mesenchymal stem cells. *Stem Cell Res Ther* 1(1): 8.
- Chen, S. Y. and Lechleider, R. J. 2004. Transforming growth factor-beta-induced differentiation of smooth muscle from a neural crest stem cell line. *Circulation Research* 94(9): 1195-1202.
- Chevallay, B. and Herbage, D. 2000. Collagen-based biomaterials as 3D scaffold for cell cultures: applications for tissue engineering and gene therapy. *Med Biol Eng Comput* 38(2): 211-218.
- Cho, C. H., Eliason, J. F. and Matthew, H. W. 2008. Application of porous glycosaminoglycan-based scaffolds for expansion of human cord blood stem cells in perfusion culture. *J Biomed Mater Res A* 86(1): 98-107.
- Chupa, J. M., Foster, A. M., Sumner, S. R., Madihally, S. V. and Matthew, H. W. 2000. Vascular cell responses to polysaccharide materials: in vitro and in vivo evaluations. *Biomaterials* 21(22): 2315-2322.
- Dado, D. and Levenberg, S. 2009. Cell-scaffold mechanical interplay within engineered tissue. *Semin Cell Dev Biol* 20(6): 656-664.
- Danielpour, D. 1993. Improved Sandwich Enzyme-Linked Immunosorbent Assays for Transforming Growth Factor-Beta-1. *Journal of Immunological Methods* 158(1): 17-25.

- De Ugarte, D. A., Morizono, K., Elbarbary, A., Alfonso, Z., Zuk, P. A., Zhu, M., Dragoo, J. L., Ashjian, P., Thomas, B., Benhaim, P., Chen, I., Fraser, J. and Hedrick, M. H. 2003. Comparison of multi-lineage cells from human adipose tissue and bone marrow. *Cells Tissues Organs* 174(3): 101-109.
- Dikovsky, D., Bianco-Peled, H. and Seliktar, D. 2008. Defining the role of matrix compliance and proteolysis in three-dimensional cell spreading and remodeling. *Biophys J* 94(7): 2914-2925.
- Discher, D. E., Janmey, P. and Wang, Y. L. 2005. Tissue cells feel and respond to the stiffness of their substrate. *Science* 310(5751): 1139-1143.
- Dong, Y. M., Ruan, Y. H., Wang, H. W., Zhao, Y. G. and Bi, D. X. 2004. Studies on glass transition temperature of chitosan with four techniques. *Journal of Applied Polymer Science* 93(4): 1553-1558.
- Engelmayr, G. C., Jr., Rabkin, E., Sutherland, F. W., Schoen, F. J., Mayer, J. E., Jr. and Sacks, M. S. 2005. The independent role of cyclic flexure in the early in vitro development of an engineered heart valve tissue. *Biomaterials* 26(2): 175-187.
- Engelmayr, G. C., Jr., Sales, V. L., Mayer, J. E., Jr. and Sacks, M. S. 2006. Cyclic flexure and laminar flow synergistically accelerate mesenchymal stem cell-mediated engineered tissue formation: Implications for engineered heart valve tissues. *Biomaterials* 27(36): 6083-6095.
- Engler, A. J., Griffin, M. A., Sen, S., Bonnemann, C. G., Sweeney, H. L. and Discher, D. E. 2004. Myotubes differentiate optimally on substrates with tissue-like stiffness: pathological implications for soft or stiff microenvironments. *J Cell Biol* 166(6): 877-887.

- Engler, A. J., Sen, S., Sweeney, H. L. and Discher, D. E. 2006. Matrix elasticity directs stem cell lineage specification. *Cell* 126(4): 677-689.
- Even-Ram, S., Artym, V. and Yamada, K. M. 2006. Matrix control of stem cell fate. *Cell* 126(4): 645-647.
- Fan, J. Y., Shang, Y., Yuan, Y. J. and Yang, J. 2010. Preparation and characterization of chitosan/galactosylated hyaluronic acid scaffolds for primary hepatocytes culture. *Journal of Materials Science-Materials in Medicine* 21(1): 319-327.
- Filova, E., Straka, F., Mirejovsky, T., Masin, J. and Bacakova, L. 2009. Tissue-engineered heart valves. *Physiol Res* 58 Suppl 2: S141-158.
- Flanagan, T. C. and Pandit, A. 2003. Living artificial heart valve alternatives: a review. *Eur Cell Mater* 6: 28-45; discussion 45.
- Freed, L. E., Guilak, F., Guo, X. E., Gray, M. L., Tranquillo, R., Holmes, J. W., Radisic, M., Sefton, M. V., Kaplan, D. and Vunjak-Novakovic, G. 2006. Advanced tools for tissue engineering: scaffolds, bioreactors, and signaling. *Tissue Eng* 12(12): 3285-3305.
- Gallagher, J. T. 2001. Heparan sulfate: growth control with a restricted sequence menu. *Journal of Clinical Investigation* 108(3): 357-361.
- Goycoolea, F. M., Arguelles-Monal, W. M., Lizardi, J., Peniche, C., Heras, A., Galed, G. and Diaz, E. I. 2007. Temperature and pH-sensitive chitosan hydrogels: DSC, rheological and swelling evidence of a volume phase transition. *Polymer Bulletin* 58(1): 225-234.

- Grassl, E. D., Oegema, T. R. and Tranquillo, R. T. 2002. Fibrin as an alternative biopolymer to type-I collagen for the fabrication of a media equivalent. *J Biomed Mater Res* 60(4): 607-612.
- Gulbins, H., Pritisanac, A., Uhlig, A., Goldemund, A., Meiser, B. M., Reichart, B. and Daebritz, S. 2005. Seeding of human endothelial cells on valve containing aortic mini-roots: development of a seeding device and procedure. *Ann Thorac Surg* 79(6): 2119-2126.
- Hirano, S. and Midorikawa, T. 1998. Novel method for the preparation of N-acylchitosan fiber and N-acylchitosan-cellulose fiber. *Biomaterials* 19(1-3): 293-297.
- Hirano, S., Nagamura, K., Zhang, M., Kim, S. K., Chung, B. G., Yoshikawa, M. and Midorikawa, T. 1999. Chitosan staple fibers and their chemical modification with some aldehydes. *Carbohydrate Polymers* 38(4): 293-298.
- Hoerstrup, S. P., Kadner, A., Melnitchouk, S., Trojan, A., Eid, K., Tracy, J., Sodian, R., Visjager, J. F., Kolb, S. A., Grunenfelder, J., Zund, G. and Turina, M. I. 2002. Tissue engineering of functional trileaflet heart valves from human marrow stromal cells. *Circulation* 106(12 Suppl 1): I143-150.
- Hoerstrup, S. P., Sodian, R., Daebritz, S., Wang, J., Bacha, E. A., Martin, D. P., Moran, A. M., Guleserian, K. J., Sperling, J. S., Kaushal, S., Vacanti, J. P., Schoen, F. J. and Mayer, J. E., Jr. 2000. Functional living trileaflet heart valves grown in vitro. *Circulation* 102(19 Suppl 3): III44-49.
- Hoerstrup, S. P., Sodian, R., Sperling, J. S., Vacanti, J. P. and Mayer, J. E., Jr. 2000. New pulsatile bioreactor for in vitro formation of tissue engineered heart valves. *Tissue Eng* 6(1): 75-79.

- Ikari, Y., Yee, K. O. and Schwartz, S. M. 2000. Role of alpha5beta1 and alphavbeta3 integrins on smooth muscle cell spreading and migration in fibrin gels. *Thromb Haemost* 84(4): 701-705.
- Ingber, D. E. 2006. Mechanical control of tissue morphogenesis during embryological development. *International Journal of Developmental Biology* 50(2-3): 255-266.
- Iop, L., Renier, V., Naso, F., Piccoli, M., Bonetti, A., Gandaglia, A., Pozzobon, M., Paolin, A., Ortolani, F., Marchini, M., Spina, M., De Coppi, P., Sartore, S. and Gerosa, G. 2009. The influence of heart valve leaflet matrix characteristics on the interaction between human mesenchymal stem cells and decellularized scaffolds. *Biomaterials* 30(25): 4104-4116.
- Jeon, E. S., Moon, H. J., Kim, Y. M. and Kim, J. H. 2006. Sphingosylphosphorylcholine induces differentiation of human mesenchymal stem cells into smooth muscle cells. *Febs Journal* 273: 130-130.
- Jockenhoevel, S., Chalabi, K., Sachweh, J. S., Groesdonk, H. V., Demircan, L., Grossmann, M., Zund, G. and Messmer, B. J. 2001. Tissue engineering: Complete autologous valve conduit - A new moulding technique. *Thoracic and Cardiovascular Surgeon* 49(5): 287-290.
- Jockenhoevel, S., Zund, G., Hoerstrup, S. P., Chalabi, K., Sachweh, J. S., Demircan, L., Messmer, B. J. and Turina, M. 2001. Fibrin gel -- advantages of a new scaffold in cardiovascular tissue engineering. *Eur J Cardiothorac Surg* 19(4): 424-430.
- Kiel, M. J., Yilmaz, O. H., Iwashita, T., Yilmaz, O. H., Terhorst, C. and Morrison, S. J. 2005. SLAM family receptors distinguish hematopoietic stem and progenitor cells and reveal endothelial niches for stem cells. *Cell* 121(7): 1109-1121.

- Knaul, J. Z., Hudson, S. M. and Creber, K. A. M. 1999. Improved mechanical properties of chitosan fibers. *Journal of Applied Polymer Science* 72(13): 1721-1732.
- Koch, S., Flanagan, T. C., Sachweh, J. S., Tanios, F., Schnoering, H., Deichmann, T., Ella, V., Kellomaki, M., Gronloh, N., Gries, T., Tolba, R., Schmitz-Rode, T. and Jockenhoevel, S. 2010. Fibrin-poly(lactide)-based tissue-engineered vascular graft in the arterial circulation. *Biomaterials* 31(17): 4731-4739.
- Kolhe, P. and Kannan, R. M. 2003. Improvement in ductility of chitosan through blending and copolymerization with PEG: FTIR investigation of molecular interactions. *Biomacromolecules* 4(1): 173-180.
- Kratz, G., Arnander, C., Swedenborg, J., Back, M., Falk, C., Gouda, I. and Larm, O. 1997. Heparin-chitosan complexes stimulate wound healing in human skin. *Scand J Plast Reconstr Surg Hand Surg* 31(2): 119-123.
- Kurpinski, K., Lam, H., Chu, J., Wang, A., Kim, A., Tsay, E., Agrawal, S., Schaffer, D. V. and Li, S. 2010. Transforming growth factor-beta and notch signaling mediate stem cell differentiation into smooth muscle cells. *Stem Cells* 28(4): 734-742.
- Lee, S. H., Kim, Y. and Kim, Y. 2007. Effect of the concentration of sodium acetate (SA) on crosslinking of chitosan fiber by epichlorohydrin (ECH) in a wet spinning system. *Carbohydrate Polymers* 70(1): 53-60.
- Lee, S. H., Park, S. Y. and Choi, J. H. 2004. Fiber formation and physical properties of chitosan fiber crosslinked by epichlorohydrin in a wet spinning system: The effect of the concentration of the crosslinking agent epichlorohydrin. *Journal of Applied Polymer Science* 92(3): 2054-2062.

- Lewus, K. E. and Nauman, E. A. 2005. In vitro characterization of a bone marrow stem cell-seeded collagen gel composite for soft tissue grafts: effects of fiber number and serum concentration. *Tissue Eng* 11(7-8): 1015-1022.
- Li, X., Feng, Q., Liu, X., Dong, W. and Cui, F. 2006. Collagen-based implants reinforced by chitin fibres in a goat shank bone defect model. *Biomaterials* 27(9): 1917-1923.
- Li, X., Feng, Q., Wang, W. and Cui, F. 2006. Chemical characteristics and cytocompatibility of collagen-based scaffold reinforced by chitin fibers for bone tissue engineering. *J Biomed Mater Res B Appl Biomater* 77(2): 219-226.
- Li, X., Liu, X., Dong, W., Feng, Q., Cui, F., Uo, M., Akasaka, T. and Watari, F. 2009. In vitro evaluation of porous poly(L-lactic acid) scaffold reinforced by chitin fibers. *J Biomed Mater Res B Appl Biomater* 90(2): 503-509.
- Lichtenberg, A., Tudorache, I., Cebotari, S., Ringes-Lichtenberg, S., Sturz, G., Hoeffler, K., Hurschler, C., Brandes, G., Hilfiker, A. and Haverich, A. 2006. In vitro re-endothelialization of detergent decellularized heart valves under simulated physiological dynamic conditions. *Biomaterials* 27(23): 4221-4229.
- Lindahl, U. and Hook, M. 1978. Glycosaminoglycans and their binding to biological macromolecules. *Annu Rev Biochem* 47: 385-417.
- Lucia, M. S., Sporn, M. B., Roberts, A. B., Stewart, L. V. and Danielpour, D. 1998. The role of transforming growth factor-beta 1, -beta 2, and -beta 3 in androgen-responsive growth of NRP-152 rat prostatic epithelial cells. *Journal of Cellular Physiology* 175(2): 184-192.

- Madihally, S. V., Flake, A. W. and Matthew, H. W. 1999. Maintenance of CD34 expression during proliferation of CD34+ cord blood cells on glycosaminoglycan surfaces. *Stem Cells* 17(5): 295-305.
- Madihally, S. V. and Matthew, H. W. 1999. Porous chitosan scaffolds for tissue engineering. *Biomaterials* 20(12): 1133-1142.
- Matthews, N. C., Wadhwa, M., Bird, C., Borrás, F. E. and Navarrete, C. V. 2000. Sustained expression of CD154 (CD40L) and proinflammatory cytokine production by alloantigen-stimulated umbilical cord blood T cells. *J Immunol* 164(12): 6206-6212.
- Mi, F. L., Chen, C. T., Tseng, Y. C., Kuan, C. Y. and Shyu, S. S. 1997. Iron(III)-carboxymethylchitin microsphere for the pH-sensitive release of 6-mercaptopurine. *Journal of Controlled Release* 44(1): 19-32.
- Miao, Z., Jin, J., Chen, L., Zhu, J., Huang, W., Zhao, J., Qian, H. and Zhang, X. 2006. Isolation of mesenchymal stem cells from human placenta: comparison with human bone marrow mesenchymal stem cells. *Cell Biol Int* 30(9): 681-687.
- Mol, A. and Hoerstrup, S. P. 2004. Heart valve tissue engineering -- where do we stand? *Int J Cardiol* 95 Suppl 1: S57-58.
- Mol, A., Rutten, M. C., Driessen, N. J., Bouten, C. V., Zund, G., Baaijens, F. P. and Hoerstrup, S. P. 2006. Autologous human tissue-engineered heart valves: prospects for systemic application. *Circulation* 114(1 Suppl): I152-158.
- Narita, Y., Yamawaki, A., Kagami, H., Ueda, M. and Ueda, Y. 2008. Effects of transforming growth factor-beta 1 and ascorbic acid on differentiation of human



- bone-marrow-derived mesenchymal stem cells into smooth muscle cell lineage. *Cell and Tissue Research* 333(3): 449-459.
- Neidert, M. R., Lee, E. S., Oegema, T. R. and Tranquillo, R. T. 2002. Enhanced fibrin remodeling in vitro with TGF-beta1, insulin and plasmin for improved tissue-equivalents. *Biomaterials* 23(17): 3717-3731.
- Neuenschwander, S. and Hoerstrup, S. P. 2004. Heart valve tissue engineering. *Transpl Immunol* 12(3-4): 359-365.
- Niklason, L. E. and Langer, R. S. 1997. Advances in tissue engineering of blood vessels and other tissues. *Transpl Immunol* 5(4): 303-306.
- Notin, L., Viton, C., David, L., Alcouffe, P., Rochas, C. and Domard, A. 2006. Morphology and mechanical properties of chitosan fibers obtained by gel-spinning: influence of the dry-jet-stretching step and ageing. *Acta Biomater* 2(4): 387-402.
- Paszek, M. J., Zahir, N., Johnson, K. R., Lakins, J. N., Rozenberg, G. I., Gefen, A., Reinhart-King, C. A., Margulies, S. S., Dembo, M., Boettiger, D., Hammer, D. A. and Weaver, V. M. 2005. Tensional homeostasis and the malignant phenotype. *Cancer Cell* 8(3): 241-254.
- Perry, T. E., Kaushal, S., Sutherland, F. W., Guleserian, K. J., Bischoff, J., Sacks, M. and Mayer, J. E. 2003. Thoracic Surgery Directors Association Award. Bone marrow as a cell source for tissue engineering heart valves. *Ann Thorac Surg* 75(3): 761-767; discussion 767.
- Pittenger, M. F., Mackay, A. M., Beck, S. C., Jaiswal, R. K., Douglas, R., Mosca, J. D., Moorman, M. A., Simonetti, D. W., Craig, S. and Marshak, D. R. 1999.

- Multilineage potential of adult human mesenchymal stem cells. *Science* 284(5411): 143-147.
- Rao, M. S. and Mattson, M. P. 2001. Stem cells and aging: expanding the possibilities. *Mechanisms of Ageing and Development* 122(7): 713-734.
- Rebelatto, C. K., Aguiar, A. M., Moretao, M. P., Senegaglia, A. C., Hansen, P., Barchiki, F., Oliveira, J., Martins, J., Kuligovski, C., Mansur, F., Christofis, A., Amaral, V. F., Brofman, P. S., Goldenberg, S., Nakao, L. S. and Correa, A. 2008. Dissimilar differentiation of mesenchymal stem cells from bone marrow, umbilical cord blood, and adipose tissue. *Exp Biol Med (Maywood)* 233(7): 901-913.
- Rothenburger, M., Vischer, P., Volker, W., Glasmacher, B., Berendes, E., Scheld, H. H. and Deiwick, M. 2001. In vitro modelling of tissue using isolated vascular cells on a synthetic collagen matrix as a substitute for heart valves. *Thorac Cardiovasc Surg* 49(4): 204-209.
- Sakurai, K., Maegawa, T. and Takahashi, T. 2000. Glass transition temperature of chitosan and miscibility of chitosan/poly(N-vinyl pyrrolidone) blends. *Polymer* 41(19): 7051-7056.
- Sarkar, S., Schmitz-Rixen, T., Hamilton, G. and Seifalian, A. M. 2007. Achieving the ideal properties for vascular bypass grafts using a tissue engineered approach: a review. *Med Biol Eng Comput* 45(4): 327-336.
- Scandola, M., Ceccorulli, G. and Pizzoli, M. 1991. Molecular Motions of Polysaccharides in the Solid-State - Dextran, Pullulan and Amylose. *International Journal of Biological Macromolecules* 13(4): 254-260.

- Schmidt, D., Mol, A., Breymann, C., Achermann, J., Odermatt, B., Gossi, M., Neuenschwander, S., Pretre, R., Genoni, M., Zund, G. and Hoerstrup, S. P. 2006. Living autologous heart valves engineered from human prenatally harvested progenitors. *Circulation* 114(1 Suppl): I125-131.
- Shah, N. M., Groves, A. K. and Anderson, D. J. 1996. Alternative neural crest cell fates are instructively promoted by TGF beta superfamily members. *Cell* 85(3): 331-343.
- Shinoka, T., Breuer, C. K., Tanel, R. E., Zund, G., Miura, T., Ma, P. X., Langer, R., Vacanti, J. P. and Mayer, J. E., Jr. 1995. Tissue engineering heart valves: valve leaflet replacement study in a lamb model. *Ann Thorac Surg* 60(6 Suppl): S513-516.
- Shinoka, T., Ma, P. X., Shum-Tim, D., Breuer, C. K., Cusick, R. A., Zund, G., Langer, R., Vacanti, J. P. and Mayer, J. E., Jr. 1996. Tissue-engineered heart valves. Autologous valve leaflet replacement study in a lamb model. *Circulation* 94(9 Suppl): II164-168.
- Shu, X. Z., Zhu, K. J. and Song, W. H. 2001. Novel pH-sensitive citrate cross-linked chitosan film for drug controlled release. *International Journal of Pharmaceutics* 212(1): 19-28.
- Simon, P., Kasimir, M. T., Seebacher, G., Weigel, G., Ullrich, R., Salzer-Muhar, U., Rieder, E. and Wolner, E. 2003. Early failure of the tissue engineered porcine heart valve SYNERGRAFT in pediatric patients. *Eur J Cardiothorac Surg* 23(6): 1002-1006; discussion 1006.

- Sinha, S., Hoofnagle, M. H., Kingston, P. A., McCanna, M. E. and Owens, G. K. 2004. Transforming growth factor-beta 1 signaling contributes to development of smooth muscle cells from embryonic stem cells. *American Journal of Physiology-Cell Physiology* 287(6): C1560-C1568.
- Sodian, R., Hoerstrup, S. P., Sperling, J. S., Daebritz, S., Martin, D. P., Moran, A. M., Kim, B. S., Schoen, F. J., Vacanti, J. P. and Mayer, J. E., Jr. 2000. Early in vivo experience with tissue-engineered trileaflet heart valves. *Circulation* 102(19 Suppl 3): III22-29.
- Sodian, R., Hoerstrup, S. P., Sperling, J. S., Martin, D. P., Daebritz, S., Mayer, J. E., Jr. and Vacanti, J. P. 2000. Evaluation of biodegradable, three-dimensional matrices for tissue engineering of heart valves. *ASAIO J* 46(1): 107-110.
- Sodian, R., Lueders, C., Kraemer, L., Kuebler, W., Shakibaei, M., Reichart, B., Daebritz, S. and Hetzer, R. 2006. Tissue engineering of autologous human heart valves using cryopreserved vascular umbilical cord cells. *Ann Thorac Surg* 81(6): 2207-2216.
- Sodian, R., Sperling, J. S., Martin, D. P., Egozy, A., Stock, U., Mayer, J. E., Jr. and Vacanti, J. P. 2000. Fabrication of a trileaflet heart valve scaffold from a polyhydroxyalkanoate biopolyester for use in tissue engineering. *Tissue Eng* 6(2): 183-188.
- Song, Y. S., Lee, H. J., Park, I. H., Kim, W. K., Ku, J. H. and Kim, S. U. 2007. Potential differentiation of human mesenchymal stem cell transplanted in rat corpus cavernosum toward endothelial or smooth muscle cells. *Int J Impot Res* 19(4): 378-385.

- Song, Z. C., Shu, R. and Zhang, X. L. 2010. Cellular responses and expression profiling of human bone marrow stromal cells stimulated with enamel matrix proteins in vitro. *Cell Prolif* 43(1): 84-94.
- Steinhoff, G., Stock, U., Karim, N., Mertsching, H., Timke, A., Meliss, R. R., Pethig, K., Haverich, A. and Bader, A. 2000. Tissue engineering of pulmonary heart valves on allogenic acellular matrix conduits: in vivo restoration of valve tissue. *Circulation* 102(19 Suppl 3): III50-55.
- Stradins, P., Lacis, R., Ozolanta, I., Purina, B., Ose, V., Feldmane, L. and Kasyanov, V. 2004. Comparison of biomechanical and structural properties between human aortic and pulmonary valve. *Eur J Cardiothorac Surg* 26(3): 634-639.
- Suh, J. K. and Matthew, H. W. 2000. Application of chitosan-based polysaccharide biomaterials in cartilage tissue engineering: a review. *Biomaterials* 21(24): 2589-2598.
- Sutherland, F. W., Perry, T. E., Yu, Y., Sherwood, M. C., Rabkin, E., Masuda, Y., Garcia, G. A., McLellan, D. L., Engelmayer, G. C., Jr., Sacks, M. S., Schoen, F. J. and Mayer, J. E., Jr. 2005. From stem cells to viable autologous semilunar heart valve. *Circulation* 111(21): 2783-2791.
- Suzuki, S., Narita, Y., Yamawaki, A., Murase, Y., Satake, M., Mutsuga, M., Okamoto, H., Kagami, H., Ueda, M. and Ueda, Y. 2010. Effects of extracellular matrix on differentiation of human bone marrow-derived mesenchymal stem cells into smooth muscle cell lineage: utility for cardiovascular tissue engineering. *Cells Tissues Organs* 191(4): 269-280.

- Tang, G. H., Fazel, S., Weisel, R. D., Van Arsdell, G. S. and Li, R. K. 2005. Cardiovascular tissue engineering therapy: so near, so far? *Ann Thorac Surg* 79(6): 1831-1833.
- Taylor, P. M., Allen, S. P., Dreger, S. A. and Yacoub, M. H. 2002. Human cardiac valve interstitial cells in collagen sponge: a biological three-dimensional matrix for tissue engineering. *J Heart Valve Dis* 11(3): 298-306; discussion 306-297.
- Thubrikar, M. J. 1990. *Geometry of The Aortic Valve. The Aortic Valve.* M. J. Thubrikar. Boca Raton, Florida, CRC Press, Inc.: 8-18.
- Tschoeke, B., Flanagan, T. C., Koch, S., Harwoko, M. S., Deichmann, T., Ella, V., Sachweh, J. S., Kellomaki, M., Gries, T., Schmitz-Rode, T. and Jockenhoevel, S. 2009. Tissue-engineered small-caliber vascular graft based on a novel biodegradable composite fibrin-poly lactide scaffold. *Tissue Eng Part A* 15(8): 1909-1918.
- Turnbull, J., Powell, A. and Guimond, S. 2001. Heparan sulfate: decoding a dynamic multifunctional cell regulator. *Trends Cell Biol* 11(2): 75-82.
- Tuzlakoglu, K., Alves, C. M., Mano, J. F. and Reis, R. L. 2004. Production and characterization of chitosan fibers and 3-D fiber mesh scaffolds for tissue engineering applications. *Macromolecular Bioscience* 4(8): 811-819.
- Unsworth, B. R. and Lelkes, P. I. 1998. Growing tissues in microgravity. *Nat Med* 4(8): 901-907.
- Uygun, B. E., Bou-Akl, T., Albanna, M. and Matthew, H. W. 2010. Membrane thickness is an important variable in membrane scaffolds: Influence of chitosan membrane structure on the behavior of cells. *Acta Biomater* 6(6): 2126-2131.

- Uygun, B. E., Stojisih, S. E. and Matthew, H. W. T. 2009. Effects of Immobilized Glycosaminoglycans on the Proliferation and Differentiation of Mesenchymal Stem Cells. *Tissue Engineering Part A* 15(11): 3499-3512.
- VandeVord, P. J., Matthew, H. W., DeSilva, S. P., Mayton, L., Wu, B. and Wooley, P. H. 2002. Evaluation of the biocompatibility of a chitosan scaffold in mice. *J Biomed Mater Res* 59(3): 585-590.
- Vogel, V. and Sheetz, M. 2006. Local force and geometry sensing regulate cell functions. *Nat Rev Mol Cell Biol* 7(4): 265-275.
- Wang, X., Song, G., Lou, T. and Peng, W. 2009. Fabrication of nano-fibrous PLLA scaffold reinforced with chitosan fibers. *J Biomater Sci Polym Ed* 20(14): 1995-2002.
- Wei, Y. C., Hudson, S. M., Mayer, J. M. and Kaplan, D. L. 1992. The Cross-Linking of Chitosan Fibers. *Journal of Polymer Science Part a-Polymer Chemistry* 30(10): 2187-2193.
- Weinberg, C. B. and Bell, E. 1986. A blood vessel model constructed from collagen and cultured vascular cells. *Science* 231(4736): 397-400.
- Wilson, G. J., Courtman, D. W., Klement, P., Lee, J. M. and Yeger, H. 1995. Acellular matrix: a biomaterials approach for coronary artery bypass and heart valve replacement. *Ann Thorac Surg* 60(2 Suppl): S353-358.
- Yacoub, M. H. and Takkenberg, J. J. 2005. Will heart valve tissue engineering change the world? *Nat Clin Pract Cardiovasc Med* 2(2): 60-61.

- Ye, Q., Zund, G., Benedikt, P., Jockenhoevel, S., Hoerstrup, S. P., Sakyama, S., Hubbell, J. A. and Turina, M. 2000. Fibrin gel as a three dimensional matrix in cardiovascular tissue engineering. *Eur J Cardiothorac Surg* 17(5): 587-591.
- Zhou, L., Isenberg, J. S., Cao, Z. and Roberts, D. D. 2006. Type I collagen is a molecular target for inhibition of angiogenesis by endogenous thrombospondin-1. *Oncogene* 25(4): 536-545.
- Zimmermann, W. H. and Eschenhagen, T. 2003. Cardiac tissue engineering for replacement therapy. *Heart Fail Rev* 8(3): 259-269.



**ABSTRACT****REINFORCED CHITOSAN-BASED HEART VALVE SCAFFOLD AND UTILITY OF BONE MARROW-DERIVED MESENCHYMAL STEM CELLS FOR CARDIOVASCULAR TISSUE ENGINEERING**

by

**MOHAMMAD ZAKI ALBANNA****May 2011****Advisor:** Dr. Howard W. T. Matthew**Major:** Biomedical Engineering**Degree:** Doctor of Philosophy

Recent research has demonstrated a strong correlation between the differentiation profile of mesenchymal stem cells (MSCs) and scaffold stiffness. Chitosan is being widely studied for tissue engineering applications due to its biocompatibility and biodegradability. However, its use in load-bearing applications is limited due to moderate to low mechanical properties. In this study, we investigated the effectiveness of a fiber reinforcement method for enhancing the mechanical properties of chitosan scaffolds. Chitosan fibers were fabricated using a solution extrusion and neutralization method and incorporated into porous chitosan scaffolds. The effects of different fiber/scaffold mass ratios, fiber mechanical properties and fiber lengths on scaffold mechanical properties were studied. The results showed that incorporating fibers improved scaffold strength and stiffness in proportion to the fiber/scaffold mass ratio. A fiber-reinforced heart valve leaflet scaffold achieved strength values comparable to the radial values of human pulmonary and aortic valves. Additionally, the effects of

shorter fibers (2 mm) were found to be up to 3-fold greater than longer fibers (10 mm). Despite this reduction in fiber mechanical properties caused by heparin crosslinking, the heparin-modified fibers still improved the mechanical properties of the reinforced scaffolds, but to a lesser extent than the unmodified fibers. The results demonstrate that chitosan fiber-reinforcement can be used to generate tissue-matching mechanical properties in porous chitosan scaffolds and that fiber length and mechanical properties are important parameters in defining the degree of mechanical improvement. We further studied various chemical and physical treatments to improve the mechanical properties of chitosan fibers. With combination of chemical and physical treatments, fiber stiffness improved 40fold compared to unmodified fibers. We also isolated ovine bone marrow-derived MSCs and evaluated their utility for cardiovascular tissue engineering applications. Moreover, we evaluated the effect of various glycosaminoglycans (GAGs) on MSCs morphology and proliferation. Lastly, we studied the effect of stiffness of mechanically improved chitosan fibers on MSCs viability, attachment and proliferation. Results showed that MSCs proliferation improved in proportion to fiber stiffness.

**AUTOBIOGRAPHICAL STATEMENT****EDUCATION**

M.Sc., Biomedical Engineering, Wayne State University, (WSU), December 2009

M.Sc., Electrical and Computer Engineering, Southern Illinois University at Carbondale (SIUC), July 2007

B.Sc., Biomedical Engineering, The Hashemite University, June 2006

**REFEREED PROFESSIONAL JOURNALS:**

Uygun BE, Bou-Akl T, **Albanna M**, Matthew HW (Jun 2010). *“Membrane thickness is an important variable in membrane scaffolds: Influence of chitosan membrane structure on the behavior of cells”*. Acta Biomaterialia, 6 (6), 2126-31

**PAPERS IN REFEREED JOURNALS AWAITING REVIEW:**

**Mohammad Z. Albanna**, Therese H. Bou-Akl, Henry L. Walters III, Howard W.T. Matthew. *“A Novel Approach for Improving the Mechanical Properties of Chitosan-Based Heart Valve Scaffolds”*. In Review in Journal of the Mechanical Behavior of Biomedical Materials, December 2010.

**Mohammad Z. Albanna**, Henry L. Walters III, Howard W.T. Matthew. *“Processed Chitosan fibers with Improved Mechanical Properties for Tissue Engineering Applications”*. Submitted to Journal of the Mechanical Behavior of Biomedical Materials, December 2010.

**CONFERENCE PRESENTATIONS (More than 10 oral presentations)**

**Mohammad Z. Albanna**, Therese H. Bou-Akl, Henry L. Walters III, Howard W.T. Matthew. *“Dynamic Culturing of Chitosan-Glycosaminoglycans Scaffolds with Bone Marrow Mesenchymal Stem Cells for Heart Valve Tissue Engineering”*. Transactions of the Society for Biomaterials (SFB), April 2011. Orlando, Florida, USA